Breast Cancer Diagnosis Using Deep Learning Models

A Doctoral Dissertation
Submitted to the Council of Erbil Technical Engineering College, at Erbil Polytechnic University in Partial Fulfillment of the Requirements for the Degree of Doctor of Philosophy in Information Systems Engineering.

by

Chiman Haydar Salh

B.Sc. in Computer Sciences (2013)

M.Sc. in Electrical and Electronic Engineering (2017)

Supervised by

Assistant Prof. Dr. Abbas M. Ali Mohamad

Erbil, Kurdistan Region of Iraq

December 2023

DECLARATION

I declare that the PhD Dissertation entitled: ***Breast Cancer Diagnosis Using Deep Learning Models,*** is my own original work, and hereby I certify that unless stated, all work contained within this dissertation is my own independent research and has not been submitted for the award of any other degree at any institution, except where due acknowledgment is made in the text.

Signature:

Student Name: Chiman Haydar Salh

Date: / / 2023

LINGUISTIC REVIEW

I confirmed that I have reviewed the Ph.D. dissertation entitled:

Breast Cancer Diagnosis Using Deep Learning Models.

from the English linguistic point of view, and I can confirm that it is free of grammatical and spelling errors.

Signature:

Name of Reviewer: Awat Mohammed Mustafa

Lecturer, MA in LTE.

Phone No.07504899129

Email address: awat.mustafa@epu.edu.iq

Date: / / 2023

SUPERVISOR CERTIFICATE

This dissertation entitled "***Breast Cancer Diagnosis Using Deep Learning Models***" is presented by "***Chiman Haydar Salh***" and has been written under my supervision and has been submitted for the award of the Doctor of Philosophy in Information Systems Engineering with my approval as supervisor.

Signature:

Name: Assistance Prof. Dr. Abbas M. Ali Mohamad
(Supervisor)

Date: / /2023

I confirm that all requirements have been fulfilled.

Signature:

Name: Byad Abdullqader Ahmed

Head of the Department of Information Systems Engineering

Date: / / 2023

I confirm that all requirements have been fulfilled.

Postgraduate Office

Signature:

Name: Byad Abdullqader Ahmed

Date: / / 2023

EXAMINING COMMITTEE CERTIFICATION

We certify that we have read this dissertation: "***Breast Cancer Diagnosis Using Deep Learning Models"*** and as an examining committee examined the student (***Chiman Haydar Salh***) in its content and what related to it. We approve that it meets the standards of a dissertation for the degree of Doctor of Philosophy (Ph.D.) in Information System Engineering.

Signature:
Name:
(Chairman)
Date: / / 2023

Signature:
Name: Assist. Prof.
(Member)
Date: / / 2023

Signature:
Name:
(Member)
Date: / /2023

Signature:
Name: Assist. Prof.
(Member)
Date: / /2023

Signature:
Name: Assist. Prof.
(Member)
Date: / /2023

Signature:
Name: Asst. Prof. Dr. Abbas M. Ali Mohamad
(Supervisor-Member)
Date: / /2023

Signature
Name: Prof. Dr. Ayad Zaki Saber Agha
Dean of the College of Erbil Technical Engineering
Date: / / 2023

ACKNOWLEDGMENT

First of all, and thankful to ALLAH Almighty for his abundant grace and blessings that gave me the strength, opportunity, and capability to complete this thesis successfully. Also honored to express my highest appreciation to my supervisor **Assistant Prof. Dr. Abbas M. Ali Mohamad** for marvelous supervision support, encouragement constant guidance and professional advice. They are sincerely thankful to the presidency of the Information System Engineering department for their support.

Moreover, extend my deepest gratitude to my family for allowing me to realize my own potential. All the support they have provided me over the years was the greatest gift anyone has ever given me for their consistent prayers, unconditional love, care, understanding, patience, and cooperation to follow my dreams.

Many thanks to the Ministry of Health and the staff at Hospitals in Erbil and Suleimani for their help in collecting the data.

I am also thankful to my two radiologist colleagues **Dr. Sawen Khasrow Dizay** and **Dr. Lana R.A. Pshtiwan** support and encouragement and for taking the time to listen. Finally, my Thanks go to all the people who supported me in completing this dissertation, directly or indirectly.

ABSTRACT

Breast Cancer (BC) is a prevalent and potentially life-threatening disease affecting women worldwide. The timely and precise identification of ailments is essential in enhancing patient outcomes and rates of survival. Deep learning models have emerged as powerful tools for medical image analysis that potentially aiding in automatic BC detection. Several studies have been done in this area, and many gaps should be considered in the survey. As there are no datasets related to the Kurdistan Region of Iraq (KRI) hospitals categorizing images based on breast cancer cases, much of the writing on this topic has focused on classification accuracy without addressing reliability until now. This dissertation intends to develop a model based on machine learning that can be used to detect BC.

In order to be able to swiftly and cost-effectively identify potential cases of breast cancer. In this dissertation, very robust approaches for detecting breast cancer, particularly mastectomy and Wide Local Excision (WLE) were developed. BC datasets have been constructed, including magnetic resonance imaging (MRI) (DCE-MRI) stands for dynamic contrast-enhanced magnetic resonance imaging and mammography.

This dissertation intends to develop a model based on deep learning that can be used to detect breast cancer. It presents three main methods which can be categorized as follows:

This novel approach aims to classify breast cancer MRI images through a three-stage process: segmentation and feature extraction using five techniques it is (Scale-Invariant Feature Transform (Sift), Histogram of Oriented Gradients (HOG), Edge-Oriented Histogram (EOH), Local Binary Patterns (LBP), and Bag of Words (BoW)), and classification using six algorithms it is (K-Nearest Neighbors (KNN), Artificial Neural Network (ANN), Support Vector Machine

(SVM), AdaBoost, Decision Tree (DT), and Random Forest(RF)). The method demonstrated promising results, with 91.9% accuracy for images from Rizgary Hospital - Erbil and Hiwa Hospital - Sulaymaniyah, 97% accuracy on the ACRIN dataset, and 92.3% accuracy for breast cancer MRI images, highlighting its effectiveness in BC diagnosis via MRI imaging.

The second models, which are convolutional neural network (CNN), ResNet152V2, and Mask Region-based Convolutional Neural Network (Mask R-CNN), have been used to develop a cancer mammography image classification and recognition model from authentic images with less training time and computation cost but high accuracy and recall which would be the target of the experiments. It has been concluded that ResNet152V2 achieved a higher accuracy of 100% in recognition of the type of breast density and normal or abnormal images. A modified CNN has been used to determine whether the mammogram image is left or right. This model used Mask RCNN to differentiate between malignant and benign tumors and find the tumor size.

The third model uses different deep-learning approaches to increase the deeper features in breast cancer MRI and DCE_MRI images. This model has EfficientNetV2L, Mask R-CNN, Detectron2, and Detectron2 with Faster RCNN. In this model, we used Yolov7 instead of Mask RCNN. Has been concluded that Mask R-CNN achieved higher accuracy in recognition by more than 10% than YoloV7. This dissertation has been extended to the automatic detection of breast cancer for mastectomy or WLE using different deep-learning models.

In conclusion, incorporating deep learning models into breast cancer diagnostics yields promising outcomes in accuracy and efficiency. These models can potentially be helpful tools for radiologists and pathologists in detecting and classifying breast cancer.

Table of Contents

pages

List of Figure

pages

List of Table

pages

List of Abbreviation

Abbreviation	Definition
ACRIN	American College of Radiology's Imaging Network
ADBMD	Automatic Detection of Breast Cancer for Mastectomy Using Different Deep Learning Models
ANN	Artificial Neural Network
AUC	Area Under Curve
BC	Breast Cancer
BI-RADS	Breast Imaging–Reporting and Data System
BoW	Bag of Words
BTRD	Breast Tumor Recognition and Classification Density Type Using Different Deep Learning Models.
CAD	Computer-Aided Detection and/or Diagnosis
CNN	Convolutional Neural Network
DCE-MRI	Dynamic Contrast-Enhanced Magnetic Resonance Imaging
DCIS	Ductal Carcinoma in Situ
DL	Deep Learning
DT	Decision Tree
EOH	Edge-Oriented Histogram
ESHMRI	Erbil and Sulaymaniyah Hospital (MRI)

FN	False Negative
FP	False Positive
HOG	Histogram of Oriented Gradient
IDE	Integrated Development Environment
IHC	Immunohistochemistry
IOU	Intersection-Over-Union
JSON	JavaScript Object Notation
KNN	K-Nearest Neighbors
KRI	Kurdistan Region of Iraq
LBP	Local Binary Patterns
LCIS	Lobular Carcinoma in Situ
Mask R-CNN	Mask- Region-Based Convolutional Neural Network
MDT	Multidisciplinary Team
ML	Machine Learning
MRI	Magnetic Resonance Imaging
NAC	Neoadjuvant Chemotherapy
NAS	Neural Architecture Search
PACS	Picture Archiving and Communication System
PPV	Positive Predictive Value
PR	Positive Rate
R-CNN	Region Convolutional neural network
ReLU	Rectified Linear Units

RF	Random Forest
ROC	Receiver Operating Characteristics
RoI	Region of Interest
RPN	Region Proposal Network
SIFT	Scale-Invariant Feature Transform
SVM	Support Vector Machines
TN	True Negative
TP	True Positive
TPR	True Positive Rate
VIA	VGG Image Annotator
WDBC	Wisconsin Diagnostic Breast Cancer
WLE	Wide Local Excision
ZIHEM	Zheen International Hospital-Erbil (Mammography)

CHAPTER ONE

1 INTRODUCTION

1.1 Overview

Breast Cancer (BC) is the world's second-biggest cause of mortality, and sophisticated algorithms and procedures are required to forecast and categorize it. Cancer is an abnormal development of cells that can spread throughout the body. It is also called malignancy, and more than a hundred types of cancer have been identified notably, breast cancer (Benjelloun et al., 2018). Medical images depicting the human body's interior are used to diagnose diseases, particularly cancer.

Medical imaging is valuable for identifying different medical disorders and evaluating research results. Biomedical imaging is most important in managing cancer (Sethy et al., 2022) (L. Wang, 2017). Breast Tumor (BT) is one of the most prevalent tumors among females. Many women are projected to experience breast cancer over their lifetime (Abdel Rahman et al., 2020). BC can be identified early by using imaging techniques, allowing patients to receive the proper treatment and boosting their chances of survival.

Medical imaging techniques include diagnostic mammography, magnetic resonance imaging (MRI), Computed tomography (CT-Scan) breast, and ultrasound (Sivasangari et al., 2022). These tasks are designed to distinguish cancer from healthy breast tissues, which may yield valuable data for additional investigation (Loizidou et al., 2021). MRI is a commonly employed medical imaging technology for detecting and diagnosing breast cancer (Y. Kim et al., 2021). Additionally, MRI is performed on patients with breast cancer tumors in two instances. The initial MRI is conducted to confirm the presence of cancer. At the same time, the second MRI is carried out following the administration of

Neoadjuvant chemotherapy (NAC), explicitly using dynamic contrast-enhanced MRI (DCE-MRI).

In current medical practice, neoadjuvant therapy imaging for assessing the response of locally advanced breast cancer has emerged as the prevailing approach. The goal of this treatment is to minimize the size of the tumor prior to surgical removal (Ren et al., 2022). Quantitative imaging is essential in the NAC situation for determining how well the intact primary tumor responds to specific systemic medications (Jones et al., 2020).

Technology must be used to integrate pathology and radiology to prevent negative consequences (M. Wang & Chen, 2020). Computer-aided detection and diagnosis (CAD) systems are proposed to assist radiologists in visually screening mammograms to prevent misdiagnosis (Ting et al., 2019). CAD systems are used to classify malignant and benign masses. Deep learning (DL) has enabled researchers to design models that predict a person's chance of acquiring breast cancer before diagnosis (Hirra et al., 2021). These models can then analyze various data sources to find patterns and provide helpful risk assessments. Using deep learning methodologies in breast cancer diagnosis and therapy has significantly transformed the field (Alzubaidi et al., 2021).

Until now, researchers have been limited in their ability to identify this disease due to the reliance on public datasets. These datasets are often incomplete and may not include all of the necessary information for accurate diagnosis. Furthermore, these data sources can be expensive or difficult to access, further limiting research capabilities and progress toward a better understanding of this condition. This dissertation aims to generate a comprehensive dataset that examines different breast types' characteristics while incorporating neoadjuvant therapy in conjunction with MRI images. This aspect holds significant relevance within the context of the study. This study utilizes a variety of deep learning

models to effectively identify malignancies through the analysis of MRI, DCE-MRI, and mammography images. Several datasets have been created based on images collected in hospitals in Erbil and Suleimani. Two radiology doctors have confirmed this, and software has been used to correct and fix the images.

The main goal of this dissertation is to provide a comprehensive analysis of the current state of utilizing deep learning models for diagnosing breast cancer. It also explores the various strategies and solutions that can be used to improve the performance of this technology. The study's methodology is focused on developing a set of solutions commonly used in classifying images, like DL models. They are then tested to evaluate their performance against existing systems. A number of these will then be used in practice to improve the performance of the new technology.

In this dissertation, many automated breast tumor detection algorithms have been implemented. More importantly, the detection of breast cancer has been compared between many papers using different models.

1.2 Problem Statement

The development of accurate deep learning models for breast cancer diagnosis and classification has the potential to revolutionize healthcare, improving diagnostic accuracy and reducing workloads for radiologists. However, the challenge of data collection and annotation is a major barrier to progress.

One primary obstacle in training deep learning models for medical imaging is the need for large, labeled training datasets. Annotating medical imaging data is time-consuming and labor-intensive, requiring extensive expertise to eliminate human error. This poses a significant challenge for breast cancer diagnosis and

classification, as mammography, MRI, and DCE-MRI images can be complex and difficult to interpret, even for experienced radiologists.

A. The tedious and time-consuming task of manually annotating massive amounts of medical imaging data to eliminate human error is a major challenge for training deep-learning models to diagnose breast cancer from mammograms, and MRIs. This is because cancer lesions can appear anywhere and look different in different images.

B. Thus far, despite improved techniques, mislabeling of cancerous conditions has persisted because medical imaging data is complex and variable.

C. Several BC datasets are available online for the development of computer-aided detection (CADs), but not KRI Hospital cases, which pose challenges in their classification through deep learning models.

D. Detecting lesions within mammography images and identifying breast cancer subtypes C and D poses significant challenges. Consequently, the utilization of magnetic resonance imaging (MRI) emerges as an effective approach for accurately identifying tumors.

1.3 Objectives of the Study

The main objective of this dissertation is to identify and categorize the spatial extent of a malignant tumor in the breast. CAD has greatly revolutionized medicine by providing clinicians with a more thorough understanding of malignant tumors. Through a comprehensive examination of the image and a meticulous analysis of its many properties, medical professionals can precisely identify the specific regions impacted by cancer and ascertain the corresponding stage of the disease. The objectives of this dissertation are:

A. This dissertation goals to collect data on breast cancer from MRI, mammography, and DCE-MRI images.

B. In order to compare machine learning and deep learning algorithms to diagnose breast cancer disorders across various species.

C. To achieve precise detection of breast cancer in MRI images, the approach involves employing optimized machine learning techniques and multi-step feature extraction procedures. Furthermore, various classification algorithms are applied for the diagnosis of breast cancer.

D. In order to employ deep learning techniques to effectively categorize images from the testing dataset into various categories of breast cancer tumors or healthy images.

E. To gain expertise in the realm of medical image recognition, annotation, quantification, and computer vision orientation for effectively discerning relevant factors during the learning process.

1.4 Scope of the Study

This dissertation is done on BC images provided by the Ministry of Health's datasets. This dissertation uses breast cancer MRI, DCE-MRI, and mammography images as input images for classification, recognition, and detection. Numerous supervised ML methods can be used for to achieve the objective of image classification. Supervised machine learning techniques (KNN, DT, ANN, SVM, RF, and AdaBoost) and transfer deep learning convolutional neural networks (CNN, ResNet152V2, and EfficientNetV2L).

Also evaluates the performance of three different object detection models (Mask R-CNN, Detectron2, and Detectron2 with Faster R-CNN). It was determined which of the three models performed the best in a detection

comparison. By assisting two radiology doctors, have achieved our objective of reducing the error rate using datasets in this dissertation.

The dissertation has the potential to develop new methods for the classification, recognition, and detection of BC, which could help radiologists diagnose BC more accurately and efficiently.

1.5 Contribution

In addition to determining the best model for identifying and categorizing breast malignancies, this dissertation aims to establish the optimal method for detecting and classifying the disease. In this section, they will discuss the following main contributions to this dissertation:

1. Computer-aided classification and detection models can help radiologists identify and classify breast cancer lesions more accurately and efficiently. This can lead to earlier diagnosis and more effective treatment for patients.
2. The proposed model can accurately identify and classify breast cancers on mammograms, compare breast density types, and measure tumor size.
3. The proposed approach can accurately identify and classify malignant breasts on MRI images, aiding in mastectomy or wide local excision decisions.
4. The proposed model accurately identifies and classifies malignant BC on MRI images, including pre-and post- post-Neoadjuvant chemotherapy (NAC) treatment tumors, based on patterns of breast carcinoma.
5. Mask R-CNN and Detectron2 are powerful deep-learning models that can be used to achieve exceptional results in identifying malignant tumors due to their advanced architecture and features.

6. The proposed MRI and mammography models can automatically determine whether the breast is on the right or left side, which can aid in surgical planning and other treatments.

1.6 Thesis Layout

This dissertation is divided into five chapters and organized as follows: The first chapter gives an overview of the dissertation topic, problem statements, dissertation objectives, and dissertation organization.

The second chapter presents the literature review regarding fault detection and the theoretical background of algorithms. Based on the literature, theoretical machine-learning methods for breast cancer diagnosis are discussed. Also covered are deep-learning breast cancer diagnosis studies. This chapter covers the leading digital image processing components.

The third chapter covers research methodologies and frameworks. This chapter proposes the thesis's new breast cancer model-initial breast cancer detection using ML and DL algorithm performance. The chapter finishes with accuracy, confusion matrix, specificity, and sensitivity reviews.

Simulation implementation and numerical results are in chapter four. The results are compared to other research for a thorough analysis. The concluding and fifth chapters outline future work. This chapter also discusses research and development opportunities to enhance the proposed algorithms.

CHAPTER TWO

2 BACKGROUND AND LITERATURE REVIEW

2.1 Introduction

Cancer results from abnormal cell growth. This illness causes cells to develop tumors frequently visible on X-ray or mammography modalities regularly. Breast cancer is one of the foremost causes of death for women globally (Michael et al., 2021).

Mammography is among the most crucial and helpful tools for detecting breast cancer early (N. Cai et al., 2021). Adopting a low-energy technology to obtain visual images of the interior structure of breasts has been demonstrated as a trustworthy and vital screening technique. However, manually reviewing many mammograms takes time, and there is a 10%–30% mistake rate due to human factors (K. Zhou et al., 2022).

The early detection of breast cancer now relies heavily on the computer-aided detection system based on image processing. As a result, many preprocessing techniques have been recommended to improve the quality of mammograms and enable more precise analysis. Image processing is required to identify breast cancer accurately (Zhao et al., 2022).

The different machine learning techniques and technologies that are required for better breast cancer diagnosis are introduced in this chapter (Moy et al., 2020). The chapter also provides background information on breast cancer, including examples of the disease's forms and symptoms. The review of the literature was a type of analysis in which data from past studies was collected and compared. The technological advancements in this area have significantly changed how to approach image classification. The collected information enabled

the making of conclusions and the identification of challenges. These factors enabled the researcher to outline recommendations for improving DL, which can enhance the process of medical diagnostic imaging, especially in responding to the challenges involved.

2.2 Breast Cancer

Breast cancer is a form of cancer that develops from breast cells. Typically, breast cancer originates in the inner lining of milk ducts or the lobules that supply them with milk (American Cancer Society, 2022). A malignant tumor is capable of spreading to other areas of the body. Lobular carcinoma refers to breast cancer originating from the lobules, while ductal carcinoma refers to cancer originating from the ducts (Tamimi et al., 2016).

These factors can interact, further increasing the risk of cancer. For example, individuals with a family history of cancer and specific genetic mutations may be more susceptible to developing the disease if exposed to environmental carcinogens or engage in unhealthy lifestyle choices (Flavahan et al., 2017). When this uncontrolled cell development occurs in breast tissue, it is known as 'breast cancer.' The disease known as breast cancer is brought on by abnormal cell proliferation inside the breast's internal tissues (Runowicz et al., 2016). Generally, the breast is composed of an endocrine gland with adipose tissue protected by a structure of loose fibrous connective tissue, glandular tissue, and tubules connecting the lobes to the nipple (Mahmood et al., 2022).

2.2.1 Breast Tumors

Breast tumors can be divided into three categories: benign breast tumors, in situ breast cancer, and invasive breast cancer (Goh et al., 2021). Numerous terms describe the distinct subtypes of breast cancer (García Marcos, 2018). The precise breast cells that become malignant characterize the type of breast cancer. Varieties of breast cancer are determined by the afflicted breast area and cell type (Sivasangari et al., 2022). Ductal carcinoma in situ (DCIS) explicitly affects the breast's milk ducts, while lobular carcinoma in situ (LCIS) is found in the lobules responsible for producing milk. These types of cancer are considered non-invasive, as they have not spread beyond the site where they originated (Dawoud et al., 2022).

2.2.1.1 Benign Breast Tumors

It is referred to as invasive ductal cancer. It is the most prevalent form of breast cancer, accounting for approximately 80% of all cases detected by mammography (Goh et al., 2021). As the name indicates, these are noncancerous growths that cannot penetrate surrounding tissues or spread to other organs. In such cases, further tests like biopsies may be needed to accurately determine if the mass is benign or malignant (Webber et al., 2020).

2.2.1.2 Malignant Breast Cancer

Malignant mammary tumors can be divided into two categories: Invasive cancer is more aggressive and has a higher risk of spreading to other body parts.

On the other hand, noninvasive or in situ cancer is typically confined to the breast and has a lower risk of metastasis (L. Jiang, 2013). DCIS is the most prevalent noninvasive breast cancer characterized by abnormal cells confined to the milk ducts. In contrast, LCIS is less prevalent and involves abnormal cells in the breast lobules (J. Feng & Jiang, 2022) (Adusei, 2020). LC begins in the lobules of the breast glands that produce milk. It, like IDC, can spread (metastasize) to other body regions, as shown in Fig. 2. 1. (American Cancer Society, 2022).

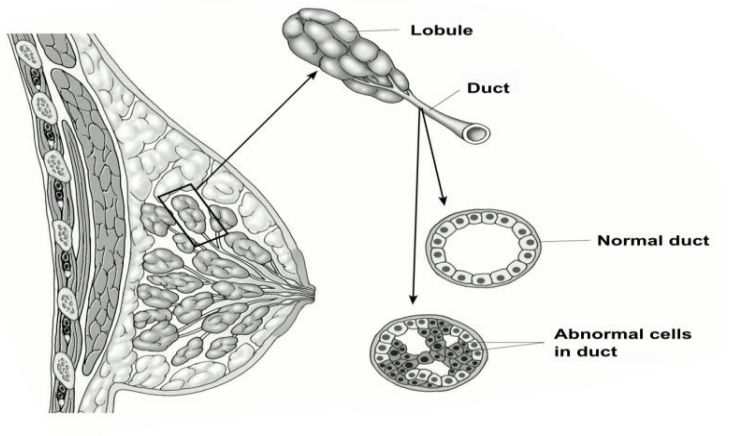

Figure 2.1 Ductal and lobular breast cancer (American Cancer Society, 2022).

Early detection of breast cancer improves treatment outcomes and survival rates significantly. Therefore, regular screenings and self-examinations are essential for detecting the disease in its earliest stages (Smith et al., 2018).

2.2.1.2.1 Mastectomy Breast Cancer

A *mastectomy* is a surgical procedure that removes the entire breast, which can effectively treat certain forms of breast cancer. It is often recommended for cases with a high risk of cancer spreading or recurring, as well as for individuals

with a strong family history of breast cancer (D. Y. Kim et al., 2022). Additionally, a mastectomy may also be considered for patients who prefer to remove the entire breast to reduce the chances of future cancer development (Khalil et al., 2020).

2.2.1.2.2 Wide Local Excision (WLE) Breast Cancer

A wide local excision (WLE) or lumpectomy is a surgical treatment that removes a small region of diseased or troublesome tissue while leaving a healthy margin. This method is typically used to treat breast and skin lesions but can be used on any body part. It could be challenging to decide between a mastectomy and a lumpectomy (Di Micco et al., 2017). Both techniques are equally effective in preventing breast cancer recurrence. A lumpectomy, however, is not an option for everyone with breast cancer, and some choose a mastectomy (Burbank, 2006).

2.3 Medical Image Models

Medical imaging is one of the growing standards for medical therapy for diseases such as cancer and many other ailments. Applying sophisticated machine learning algorithms and image processing methodologies to expedite the identification and diagnosis of tumors can enhance the precision of breast cancer diagnoses (Abas, 2022) (Latif et al., 2019). Any technology can provide specific information about the body part being examined or treated (Yassin et al., 2018). The primary objective of medical imaging research is to classify the precise positioning, measurements, and organ-specific attributes. This is done to extract usable information from vast quantities of data. As a result, several researchers concentrated on creating and analyzing medical images to classify the

overwhelming majority of diseases (Murtaza et al., 2020). In recent years, medicine has witnessed substantial advancements and notable contributions from artificial intelligence (AI) and machine learning, particularly in image processing (H. Cai et al., 2019). Medical imaging is well-recognized as a productive approach to detecting breast cancer. This diagnostic technique encompasses a diverse range of modalities, such as computed tomography (CT), mammography, positron emission tomography (PET), magnetic resonance imaging (MRI), duplex ultrasounds, and radiography (Y. Feng et al., 2018).

2.3.1 Mammography Image

Mammography is an early breast cancer diagnosis for women, allowing radiologists to check for anomalies and detect improvement (Al-masni et al., 2018). Due to its low radiation requirements, mammography poses fewer risks to patients. According to the American Cancer Society, a patient receiving radiation during an examination receives nearly as much radiation as someone receiving radiation from their surroundings over three months. A single reading, double reading, or application of CAD can be used for a patient and depends on the results being analyzed, as illustrated in Fig. 2. 2 (Xi et al., 2018). Research has demonstrated that film-screen and digital mammography are trustworthy and valuable for the early detection of breast cancer. Furthermore, it has been established that the utilization of breast tomosynthesis enhances the diagnostic accuracy of breast cancer and reduces the requirement for women to undergo further testing following an unfavorable examination result, as depicted in Table 2. 1 (Henriksen et al., 2019).

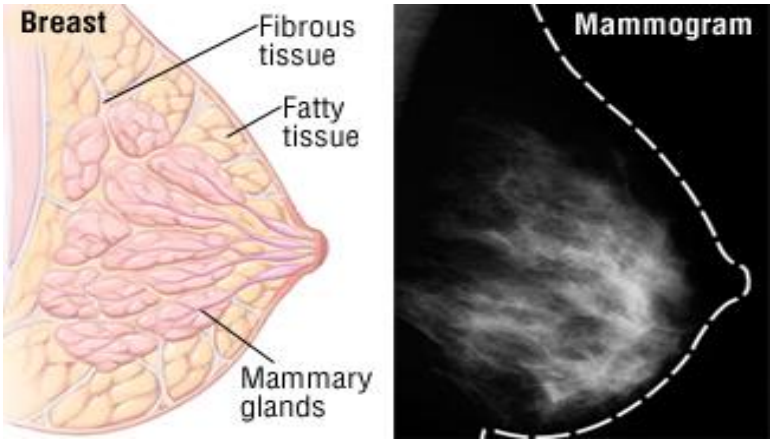

Figure 2.2 Mammography structure. (Henriksen et al., 2019).

Table 2.1 Comparison of mammography techniques

No.	Digital Mammography	Breast Tomosynthesis	Computer-Aided Detection and Diagnosis
1.	Less radiation	Less radiation	Less radiation
2.	Digital mammographic images	3 Dimensional images	Reviews digital mammographic images
3.	Uses electrons	digital x-ray	Computerized system
4.	Clear images	Highly Clear images	Highly Clear images
5.	Accurate	Highly accurate	Highly accurate

2.3.2 Magnetic Resonance Imaging (MRI)

Magnetic resonance imaging (MRI) is the most appealing alternative to mammography and another method for the early identification and diagnosis of

cancer cells. Some tumors mammography might miss can be found with MRI sensitivity (De Filippis et al., 2019). Moreover, MRI in discerning the phase of the illness enables radiologists and other healthcare practitioners to make informed decisions on the appropriate treatment strategies for individuals diagnosed with breast cancer (Qi et al., 2019). Using magnetic fields in MRI renders it devoid of any detrimental impacts on human physiology. Nevertheless, MRI is characterized by a somewhat lengthy execution time and incurs a significantly higher cost than mammography, exceeding it by more than tenfold. MRI employs magnetic fields rather than X-rays to generate exact transverse representations of three-dimensional structures, as depicted in Fig. 2. 3 (H. Feng et al., 2020).

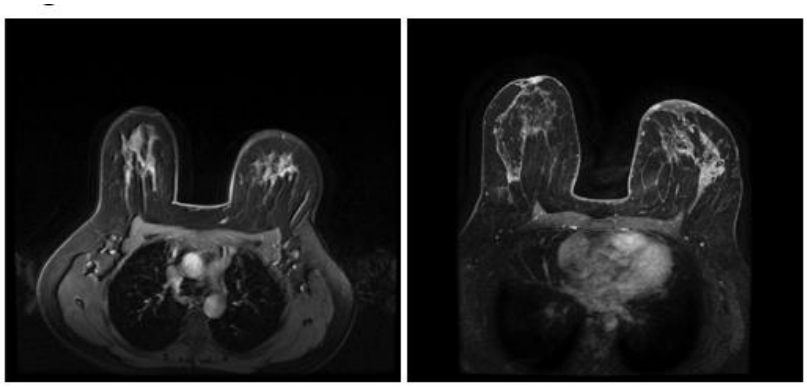

Figure 2.3 MRI image sample

2.3.3 Dynamic Contrast Enhanced MRI (DCE-MRI)

DCE-MRI is a valuable imaging technique for assessing breast cancer. Screening for breast cancer in high-risk women frequently involves using DCE-MRI. Furthermore, it can be used to gauge the extent of locally aggressive breast cancer and help plan for further rounds of treatment (neoadjuvant and adjuvant) (Conti et al., 2021). DCE-MRI significantly improves early breast cancer

identification, especially in highly susceptible individuals. It assesses vascular density, morphology, and aggressive characteristics, making it the preferred method in healthcare practice for high-resolution images of breast malignancies and vascular structures (Leithner et al., 2018), as shown in Fig. 2. 4.

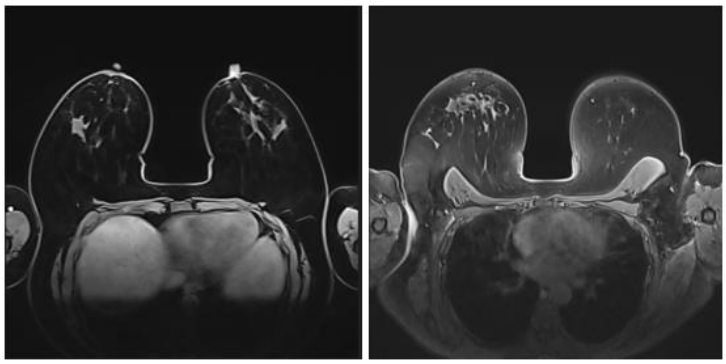

Figure 2.4 Pre-NAC and Post-NAC image sample

2.3.4 Available Datasets

Several datasets containing breast cancer images are available for training and testing models for various tasks, including cancer recognition. By leveraging these images, can build more comprehensive and accurate models that are better equipped to identify and diagnose potential cases of breast cancer in an increasingly efficient manner (Mendel et al., 2019). Furthermore, this approach allows us to leverage the expertise of healthcare professionals who have acquired extensive knowledge about different stages and types of breast cancers from their clinical experiences.

In this dissertation, two datasets have been sourced from the mentioned website (https://wiki.cancerimagingarchive.net), which hosts a comprehensive collection of cancer images from the human body.

2.4 Image Classification

Image categorization is an exciting subject that has progressed dramatically in recent years. Classification organizes data into categories using quantitative attributes. Data points must be classified as benign or malignant to detect breast cancer. The classification process involves training and assessment. The classifier is trained using feature vectors with class labels. Cases for the classifier to learn from are feature vectors. After learning to classify, the samples can evaluate a feature vector for an unexpected class. The final stage of the feature detection process for an image is the last step.

Feature categorization is a fundamental process in medical imaging, playing a critical role in identifying and detecting tumors. Additionally, this process finds use in many domains, such as robotics and voice recognition. Its primary function is classifying features into multiple groups based on diverse qualities (Chen et al., 2021). The competition results will be used to demonstrate advances in image recognition. These methods can be used to identify images of breast cancer.

2.4.1 Traditional Approach used for Breast Cancer Recognition

According to studies published in machine learning was used to diagnose breast cancer. Research in this area has been concerned chiefly with using machine-learning strategies for diagnosing and classifying breast cancer (Zheng et al., 2020). Among the many components of AI, machine learning is well acknowledged. It also stresses how complex knowledge is required for understanding diseases or infections through digital imaging. This finding highlights the significance of machine learning's role in the diagnosis of disease

(Abas, 2022) (Latif et al., 2019). ML encompasses various statistical analysis methods that undergo iterative improvement through training data to construct models capable of making autonomous predictions. In essence, the performance of computer programs exhibits automatic enhancement as a consequence of accumulated experience. Machine learning algorithms aim to construct a mathematical model accurately representing the dataset (Yassin et al., 2018). For the efficient process of medical diagnostic imaging, different types of ML techniques are considered essential.

This chapter analyzes machine learning for breast cancer imaging, analyzing medical diagnosis, challenges, and arguments from various sources and comparing researchers' perspectives (Sannasi Chakravarthy & Rajaguru, 2022). Machine learning challenges in breast cancer imaging are explained, focusing on the evolution of algorithms like SVM, KNN, ANN, DT, and RF for medical diagnostics (Quintanilla-Domínguez et al., 2018). The right strategy depends on the problem, dataset size, and feature complexity. Researchers often use feature engineering to preprocess data and extract useful features for improved performance (Esgario & Krohling, 2022). Machine learning algorithms like SVM are best for detecting breast cancer tumors, achieving the highest accuracy, and results appear in Fig. 2. 5 according to the best accuracy and depending on the datasets used for breast cancer.

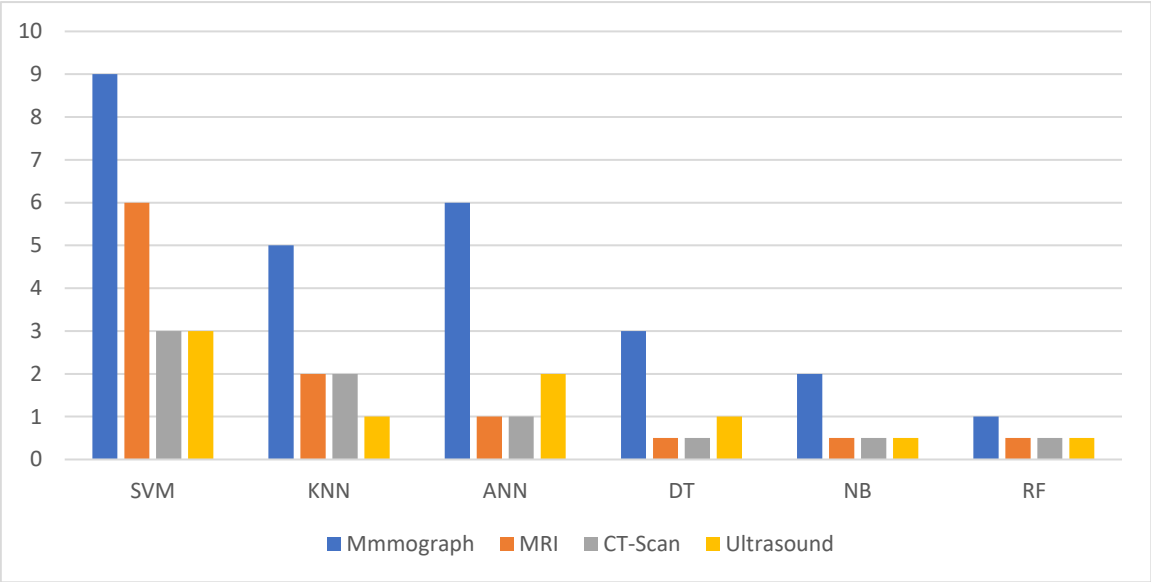

Figure 2.5 Machine learning employs several algorithms and image analysis techniques to detect breast cancer

2.4.1.1 Scale-Invariant Feature Transform (SIFT)

David Lowe developed the SIFT as a technique for extracting distinguishing visual characteristics. This method has four separate stages (Shiji et al., 2017). One of the first stages is locating important image points. The next step is computing visual descriptors, or features, in critical areas. The third stage assigns orientations, while the fourth refines important point positioning (Tang et al., 2022). The methodology defines an image as a collection of feature vectors unaffected by translation, scaling, or rotation (Sasikala et al., 2020). The process of extracting SIFT features is primarily distinguished by two critical parameters: the peak and edge threshold. The subsequent methods are the primary computational procedures employed to generate the collection of image features, as shown in Figure 2. 6 (Pei et al., 2018).

$$I(x, y, \sigma) = I(x, y) * G(x, y, \sigma) \quad \text{.....(2.1)}$$

In the first step scale-space of an image I (x, y, σ) is formed by convolving the image I (x, y) with a variable scale Gaussian (x, y, σ).

Establishing scale space is a fundamental concept in image processing and computer vision. The construction of a Gaussian pyramid involves the application of Gaussian smoothing to a pair of images, denoted as I (x, y). The point (x, y) is located within an M × N-sized region, and a series of s + 3 Gaussian images are constructed in the initial scale space.

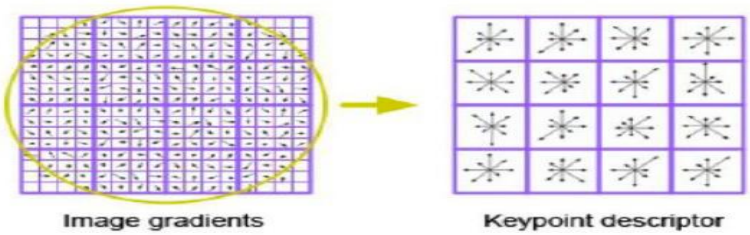

Figure 2.6 The SIFT descriptor generation (Adel et al., 2014).

2.4.1.2 Histogram of Oriented Gradients (HOG)

Dalal and Triggs developed the HOG approach to detect human bodies. However, it has since become one of the most popular descriptors in computer vision and pattern recognition (Pomponiu et al., 2014). The texture is vital for medical image identification. In computer image analysis, intensity and color are critical for classification, detection, and segmentation. This study extracted features using the HOG method. The computer vision community has successfully employed these features for object detection and localization. The HOG technique assumes that a highly sampled grid's histogram of local intensity gradients or edge directions may capture the local look and shape (Mu'jizah & Novitasari, 2021). The histogram of directed gradients uses intensity or edge directions to describe object appearance. The above feature is helpful for edges and corners since it

conveys more object shape information than flat regions, as shown in Figure 2. 7 (Kadhim & Kamil, 2022).

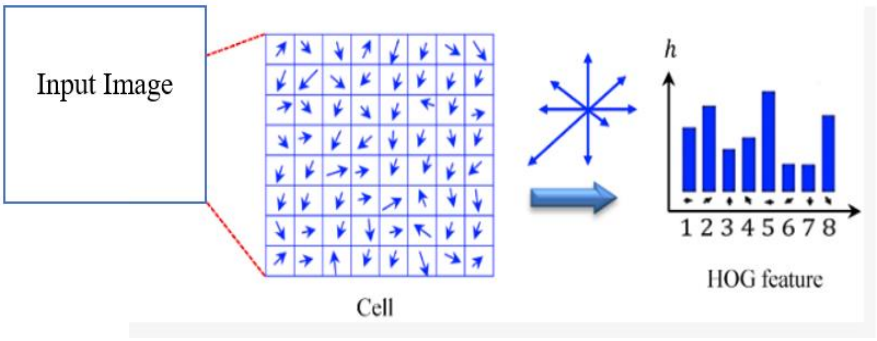

Figure 2.7 The process to extract HOG features (Bakheet & Al-Hamadi, 2021).

2.4.1.3 Edge Oriented Histogram (EOH)

The initial stage in creating EOH involves the calculation of descriptors by utilizing edge pixels surrounding each feature point. In contrast, EOH has a heightened sensitivity to intricate textures. The creation of EOH involves the utilization of edge direction, which is obtained by extracting edges from the image (Timotius & Setyawan, 2014). This information can then be employed as a characteristic feature of the image. The equation is employed to determine an edge.

$$m_{i,j} = \sqrt{Gx(i,j)^2 + G_y\,(i,j)^2} \quad \text{.....(2.2)}$$

$$G_x = \text{Sob1}(I_{ROI}), G_y = \text{Sob1}(I_{ROI}) \quad \text{.....(2.3)}$$

$m_{i,\,j}$: is the magnitude of the edge at pixel (i, j). Gx $(i, j)^2$: is the gradient of the image at pixel (i, j) in the x-direction. Gy $(i, j)^2$: is the gradient of the image at pixel (i, j) in the y-direction.

2.4.1.4 Local Binary Patterns (LBP)

The LBP technique is widely employed for extracting texture features in recognition algorithms. The features that have been obtained can be utilized to classify anomalies related to breast cancer in MRI images (L. Cai et al., 2015). Calculating the LBP code for a pixel in an image involves comparing the pixel and its neighboring pixels. The parameters P (number of neighbors) and R (relative distance) are user-defined variables that are utilized in the LBP algorithm to determine the radius of comparisons (Lenc & Kr, 2014). Determine the sign parameter of the adjacent pixel within the neighborhood. Applications that rely on image processing extensively employ this technique (Praveen et al., 2022). LBP uses a 3x3 block size, as seen in Fig. 2. 8. In this setup, the central pixel sets the surrounding pixels' threshold. The LBP code for a central pixel is calculated by encoding the threshold value in decimal. The LBP is mathematically defined as: (Naresh & Vani, 2015).

$$LBP_{P,R} = \sum_{P=0}^{P-1} S(g_p - g_c)2^p, S(x) = \begin{cases} 1, x \geq 0 \\ 0, x < 0 \end{cases} \quad \text{.....(2.4)}$$

$LBP_{P,\ R}$: is the LBP value for the central pixel. ***P*** is the number of neighboring pixels. ***R*** is the radius of the neighborhood. g_c is the gray level of the central pixel. g_p: is the gray level of the p-th neighboring pixel. S(x) is a step function that returns 0 if x is less than 0 and 1 if x is greater than or equal to 0. The step function S(x) is used to binarize the difference between the gray levels of the central pixel and its neighboring pixels. This means that the LBP value for a given pixel is a binary number that represents the local spatial pattern and gray scale contrast in the neighborhood of that pixel.

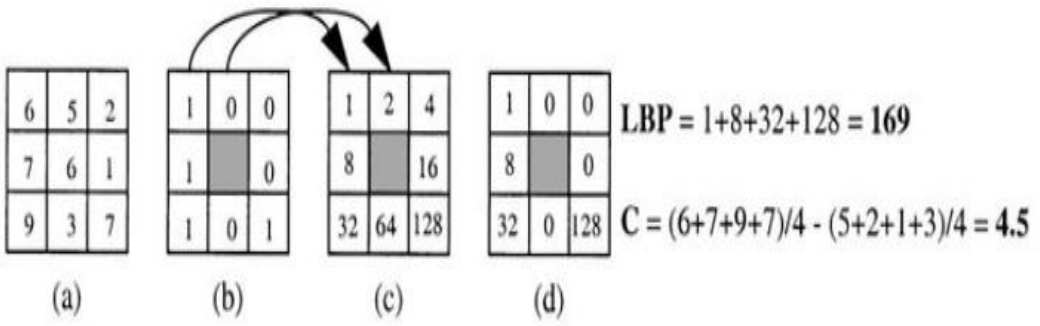

Figure 2.8 Calculating the original LBP (Naresh & Vani, 2015).

2.4.1.5 Bag of Words (BoW)

The BoW method extracts features from the text. These traits could be used to train machine-learning algorithms. This technology generates dictionaries from training data using k-means clustering. These dictionaries determine the BoW model and the final image depiction (Rojas et al., 2017). BoW feature coding is commonly used for the classification of medical and natural images. To construct the bag of words model, must be first cluster the retrieved local descriptors into a visual vocabulary (codebook) (Bardou et al., 2018). K-means is used to cluster the descriptor sets recovered from the training set into K-clusters.

2.4.1.6 K-Nearest Neighbor (KNN)

The k-nearest neighbor algorithm is a non-parametric and lazy approach (Tahmooresi et al., 2018). The selection of the nearest neighbors is determined by calculating the Euclidean distance between the x and y vectors, as specified in equation (2–6). The outcome of the K-nearest neighbors (KNN) algorithm exhibits variability when alternative values of K are employed. An elevated value of K

leads to class overlaps, whereas a reduced value of K results in increased computational requirements as shown in Fig. 2. 9 (Bharat et al., 2018).

Euclidean Distance= $\sqrt{\sum_{i=1}^{k}(X_i - Y_i)^2}$ ……..…..….(2.5)

k is the number of dimensions. X_i and Y_i are the coordinates of the two points in the i-th dimension.

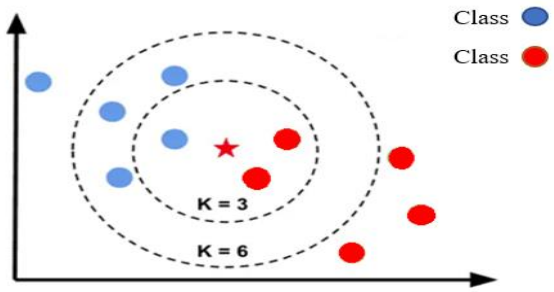

Figure 2.9 KNN illustration (Sharma et al., 2018).

2.4.1.7 Decision Tree (DT)

A decision tree is a tree-like model of choices and the results that can be expected from them (Tahmooresi et al., 2018). The decision tree is built utilizing the entropy or information gain of each attribute, and the core algorithm of a DT is termed iterative dichotomies (Silva et al., 2019) (Obaid et al., 2018). There are a number of parameters that can be used to tune a decision tree. Some of the most important parameters include. Decision tree using its max-depth, min-samples-leaf, and max-leaf-nodes properties (Magboo & Magboo, 2021).

$E(S) = \sum_{i=1}^{c} -P_i \ log_2 \ P_i$ ……...….(2.6)

c is the number of classes in the set. $\boldsymbol{P_i}$ is the probability of class ***i*** in the set.

2.4.1.8 Random Forests (RF)

Random forests are a type of ensemble method utilized for the purposes of categorization, regression, and differentiation in several domains (Benhassine et al., 2020). This approach involves the generation of decision trees during the training phase. Random forests are employed as a means to address the issue of overfitting that arises in decision trees (Islam et al., 2021). Random forests consist of an ensemble of decision trees, with the ultimate decision being determined using a majority voting mechanism (Sivasangari et al., 2022).

$$\text{MSE} = \frac{1}{N}\sum_{i=1}^{N} (fi - yi)^2 \quad \text{.....(2.7)}$$

where N represents the number of data points, fi represents the value returned by the model, and (yi) represents the actual value of the data point.

2.4.1.9 Artificial Neural Network (ANN)

An artificial neural network is a computational model that draws inspiration from biological processes. It is utilized for various applications, including pattern recognition, output prediction, clustering, and optimization (Hossam et al., 2018). One of the most widely recognized models in the field of neural networks is the artificial neural network (ANN), which offers several notable advantages. Furthermore, it has been utilized in the context of detecting malignant breast nodules, hence finding practical use in the field of clinical studies. The architecture comprises an input layer, one concealed layer and one output layer (Atrey et al., 2019).

$$Z=\text{Bias}+W_1X_1 +W_2X_2 + \ldots + W_nX_n \quad \text{.....(2.8)}$$

where Z represents the denotation of the above ANN graphic representation. W represents the weights or beta coefficients, X represents the independent variables or inputs, and the bias or intercept equals W_0 shown in Fig. 2. 10.

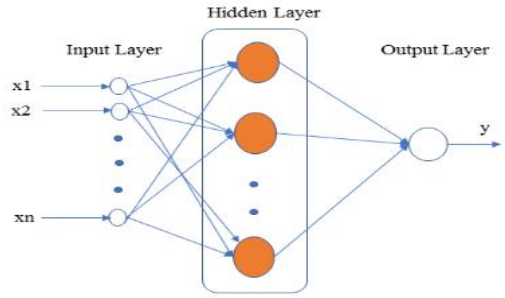

Figure 2.10 ANN architecture (Atrey et al., 2019).

2.4.1.10 Support Vector Machine (SVM)

The SVM is a machine learning technique that is founded on the principles of constrained minimization problems (M. Wang & Chen, 2020). In order to determine the maximum separation distance between objects, it is necessary to compute the dot products between the support vectors and the objects. The objective is to delineate the maximum separation between the classes (Acharya et al., 2020). The underlying principle involves transforming a non-linearly separable dataset into a higher-dimensional space, thereby enabling the identification of a hyperplane that effectively distinguishes the objects (Magboo & Magboo, 2021). The current study employs the kernel trick, specifically utilizing a radial basis kernel as depicted in the equation (Khourdifi & Bahaj, 2019).

$$h(x_i) = sign(\sum_{j=1}^{s} \alpha_j \ y_j K(x_j, x_i) \ + b) \quad \text{(2.9)}$$

$$K(v, v^-) \ = \ exp\ (\frac{||v - v^-||^2}{2\gamma^2}) \quad \text{(2.10)}$$

Here $\mathbf{x_i}$ is the (vector of values) to predict. The $\mathbf{x_j}$ are so-called support vectors which are a subset of the training data. The $\mathbf{y_j}$ is the class (-1 or +1) of each data $\mathbf{x_j}$. The $\boldsymbol{\alpha_j}$ are constants, one for each x_j. The b is a single numeric constant. Letter s is the number of support vectors. The $\boldsymbol{K}$ is a kernel function that accepts two vectors and returns a single number that is a measure of similarity between the two vectors, where 1.0 means identical and 0.0 means as different as possible.

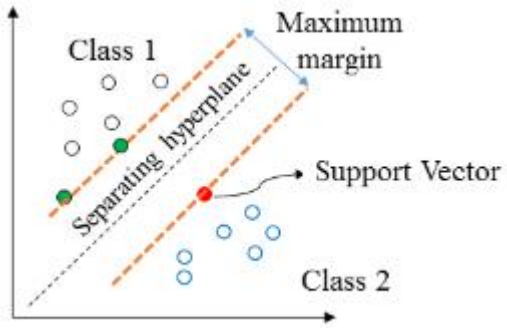

Figure 2.11 Support vector machine classification schemes (Atrey et al., 2019).

2.4.1.11 AdaBoost

The present approach is utilized for the prediction of breast cancer's presence through the implementation of regression and classification techniques (Senkamalavalli, 2017). The integration of all weak learners into a single powerful rule facilitates the transformation of weak learners into strong learners. The algorithm acquires the weight of the node and iteratively modifies it until it achieves precise outcomes. However, it is still vulnerable to variations in feature quality and the presence of noise (Tahmooresi et al., 2018).

$$H(x)=sign\left(\sum_{i=1}^{T}\alpha_t\ h_t\ (x)\right) \quad \text{.....(2.11)}$$

T is the number of weak learners. ***αt*** is the weight of the *t*-th weak learner. ***ht*** (*x*) is the prediction of the *t*-th weak learner. The sign function is used to

convert the weighted sum of the weak learner predictions into a binary classification decision.

2.4.2 Deep Learning Approaches

Deep learning (DL) is a subfield of machine learning that thinks on intricate image feature hierarchies. DL algorithms use multi layers neural networks to generate hierarchical features, allowing them to practice with millions of images. DL has gained popularity in image segmentation and classification and uses neural networks for learning and data forecasting (Abbas, 2016). The ability to produce results revealed that the neural network is capable of achieving a high degree of accuracy and a low rate of false-negative analysis. Deep-learning methodologies and convolutional neural networks (CNNs) are among the most intriguing deep-learning techniques (Dargan et al., 2020). CNN is a cutting-edge technique for image processing that employs local connection patterns and shared weights. Widespread use of deep convolutional networks in medical image analysis (Reig et al., 2020).

A CNN is a type of deep neural network commonly utilized in deep learning for the purpose of classifying visual images. CNN is a computational model that has a feed-forward architecture and possesses the ability to extract the topological characteristics of an image. CNNs are recognized as multilayer models based on perceptron's (Alzubaidi et al., 2021). CNN is comparable to neural networks in that it consists of layers: entirely linked, pooling, and convolutional. Each stratum has its own distinct function.

2.4.2.1 Convolutional Layer

The convolutional layer learns images' features by preserving pixels' spatial relationships and using filters. Images are divided into squares, where filters are estimated based on pixels' values. These filters assess intensities by multiplying pixels in the input image area and summating them. They are synchronized with image depth, such as using three filters for RGB images (Houssein et al., 2021).

The size of the convolution layer is governed by the parameters of stride, depth, and padding. The depth of the convolution layer is influenced by the characteristics of the raw images or input data. Zeros can be used to pad the features in the input layer in order to preserve the proportion and size of the output (Roslidar et al., 2019). The input array positions are filtered to build an activation map. The dimension of the output of a convolutional layer is determined by:

$$O = \frac{W - K + 2P}{S + 1} \quad \text{.....(2.12)}$$

In the given context, the symbol O denotes the output height or width, whereas W denotes the input height or width. The symbol K represents the filter size, P represents the padding, and S represents the stride. Figure 2. 12 depicts an illustrative representation of a CIFAR-10 image input image with dimensions of 32x32x3. The figure also showcases the volume of neurons present in the initial convolutional layer, along with the corresponding neurons. The equation presented below is utilized for the computation of the properties associated with the convolutional layers.

$$y^{l}_{n} = \int l \left(\sum m \longrightarrow^{l}_{n} y^{l-1}_{m)}\right) \quad \text{.....(2.13)}$$

where y^{l}_{n} is the n^{th} feature map of l-layer, $m \longrightarrow^{l}_{n}$ n is the C-kernel for feature extraction from l-layer, and y^{l-1}_{m} is the characteristic pattern linked to layer-l (Chen et al., 2021).

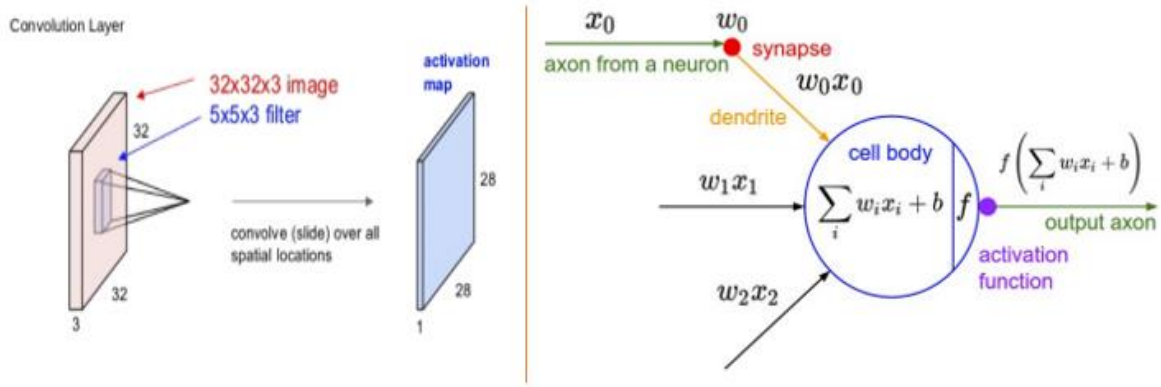

Figure 2.12 An illustration is shown, showcasing the input of a CIFAR-10 image with dimensions of 32x32x3. Additionally, the volume of neurons in the initial Convolutional layer, as well as the number of neurons (Abdelbaki, 2019).

2.4.2.2 Rectified Linear Units (ReLU) Layer

After each convolution layer, non-linearity is added. ReLU outperforms sigmoid and tanh functions without sacrificing precision. This layer also addresses the problem of vanishing gradients. As the gradient caused by back-propagation decreases exponentially with layer depth, the lower layers train exponentially more slowly (Alzubaidi et al., 2021). This is how the ReLU function is defined:

$$f(x) = \max(0, x) \quad \text{.....(2.14)}$$

$\boldsymbol{X}$ represents the input to the ReLU activation function. The ReLU function outputs the input value directly if it is positive, and otherwise outputs zero. This

means that the ReLU function is a non-linear function, which is important for training deep neural networks.

2.4.2.3 Layer of Pooling

It is sometimes referred to as the down-sampling layer. It applies a given function to a given size filter, advances through the preceding layer's input, and employs a given size filter. In a max-pooling layer, for example, the maximum of all filter values is produced. In addition to the conventional pooling layers, there are alternative types of pooling layers, namely average pooling and L2-norm pooling. This stratum serves two functions. One, by reducing the number of weight parameters, reduces the quantity of necessary calculations (Desai & Shah, 2021). It also eliminates overfitting in the model. The max-pooling illustration is depicted in Fig. 2. 13 below.

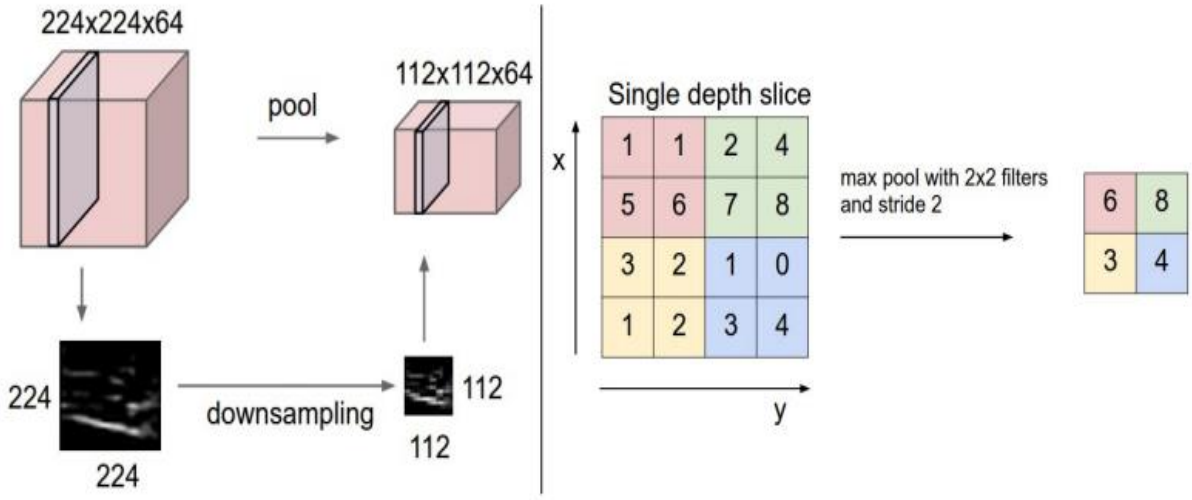

Figure 2.13 Layer of pooling CNN

Left: The [224x224x64] input volume is aggregated with filter size 2 and Stride 2 to produce the [112x112x64] output volume. Right: The most frequent down sampling operation is max, which gives rise to max Pooling, which is illustrated with a stride of 2 here. Each maximal value is divided by four integers (a 2 x 2 square) (Abdelbaki, 2019).

2.4.2.4 Dropout Layers

This layer assists in addressing the issue of overfitting. After training the network to execute on fresh samples, the weight and parameters are adjusted to the training examples. This layer removes a random activation set from another layer by setting its values to zero.

As with a typical neural network (multilayer perceptron), these unit layers are connected to each unit in the layer beneath them. Architecture of CNN: CNN's effectiveness and efficiency are significantly influenced by its architecture. Figure 2. 14 depicts CNN's architecture (Zhu et al., 2023).

The method is efficient and widely utilized in numerous computer vision applications. The CNN network has three primary layers: the convolutional layer, the pooling layer, and the fully connected layer. Each stratum is responsible for a variety of tasks. Multiple 2D matrices are considered for the input and output of the convolutional layer when classifying images. There is no restriction on the number of input and output matrices (Qader et al., 2022). Table 2. 2 illustrates the Configuration of the model used in their research.

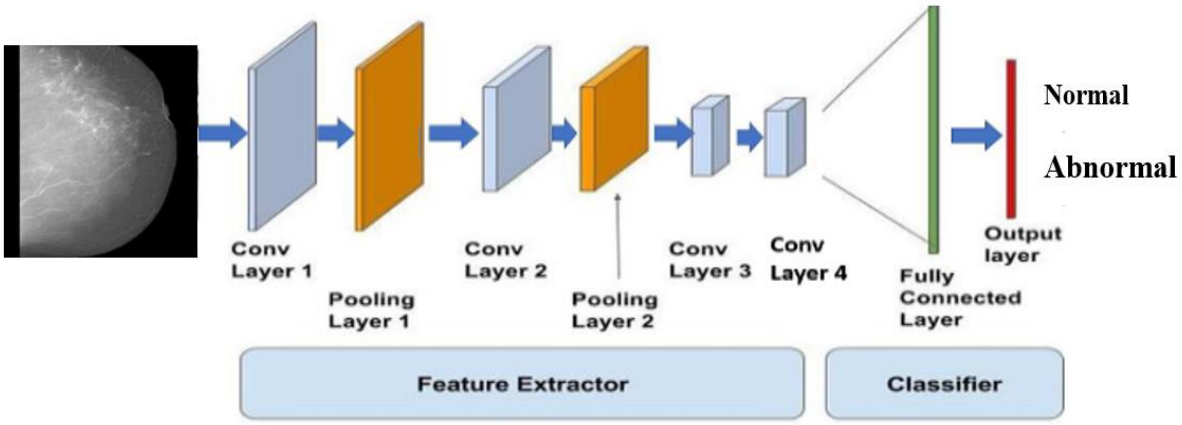

Figure 2.14 The architecture of the CNN (Kumeda et al., 2019).

Table 2.2 CNN model configuration (Howard et al., 2017).

No.	Layer	Filter size, Stride	Output
1	Input Conv ReLU Max-Pool	- 3x3,1 - 2x2,1	237x237x1 236x236x32 236x236x32 118x118x32
2	Conv ReLU Max-pool	3x3,1 - 2x2,1	116x116x64 56x56x64 58x58x64
3	Conv ReLU Max-pool	3x3,1 - 2x2,1	56x56x64 56x56x64 28x28x64
4	Conv ReLU Max-pool	5x5,1 - 2x2,1	24x24x64 24x24x64 12x12x64
5	Conv ReLU Max-pool	3x3,1 - 2x2,1	10x10x64 5x5x64
6	FC ReLU+Drop	- -	64 64
7	FC Softmax	- -	1 1

2.5 Breast Cancer Recognition Using Deep Learning CNN

Using convolutional neural networks to detect BC is an essential application of deep learning in the medical field. CNNs excel at image recognition tasks, making them ideal for analyzing mammograms and MRI breast images for BC detection. Due to the increasing significance of BC detection in numerous applications ML has been developed.

The complexity of breast cancer detection systems is attributable to the various factors that influence their accuracy, such as the unknown location of the tumor, the type of breast based on its density, and the diversity of breast tumor types. To achieve cutting-edge results, it is recommended to investigate the most recent research and best practices in medical image recognition. Since the field of deep learning is perpetually evolving and new advancements may have occurred after my knowledge it is recommended to investigate the most recent research and best practices in this area. The focus of this thesis is on transferring deep learning convolutional neural networks (CNN, ResNet152V2, and EfficientNetV2L). In addition to the above, it also evaluated the performance of different object detection models (R-CNN, Detectron2, Mask R-CNN, and Detectron2 with Faster R-CNN).

2.5.1 ResNet152V2

ResNet152V2 is a deep CNN architecture with 152 layers that was recently introduced. For experiments, 1000-class ImageNet-trained models of these networks have been pre-trained. Medical imaging applications have recently encountered widespread success with architecture. In the bottle-neck blocks that necessitate down sampling, v1 has stride = 2 in the initial 1x1 convolution, while

v2 has stride = 2 in the 3x3 convolution. Due to this distinction, ResNet152V2 is marginally more accurate than other models. The ResNet model was trained on ImageNet-1K at 224x224 resolution. In the paper Deep Residual Learning for Image Recognition, it was introduced. ResNet bypasses multiple levels of convolution simultaneously by utilizing residual blocks with skip connections between layers. It has been determined that this architecture is effective for providing a compact representation of input images and enhancing classification task performance by accelerating the convergence of a larger number of deep layers (Praveen et al., 2022).

Resnet utilized skip connections, also referred to as rapid forward connections. Before activating the ReLU, it is the principle of feeding previous levels to deeper layers. This bypass link or short route reduces the network's vanishing gradient vulnerability. The residual or identity block of Resnet is equipped with both a forward and a fast-forward link. Numerous residual units are stacked in Resnet (Bilal et al., 2022). These units are denoted as follows:

$W_l = \{W_{l,k|1\leq k\leq K}\}$ ……..……...(2.15)

$Y_l = h(x_l) + \int (x_l, W_l)$ ……..……..……(2.16)

$X_{l+1} = \int (12)(y_l)$……..……(2.17)

xl is the input variable, and xl+1 is the output of the lth unit. K is the total number of residual units. **F** is a residual function, f is a ReLU activation, and Wl is the weight and bias for the lth residual unit. The underlying identity map signal is h (xl) = xl. The objective is to learn the **F** residual function for h (xl) using h (xl) = xl, which was accomplished by means of a skip connection. v2 is enhanced by the addition of a conduit for information propagation within residual blocks and the entire network. For h (xl) and f (yl), which are both identity mappings, the

information could be disseminated throughout the entire network. The preceding two configurations greatly enhanced network performance. For a unit L that is deeper than unit l, Figure 2. 15 depicts the specific architecture of the Resnet-v2 network that has been employed.

$X_L = X_1 + \sum_{i=1}^{L-1} F\ (x_{i\ ,} W_i\ )$ ……..……...(2.18)

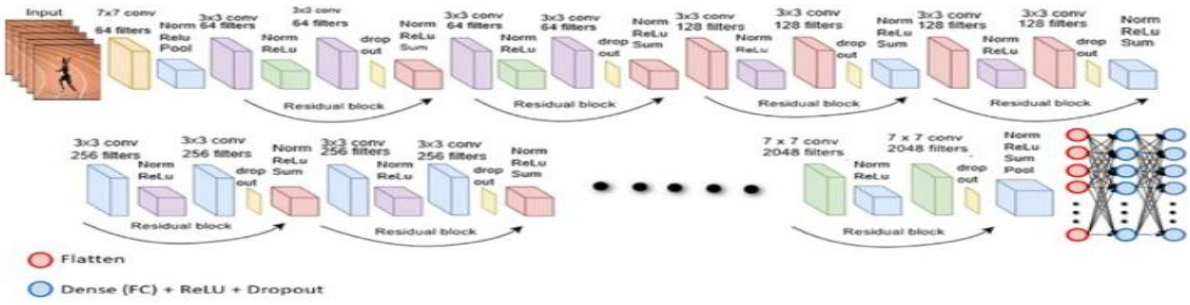

Figure 2.15 ResNet101V2 and ResNet152V2 architectures with additional layers inserted at the end for UCF-101 dataset fine-tuning (Bilal et al., 2022).

2.5.2 EfficientNetV2L

EfficientNet is a family model developed from a neural architecture search-based baseline model. Numerous researchers have attempted to scale the breadth of the network, the depth of the network, and the image resolution in order to improve performance. However, none of them define how to proportionally balance all the dimensions (Putra et al., 2020).

EfficientNetV2L, in contrast to its predecessors, is a convolutional neural network that exhibits enhanced training efficiency and improved parameter utilization. The aforementioned models exhibit reduced dimensions and enhanced speed in comparison to the majority of contemporary state-of-the-art models. The presented CNN model demonstrates that despite the widespread adoption of vision

transformers in the field of computer vision, which have exhibited superior accuracy compared to other convolutional neural networks (CNNs), the utilization of well-designed CNN models coupled with enhanced training techniques can still yield faster and superior outcomes in comparison to transformers. This further substantiates the enduring significance and relevance of CNNs in the domain of computer vision (Nayak et al., 2022). The fundamental component of the network architecture is the mobile inverted bottleneck (MBConv) layer, as initially proposed by the author. Figure 2. 16 presents the visual representation of the baseline model known as Efficient Net (Tan et al., 2019).

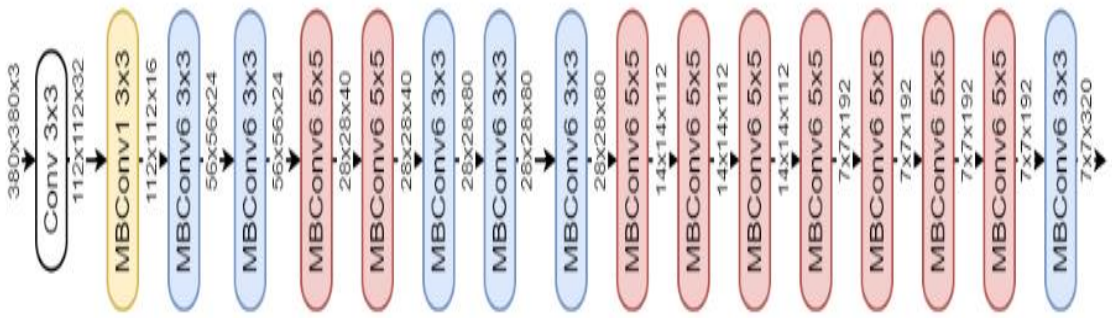

Figure 2.16 The architecture of EfficientNet (Putra et al., 2020).

Displays Table 2. 3, the performance comparison, where models tagged with 21k are pretrained compared to the recent that are specially optimized for GPUs, our EfficientNetV2-L achieves improves top-1 accuracy by 1.5% (85.3% vs. 86.8%) better accuracy with 2.8x faster inference speed.

Table 2.3 EfficientNetV2 Performance Results on ImageNet(Tan & Le, 2021).

Model		Top-1 Acc.	Parameters	FLOPs	Infer-time(ms)	Train-time(hours)
ConvNets (ours)	EfficientNetV2-S	83.9%	22M	8.8B	24	7.1
	EfficientNetV2-M	85.1%	54 M	24 B	57	13
	EfficientNetV2-L	85.3%	120 M	53 B	98	24
	EfficientNetV2-S(21K)	84.9%	22 M	8.8 B	24	9.0
	EfficientNetV2-M(21K)	86.2%	54 M	24 B	57	15
	EfficientNetV2-L (21K)	86.8%	120 M	53 B	98	26
	EfficientNetV2-XL (21k)	87.3%	208 M	94 B	-	45

2.5.3 Region Convolutional Neural Network (R-CNN)

R-CNN, a CNN-based object identification system aiming to provide a high-performance solution, was presented. They discovered that it may be more successful than low-level characteristics like histogram of oriented gradients. The pipeline, object detection, and query are the three components of the system (Girshick et al., 2014).

R-CNN provides region recommendations based on a filtered search that can be used to identify a variety of objects. Then, AlexNet is utilized to extract 4096-dimensional feature vectors from each region. The system's architecture is identical to that of the prior iteration. The only modification to the architecture is the number of units in the stratum of categorization. After the feature vectors have been extracted, they are classified using various statistical methods, such as

SVMs. R-CNN outperformed over all. in the 2013 ILSVRC data set. The Region Proposal Network (RPN) is a second alternative that is proposed. In 2015, Ren and colleagues proposed a two-stage method that generates more precise area proposals. In the initial phase, an image is sent to an RPN, which processes it using the intersection-over-union (IOU) technique (Girshick, 2015).

The second step is creating box ideas from the same feature map. The matching class probability and bounding box predict these thoughts. R-CNN has helped build two-stage detectors, but its time and resource needs make it unsuitable for future uses. The study also found that the quicker R-CNN model could increase area proposal network performance by giving more accurate cancer information.

2.5.4 Mask Region-based Convolutional Neural Network (Mask R-CNN)

The authors of the mask R-CNN framework presented a novel method for object instance segmentation that is intended to improve the performance of natural image recognition. Since the mask R-CNN is an expansion and enhancement of the Faster R-CNN, it is the most sophisticated neural network and is primarily employed for segmentation (Chiao et al., 2019).

Mask R-CNN is typically used for object detection, but since it can be generalized across a variety of datasets, as indicated in their initial research, it is also an excellent option for the vast majority of medical image analysis-based research. Previously, a faster R-CNN was utilized for drawing bounding frames and classifying the input image. Mask R-CNN is an enhanced variant of Faster R-CNN with the introduction of mask R-CNN, which takes the entire architecture of a Faster R-CNN and adds a second branch for object mask prediction. Mask R-CNN is easily trainable and applicable to a significant number of other datasets

(Zhang et al., 2020). In 2016, the mask R-CNN platform was able to outperform all single-model submissions in the annual COCO Challenge, a significant object recognition competition (Hassan & Talaa, 2022). Mask R-CNN is a technique for object recognition and segmentation. It can construct a bounding box for the target object as well as designate and categorize whether the pixels in the bounding box belong to the object or not, enabling the identification of the object, the marking of its boundary, and the detection of critical spots (Soltani et al., 2021).

In contrast, the mask-RCNN framework generates segmentation masks using a region proposal network. It employs the faster-RCNN strategy to extract features, followed by this region proposal network and an operation known as ROI-Pooling to generate outputs of standardized quantities that can be used as input to a classifier. Object detection and segmentation are techniques used to identify distinct elements in a image and generate a bounding box around a specific object. Mask R-CNN is a technique for object recognition and segmentation. Mask R-CNN provides a broad context for concurrent bulk discovery and segmentation (Min et al., 2020).

The mask R-CNN framework differs from the faster R-CNN framework in that the ROI-Pooling operation is replaced with ROI Align. It then adds a network head, which is a small fully convolutional network, to execute the required segmentations of instances. The network-head-generated segmentation masks are then separated from the class predictions. The network administrator then makes their own predictions regarding the masque (Chiao et al., 2019).

The segmentation of the region candidates is carried out concurrently by the FCN. The multi-task loss function of Mask R-CNN is shown in equation 1.

$$L = Lclass + Lbox + Lmsk \quad (2.19)$$

where L_{class} is the classification loss and L_{bbox} is the bounding box regression loss. The mask loss L_{msk} is defined as the binary cross entropy loss with a per-pixel sigmoid activation.

Where $L_{class} + L_{box}$ are identified the same as in Faster R-CNN, $L_{class} + L_{box}$ are defined as:

$$L_{class} + L_{box} = \frac{1}{N_{cls}} \sum_i L_{cls}(P_i, P_i) + \frac{1}{N_{box}} \sum_i P_i \, L_1^{smooth}(t_i - t_i^*) \quad \text{.....(2.20)}$$

$$L_{cls}(\{P_i, P_i^*\}) = P_i^* \, log P_i^* - (1 - P_i^*) \log(1 - P_i^*) \quad \text{..... (2.21)}$$

And the L_{mask} is the average binary cross-entropy loss:

$$L_{mask} = -\frac{1}{m^2} \sum_{1 \le i,j \le m} [\, y_{ij} \log o \, y_{ij}^k + (1 - y_{ij}) \log (1 - o y_{ij}^k)] \quad \text{.....(2.22)}$$

The framework's backbone network is modeled after a network developed specifically for image analysis, such as ResNet-101 or ResNet-50. The multi-scale and hierarchical properties of these networks are utilized to provide advantageous features such as semantic segmentation and object recognition. As a rule, a fully convolutional neural network serves as the backbone of a feature pyramid network. It can effectively identify objects and is frequently instructed. Figure 2. 17 depicts the algorithm for mask R-CNN (Gonzalez et al., 2019).

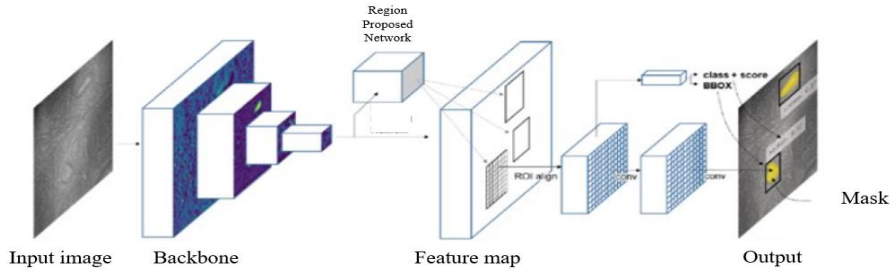

Figure 2.17 Architecture of mask R-CNN for instance segmentation (Hubert-moy et al., 2021).

2.5.5 Detectron2

Detectron2 is widely recognized as a highly potent and effective toolkit for deep learning in the field of visual perception. The design of the system prioritizes flexibility, allowing for seamless transitions between various tasks, including object detection, instance segmentation, and person key point detection (Ahmad & Mouiad, 2021).

The instance detection strategy involves the utilization of Detectron2, a contemporary open-source stance segmentation technology developed by Facebook AI Research. In this study, have been employed the Mask R-CNN with Feature Pyramid Network (Base-R-CNN FPN) as the bounding box detector. Furthermore, have been expanded its functionality to include the Mask R-CNN for creating the segmentation mask within the Detectron2 framework. Hence, the network can be described as a two-stage architecture consisting of three primary components: the backbone network, the Region Proposal Network (RPN), and the ROI head, as depicted in Figure 2. 18.

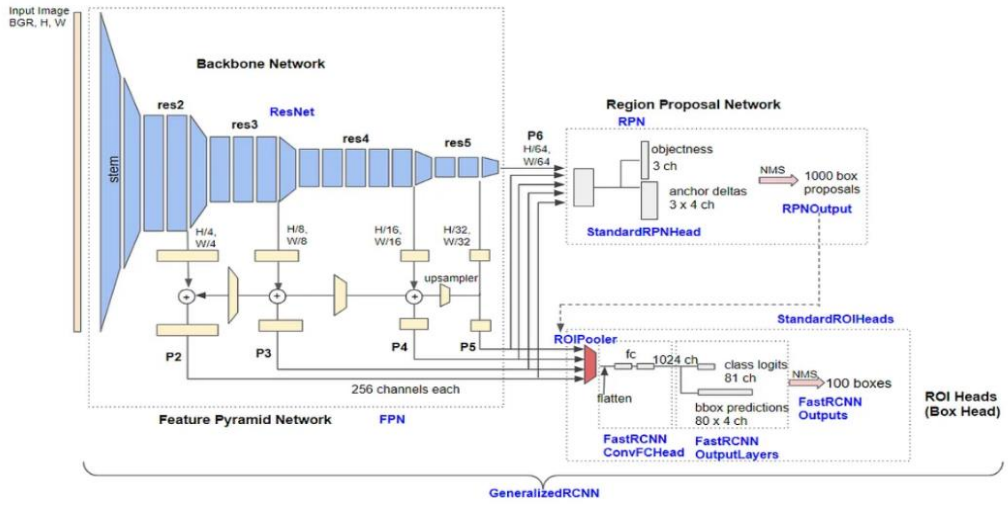

Figure 2.18 The schematic architecture of Detecron2 has been modified (Y. Wu et al., 2019).

The meta-architecture of the network is depicted in the diagram above. As can be seen, it contains three blocks:

1. Backbone Network: extracts feature maps at different scales from the image input. P2 (1/4 scale), P3 (1/8), P4 (1/16), P5 (1/32) and P6 (1/64) are the output values of Base-RCNN-FPN. The output feature of non-FPN ('C4') architecture is restricted to 1/16 scale.

2. The Region Proposal Network recognizes object regions using multi-scale characteristics. 1000 box suggestions with confidence scores are generated by default.

3. Box Head: divides and warps feature maps into multiple fixed-size features using proposed boxes and obtains fine tuned box positions and classification results through fully-connected layers. Lastly, using non-maximum suppression (NMS), 100 cells are (by default) filtered out. Box heads are one of the subclasses of ROI heads. For instance, Mask R-CNN includes additional ROI heads, such as a mask head (Sarker et al., 2021).

The feature maps in this study were obtained by employing the ResNet101 architecture with FPN as the backbone network. The ResNet101 model consists of a stem block and four bottleneck blocks. The stem block, which consists of 77 convolution layers with a stride of 2, is used to process the input image. Subsequently, a max-pooling layer with a stride of 2 is employed to further down-sample the input image. The output feature map of the stem block is denoted as 64 H/W W/4, where H and W represent the height and width of the input image, respectively. The four bottleneck blocks from the original ResNet architecture proposal are utilized in this model. Additionally, the FPN incorporates the four output feature maps from the ResNet bottleneck blocks (res1, res2, res3, and res4), as well as the lateral and output convolution layers (Pham et al., 2020).

2.5.6 Faster R-CNN with Detectron2

Faster R-CNN is an object recognition model that improves upon Fast R-CNN by combining a region proposal network (RPN) with the CNN model. The RPN and the detection network exchange full-image convolutional characteristics, allowing for virtually cost-free region recommendations. It is a fully convolutional network that predicts object limits and objectless scores at every location simultaneously. The RPN is trained from start to finish to provide Fast R-CNN with high-quality region suggestions for detection. R-CNNs are designed to locate an object within an image by suggesting possible regions of interest and subsequently classifying them (Pratiwi & Sari, 2022).

The faster RCNN algorithm is a relatively new development that builds upon the R-CNN architecture. Also, this algorithm was introduced in 2015 with the primary aim of optimizing computational efficiency compared to its predecessor. The efficacy of this algorithm in object detection has been demonstrated through its effective application in many scenarios. The topics of interest include face detection, driver's cell phone usage, and hands-on steering wheel detection (H. Jiang & Learned-Miller, 2017).

R-CNNs are utilized to locate an object within an image by proposing plausible regions of interest and then classifying them. The object detection model, faster R-CNN, is an extension of the R-CNN architecture. It consists of the following main elements: fast backbone network, region proposal network (RPN), Region of Interest (RoI) Pooling, RoI Pooling. The Head of R-CNN depicted in Fig. 2. 19 (Reiazi et al., 2018). According to the most recent update in September 2021, Faster R-CNN is a prevalent model for object identification, whereas Detectron2 is a deep learning framework created by Facebook AI Research (FAIR) that offers implementations for several computer vision applications,

including object detection. Detectron2 is a state-of-the-art deep learning framework that offers a comprehensive implementation of the Faster R-CNN algorithm, along with various alternative models for object detection. The process of integrating faster R-CNN with Detectron2 encompasses three main steps: leveraging the backbone of Detectron2, constructing faster R-CNN on the foundation of Detectron2, and conducting training and inference procedures.

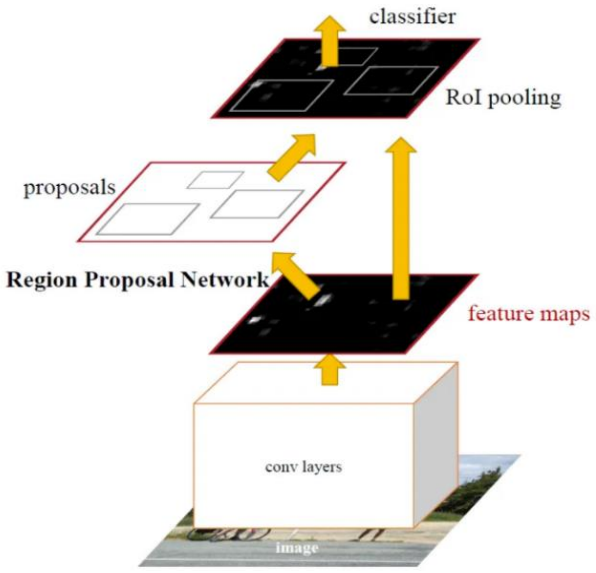

Figure 2.19 Faster RCNN network (Makone, 2020).

Using small datasets to train CNNs limits their efficacy, including overfitting, as CNNs require large-scale training data. This issue is resolved by transfer learning, which also provides a solution for small-scale datasets. Transfer learning is a technique for training deep learning networks on a large number of datasets using models that have been pre-trained on generalized datasets. This method fine-tunes models on target datasets by utilizing pre-trained and frozen weights. If the dataset is unique, additional model layers are desired. This method overcomes the limitations associated with training entire networks on large

datasets. Data augmentation is a technique that employs image modifications, such as scaling, rotation, skewing, flipping, or cropping, in conjunction with asymmetric feature-based transfer learning methods to expand datasets. Layer by layer, the feature data in a CNN structure varies. High-layer characteristics contain more semantic data but less specific data than low-layer characteristics (Chen et al., 2021). On the other hand, low-layer features contain more specific information but suffer from background noise and semantic ambiguity. This study concentrated on utilizing the ResNet152V2 and EfficientNetV2L-trained models.

2.6 Related Works

2.6.1 Machine Learning Techniques for Breast Cancer

Numerous studies have utilized Support Vector Machine, Artificial Neuron Network, and K-Nearest Neighbors algorithms to identify and categorize breast cancer through the utilization of MRI. The researchers have presented a methodology that involves applying algorithmic techniques to a public dataset to classify breast cancer as normal or abnormal, specifically benign or malignant. Studies suggested several methods wherein machine learning algorithms were employed to classify breast cancer, and their performance was compared to discover the most efficient classifier.

Machine learning methodologies include many features. These methodologies aim to develop a classification model using a dataset with designated classes. The two crucial phases in machine learning algorithms encompass dataset training and validation. Table 2. 4 presents an extensive summary of the many approaches utilized in machine learning to identify and assess breast cancer.

Table 2.4 The literature review of relevant works yields a comparison of breast cancer using different machine-learning algorithms

Authors	Method	Dataset	Purpose	Acc.	Limitation
(Khuriwal & Mishra, 2018)	ANN, Logistic	WDBC Dataset	Adaptive ensemble voting method for breast cancer diagnosis utilizing the Wisconsin Breast Cancer database.	98.50%	To understand why ANNs and logistic regression models can perform better than ensemble machine learning models for diagnosing breast cancer, even when the number of features is small.
(Benhassine et al., 2020)	ANN, Naive Bayes, SVM	MIAS, Mammographic Image	Presented a novel three-step method for extracting features from images. All obtained ROIs are subjected to the discrete cosine transform, and only the upper left corner (ULC) of the DCT coefficients are retained.	100% 92% 94%	The pre-processing step is used to narrow down the area where anomalies might be found by removing background noise and all unwanted objects. This step includes a new method for suppressing the pectoral muscles.
(Naji et al., 2021)	SVM, NB, C4.5, KNN	Wisconsin Diagnostic dataset from the UCI	To determine the most efficient and effective machine learning method for Breast Cancer diagnosis and prognosis.	98.1%	It is important to note that our results are restricted to the BCWD dataset.
(de Lima et al., 2016)	SVM	IRMA database	Identify and categorize mammographic lesions using image regions of interest.	94.11%	"Finest method of the current state-of-the-art". This means that the researchers are only comparing their model to the best-known models. It is possible that there are other models that are not as well-known, but that perform better than the proposed model.
(Arafa et al., 2019)	Nonlinear m GMM SVM	mini-MIAS dataset	The system uses GMM for the first time in the literature to segment mammogram images into ROI regions.	92.5%	The researchers used a confusion matrix to see how accurate their proposed CAD system is at detecting breast cancer in digital mammograms.
(Hazra et al., 2016)	SVM, NB, Ensemble	WDBC Dataset	Determine the smallest subset of features that can guarantee highly accurate classification of benign or malignant breast cancer.	95.1% 95.5% 95.9%	It is possible that the proposed classifier would not have the lowest time complexity on other datasets, or that its time complexity would increase on larger datasets.

(Chaurasia et al., 2018)	Naive Bayes, RBF Network, J48	Breast-cancer-Wisconsin	To present a report on breast cancer in which we utilized the available technological advances to develop breast cancer survivability prediction models.	97% 96% 93%	The researchers simplified the survival variable by converting it to a binary variable, with 1 representing malignant tumors and 0 representing benign tumors.
(De Lima et al., 2014)	SVM with RBF kernel	mini-MIAS, DDSM	The proposed task classifies the lesion in accordance with the guidelines of the American College of Radiology.	80%	The proposed work combines ELM with kernel learning. However, the authors only consider a small number of kernel functions. This could make the proposed method less effective on some datasets and tasks.
(Atrey et al., 2019)	ANN	WBCD	The level of feature dominance is proportional to the disparity between benign and malignant tumor means.	98.9%	The dominance-based filtering method can help us choose a good subset of features from the given feature set, which can make the classifier run faster without making it less accurate.
(Omondiagbe et al., 2019)	ANN, Naive Bayes, SVM	Wisconsin Diagnostic Breast Cancer	This study proposed a hybrid approach for breast cancer diagnosis by reducing the high dimensionality of features using linear discriminant analysis (LDA) and then employing the new feature dataset to Support Vector Machine.	98.82%	The CAD system could be used as a second reader to assist radiologists in making diagnoses. Alternatively, the CAD system could be used as a standalone tool to screen women for breast cancer.

2.6.2 Techniques of Deep Learning for Breast Cancer

This section presents a comprehensive summary of the latest advancements in detecting, classifying, and diagnosing breast cancer. Various studies have utilized deep learning (DL) techniques to detect and classify breast cancer in different medical imaging modalities, such as MRI, mammogram imaging, ultrasound imaging, and other relevant forms of medical images. The researchers present the results of their study on breast lesion detection and suggest an automated classification system for breast cancer images. This system is built on a fusion of deep features and advanced routing techniques. Developing the Breast Cancer Screening Framework was predicated upon the efficacy of deep learning models. Table 2. 5 presents the results of breast cancer detection achieved by utilizing diverse deep-learning methods.

Table 2.5 Comparative analysis of breast cancer detection using various Deep Learning algorithms

Author(s)	Algorithms	Dataset	Accuracy	Implementation tool
(Ahmed et al., 2020)	Deep Lab, Mask-RCNN	MIAS CBIS-DDSM	95.0% 98.0%	libraries in Python
(De Freitas Oliveira Baffa & Grassano Lattari, 2019)	CNN	DMR	98% for static and 95% for dynamic protocol	libraries in Python
(Roslidar et al., 2019)	DenseNet201 ResNet101 MobileNetV2 ShuffleNetV2	Database for Masto logy Research (DMR)	MobileNetV2 has an accuracy of 100% for static datasets and 99.6% for dynamic datasets	MATLAB
(Zuluaga-Gomez et al., 2021)	CNN	DMR-IR database	92%	libraries in Python
(Yari et al., 2020)	CNN, DensNet, ResNet	BreakHis dataset	100%	libraries in Python

(C. M. Kim et al., 2020)	CRNN	Breast Ultrasound image Mendeley data	99.75%	OpenCV-python
(Byra et al., 2019)	CNN based on VGG19	BI -RADS	AUC value: 93.6%	Python
(Ismail & Sovuthy, 2019)	VGG16- ResNet50	IRMA dataset	94% 91.7%	MATLAB
(Moy et al., 2020)	CNN	BCDR-F03	89%	Python
(Raza & Syed, 2021a)	Mask RCNN	DICOM images	85%	Python
(Zhang et al., 2022)	ResNet-101, Mask R-CNN	DCE-MRI	86%, 82%	Python
(Al-Haija & Manasra, 2020)	ResNet-50, CNN	WDBC breast cancer	99%	Python
(Bhatti et al., 2020)	CNN, Mask R-CNN	DDSM	84%, 91%	Python
(Hsieh et al., 2020)	VGG16, MaskR-CNN, Inception V3	collected dataset	87%, 89%, 90%	Python
(Min et al., 2020)	Mask R-CNN	INbreast dataset	%90	Python

A comparison between machine learning and deep learning methodologies reveals the superior performance of deep learning models. Numerous projects have been conducted to evaluate the effectiveness of deep learning and machine learning techniques for breast cancer identification using MRI, and mammography images. The deep learning approach that the authors are proposing is able to accurately identify breast cancer in medical images with greater accuracy than traditional machine learning approaches. Various architectural models such as CNN, Mask RCNN, DensNet, ResNet, and others were employed to classify breast cancer through deep learning methods. The researchers employed a CNN model for the breast cancer classification task, utilizing datasets like MIAS, CBIS-DDSM, DMR (Database for Mastology Research), DMR-IR, BreakHis, Breast Ultrasound images, Mendeley Data, and stained images for training and evaluating the model.

2.7 Summary

In this chapter, the background and literature review for this topic delve into the historical context and existing studies surrounding the application of deep learning techniques in the field of breast cancer diagnosis.

The literature review reveals that numerous studies have explored the potential of deep learning models for breast cancer diagnosis. These models have been trained on diverse datasets containing a wide range of medical images, including mammograms, MRI, and ultrasound scans. Researchers have leveraged various deep learning architectures, including Convolutional Neural Networks (CNNs) and more advanced models like ResNet and DenseNet, to classify breast cancer images with remarkable accuracy.

Moreover, these deep learning models have demonstrated the ability to identify various aspects of breast cancer diagnosis, such as tumor localization, tumor type classification, and even predicting patient outcomes. The literature also discusses the integration of deep learning with computer-aided diagnosis (CAD) systems to assist radiologists and healthcare professionals in making more accurate and timely diagnoses.

Overall, the background and literature review on breast cancer diagnosis using deep learning models underscore the growing interest and progress in this field. These models offer the potential to enhance the accuracy and efficiency of breast cancer diagnosis.

CHAPTER THREE

3 METHODOLOGIES

3.1 Introduction

In order to recognize breast cancer images, various research methods have been employed. In each research method, contributions, advantages, and disadvantages have been identified and explained. The same has been done with the proposed deep learning models. Also, the proposed methodology for this thesis contains various steps to implement breast cancer detection and diagnosis. These steps include image acquisition, pre-processing to remove unrelated noise, segmenting and clustering the tumor regions. Applying deep learning algorithms to train and test models. The field of image analysis has undergone substantial development in the past thirty years. Medical imaging and image processing progress can significantly enhance healthcare outcomes, particularly in illness categorization and diagnosis. Segmentation and machine learning algorithms are helping with BC identification and classification in medical images. Some newly proposed approaches are introduced in this chapter to overcome the limitations of the existing system, as well as an early detection and classification system for BC utilizing mammography, MRI, and DCE-MRI. These automated systems outperform existing ones in terms of efficiency.

This chapter comprises three sections: The first section discusses BC recognition based on evaluating the efficacy of machine learning algorithms using MRI image datasets. The second section advocates for automated breast density and tumor size classification using ResNet152V2 and Mask-RCNN on a mammogram dataset. The third section discusses automatic breast cancer

detection for mastectomy based on MRI images using Mask R-CNN and Detecron2 models on MRI and DCE-MRI image datasets.

3.2 Dissertation Structure

This study's primary objective is to construct a breast cancer recognition model using real and standard datasets collected from hospitals in Erbil and Suleimani and public-based datasets obtained from various sources. For this purpose, various models have been designed using different approaches, mainly deep learning. Hence, the experimental results of the proposed models will be tested and compared to find the best one.

They have been identified the main contributions of each methodology and the scenario that goes with it. The drawbacks and main negative aspects of each methodology are identified to be overcome in the next. These methodologies are used for fine-tuning, data augmentation, and designing a new model for breast cancer recognition. All the methodologies used in designing the models have the same phases but different modern methods. The main phases are:

Data collection each methodology was designed for specific breast cancer classification and detection issues therefore it needs precise data. This phase consists of two tasks shown Figure 3. 1.

Figure 3. 1 Outlines the tasks

The extraction of features is a crucial step in all the methodologies proposed in this dissertation different procedures have been proposed using different methods. Figure 3. 2 outlines the overall dissertation structure of this work.

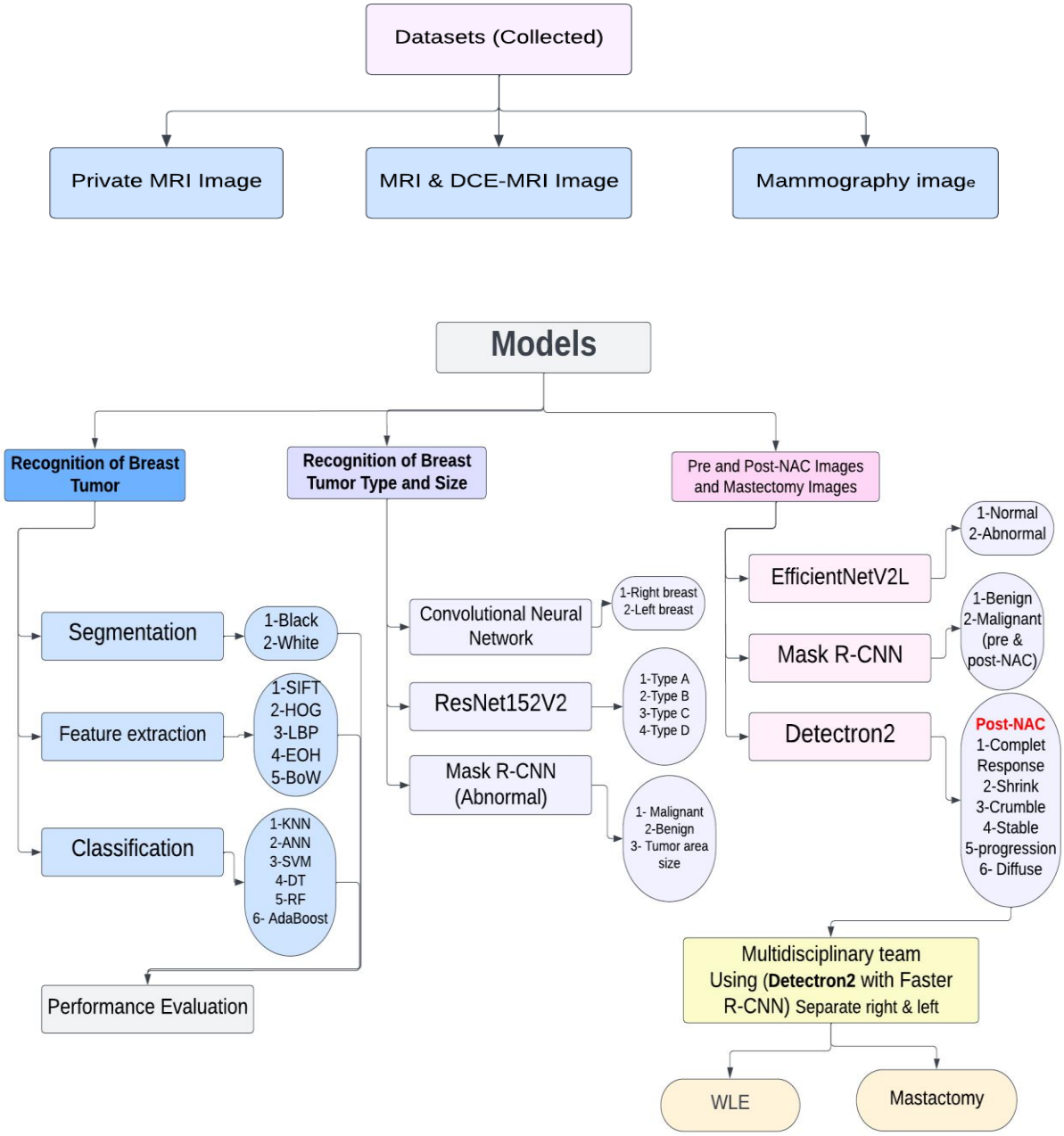

Figure 3. 2 The dissertation structure of the study

3.3 The Collected Dataset

In this dissertation, different datasets have been used that have been collected in Erbil and Sulaymaniyah hospitals and with public datasets to achieve the results by applying the methodologies. The specification of images in a breast cancer dataset may vary depending on the difference in the equipment used for breast cancer imaging between two cities, Erbil and Sulaymaniyah, or between two hospitals in the same city. However, here are some general specifications that are relevant:

1. Image format: The images are in Joint Photographic Experts Group (JPEG) image format.

2. Image resolution: All images' resolution is 512 x 512 pixels.

3. Image quality: The images collected from the website as authentic images have good quality with no blur or distortion, as this would affect the accuracy of damage assessment algorithms. Also, the images have been collected were of the same quality using a medical program, and the datasets were created with the help of two radiology doctors.

4. Multiple viewpoints: The mammography dataset includes images from different viewpoints, including the right and left breast, to provide a more comprehensive view of the cancer.

5. Image labeling: The images have been labeled with the type of breast and the tumor-malignant or benign. This information is essential for supervised machine learning models to learn how to recognize different types of cancer accurately. In this section, we will describe the dataset utilized for this dissertation.

3.3.1 Breast Mammography Image

The methodologies employed in mammography included film-screen mammography and digital mammography. Full-Field Digital Mammography (FFDM) is an alternative term for digital mammography. Although film-screen and digital mammography employ similar procedures, they have distinct differences. Film screen mammography involves using photographic films to capture images, whereas digital mammography records digital files on a computer, as depicted in Figure 3. 3. In this chapter, the focus has been on digital mammography. The dataset comprises 510 images, with each patient having two views. The dataset consists of images from 255 patients, with 133 patients diagnosed with cancer and 117 patients presenting with benign tumors also, 5 normal cases. Breast cancer images were collected from Zheen International Hospital-Erbil with a diverse age range from 25 to 70 years. The RadiAnt DICOM Viewer, a widely employed medical software in many healthcare facilities, has implemented a data scaling feature across all datasets. The mammograms were categorized into four groups by two proficient radiologists, arranged in ascending order according to the fibro glandular tissue composition levels.

Category A is characterized by a predominance of adipose tissue and a minimal presence of fibroglandular (*density describes how much of your breast tissue is considered fatty or dense*) tissue. Approximately 10% of women fall into this category. Category B refers to the presence of scattered fibroglandular tissue, which is observed in around 40% of women. Category C refers to a condition known as heterogeneously thick breasts, observed in approximately 40% of women. A high density of fibroglandular tissue characterizes category D. Approximately 10% of women exhibit the characteristics depicted in Table 3. 1. In the case of types C and D, the physician encounters difficulty accurately

determining the precise position of the tumors due to the elevated density observed in the corresponding imaging. In this scenario, it is recommended that the patient get an MRI scan. This recommendation is based on a comparative analysis of clinical breast examination, mammography, ultrasound, and MRI, demonstrating that MRI is the most precise modality for detecting tumor response and residual tumors.

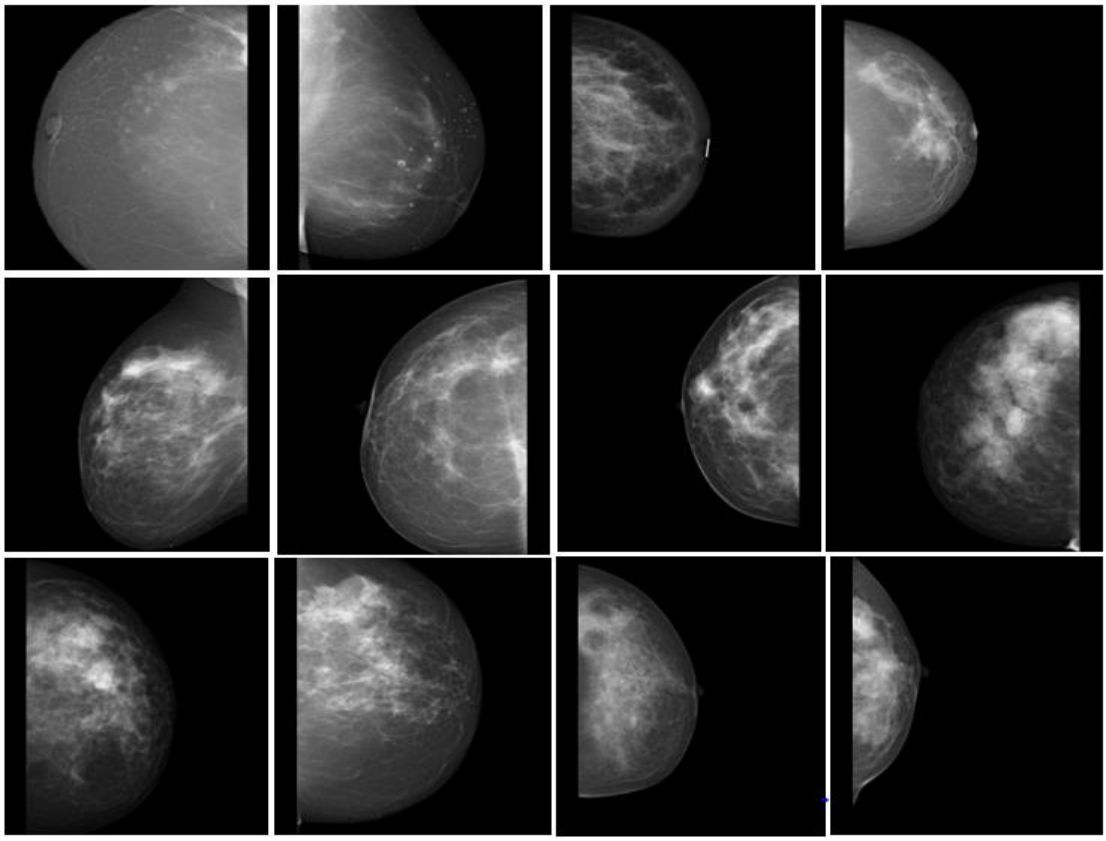

Figure 3. 3 Examples of mammography breast image datasets

Table 3. 1 Breast density types and density result percentage

Breast Types	Density Percentage	Breast Density
Type A (Fatty breast)	< (0- 25%)	10 %
Type B (Dispersed fibro glandular)	< (25%- 50%)	40 %
Type C (Heterogeneously dense)	> (50% -75%)	40 %
Type D (Extremely dense)	> (75%- 100%)	10 %

3.3.2 Breast MRI and DCE-MRI

The dataset consists of two distinct categories of breast images: magnetic resonance imaging (MRI) and dynamic contrast-enhanced (DCE) images. The magnetic resonance imaging (MRI) technique has successfully integrated many datasets. DCE-MRI is commonly employed in patients newly diagnosed with breast cancer to assess the local extent of the disease and assist in surgical and therapy planning. The dataset utilized in hospitals for this purpose is commonly referred to as pre- and post-neoadjuvant chemotherapy (NAC) or T1-weighted DCE-MRI. The dataset has 2175 images from 145 patient each contributing 15 images. Within the dataset, it was seen that 20 cases were classified as normal, 30 cases were categorized as benign, and a total of 95 patient were diagnosed with cancer.

BC images were collected at Erbil and Sulaymaniyah Hospital encompassing a diverse age range of women. The dataset was gathered throughout the period spanning from 2021 to 2022. The dataset data underwent resizing utilizing the RadiAnt application, a widely utilized medical tool across several

institutions. The dimensions of each image are 512 by 512 pixels, a size considered optimal for the visualization of cancer images, as indicated by previous research findings. The trial aimed to compare pre- and post-neoadjuvant chemotherapy (NAC) outcomes and evaluate the Breast Response Evaluation Criteria in Solid Tumors (RECIST). The post-NAC comprises five distinct categories, as depicted in Figure 3. 4: Type 0, complete response; Type 1, shrink; Type 2, crumble; Type 3, diffuse enhancement; Type 4, stable; and Type 5, progression. They have been working on something else using these images by creating a form and distributing it to the medical team. The efficacy of a multidisciplinary team (MDT) in managing malignancies following post-neoadjuvant chemotherapy was crucial to our endeavor. Figure 3.5 shows an example image of DCE-MRI.

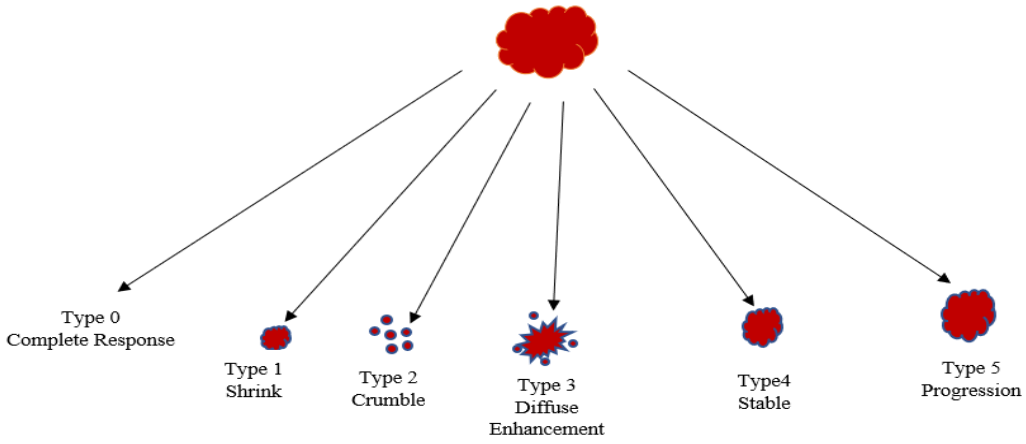

Figure 3. 4 Breast MRI response patterns of breast carcinomas during and following neoadjuvant treatment based on MRI (Goorts et al., 2018).

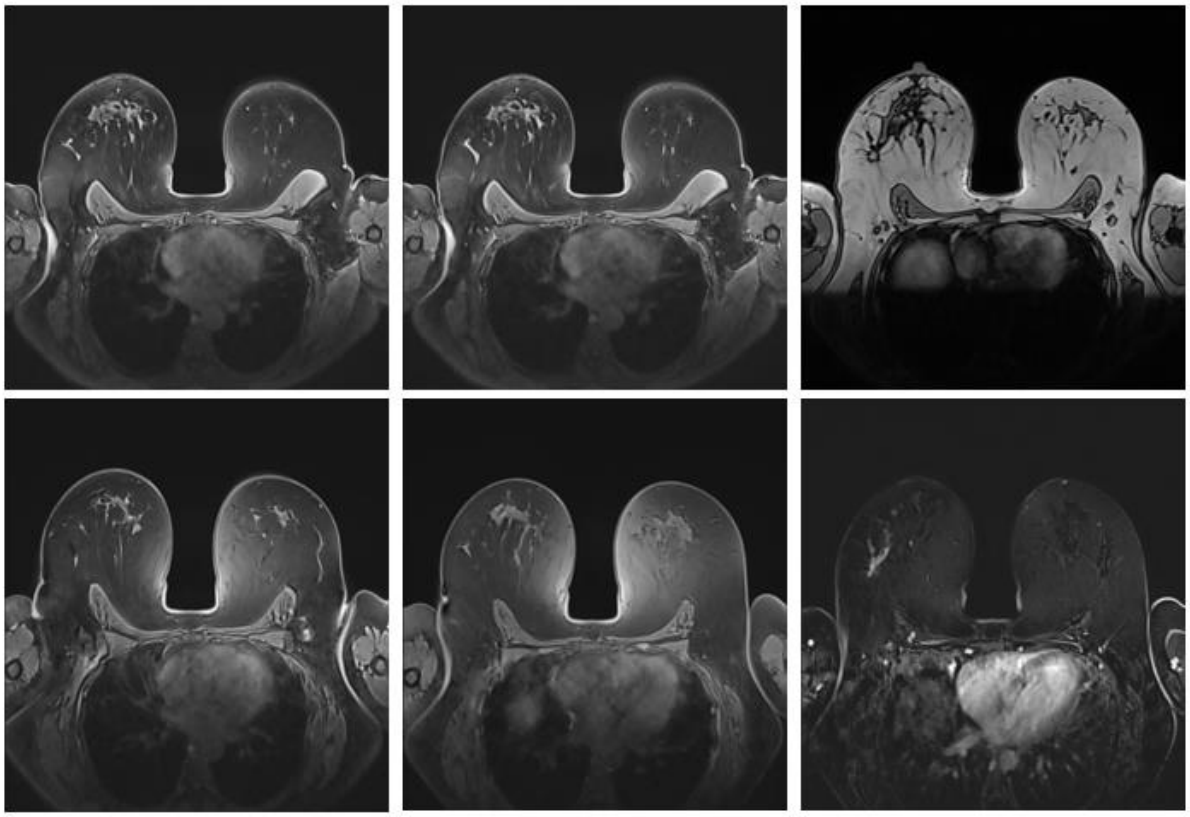

Figure 3. 5 Examples of DCE-MRI breast image datasets

3.3.3 Breast MRI Public Datasets

This dissertation utilized datasets sourced from the public image. The ACRIN (American College of Radiology's Imaging Network) first dataset contains 984 patients, but only 969 were included in the primary data analysis due to study criteria. This document contains 1280 images of 128 patients, at a rate of 10 per patient. As depicted in Figure 3. 6, the second dataset of the Wisconsin Diagnostic Breast Cancer (WDBC) MRI includes 400 images from 40 patients, 10 from each patient, with 35 patients having cancer and 5 with normal cases. All patients in this set of data have cancer data sets, collected between 2014 and 2020.

All datasets have been resized using the RadiAnt application. The dimension of each image is 512 by 512 pixels, which, according to previous research, is the optimal resolution for displaying cancer images.

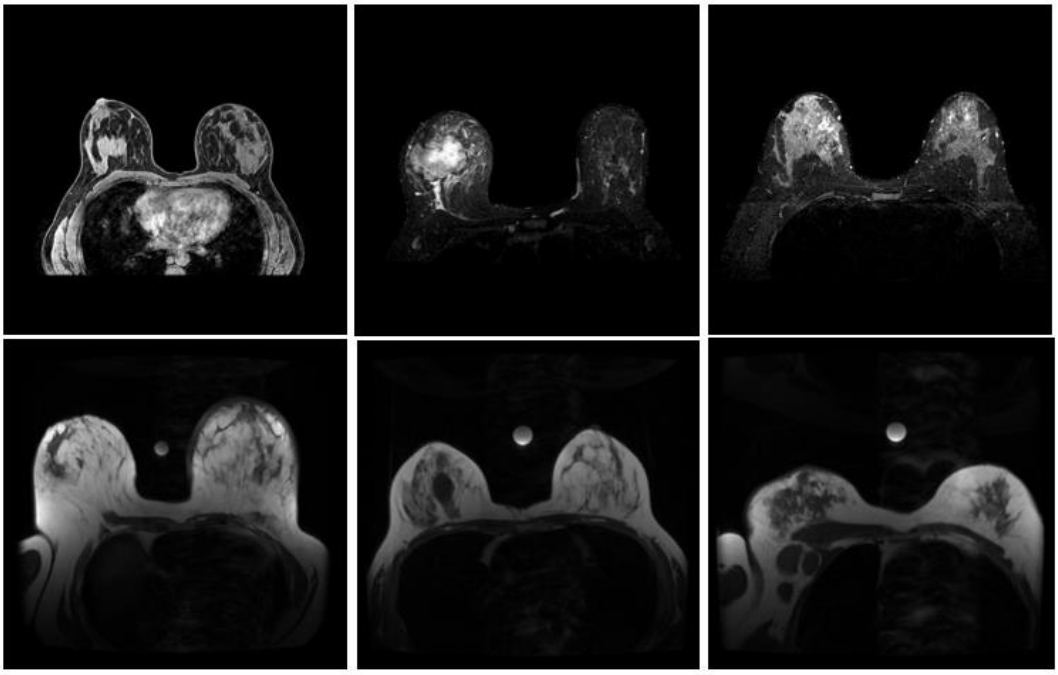

Figure 3. 6 Examples of MRI public breast image datasets

3.3.4 Data Augmentation

Data augmentation is a method for increasing the size of a dataset by randomly transforming existing data elements. This technique can generate more realistic and diverse input data, thereby enhancing the precision of machine-learning models. Data augmentation reduces overfitting by introducing additional noise into the training set, thereby reducing model complexity and enhancing generalization performance. In addition, this method permits us to make better use

of limited datasets by generating multiple versions from each sample point (Lu et al., 2019).

Adding Gaussian blur, padding, horizontal flipping, randomly flipping images from left to right, cropping, rotating, altering brightness and contrast, and adding noise are among the most popular data augmentation techniques (Yari et al., 2020), s depicted in Figure 3. 7. The preponderance of deep learning libraries, including Keras, Torch, TensorFlow, and deep neural networks, including Mack R-CNN, YOLO Detecron2, Etc., offer augmentation for classification training tasks.

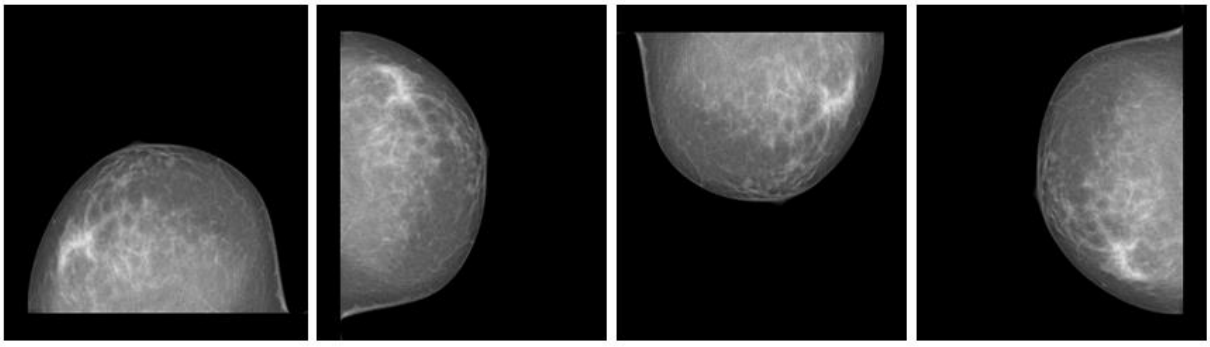

Figure 3. 7 Examples of breast cancer image data augmentation

3.4 Proposed Method 1: Breast Cancer Diagnosis Based on an Evaluation of the Efficacy of Machine Learning Algorithms

This section introduces an alternate methodology for computer-aided diagnosis (CAD) systems in breast magnetic resonance imaging images. The breast problem statement is not reliable for recognizing accuracy. They have been able to precisely detect distinct types of breast cancer tumors using three MRI image datasets and optimized machine learning techniques. Efficacy in breast

cancer using machine learning refers to the effectiveness and success of machine learning techniques and models in tasks related to breast cancer diagnosis.

The successful analysis and diagnosis of BC disorders based on MRI images require the implementation of standard methodologies. One of the processes involved is the segmentation of MRI images, followed by the extraction of characteristics for subsequent analysis. The present study aims to provide a method for the identification and performance evaluation of MRI and imaging data. This will be achieved through the utilization of four steps. The first step entails the utilization of an MRI image dataset, which comprises three datasets, with two of them being public datasets and one being a private dataset. Subsequently, the segmentation process is applied to convert the image into a binary representation consisting solely of black and white pixels. The third stage involves the process of feature extraction from the image. This step utilizes various methods, namely Scale-Invariant Feature Transform (SIFT), Histogram of Oriented Gradients (HOG), Local Binary Patterns (LBP), Bag-of-Words (BoW), and Edge Orientation Histograms (EOH). The fourth and last phase involves the implementation of various classifying machine learning algorithms, namely K-Nearest Neighbors (KNN), decision tree, Naïve Bayes, Artificial Neural Network (ANN), Support Vector Machine (SVM), Random Forest (RF), and AdaBoost. The outcomes of our proposed work demonstrate the performance evaluation, as depicted in Figure 3. 8.

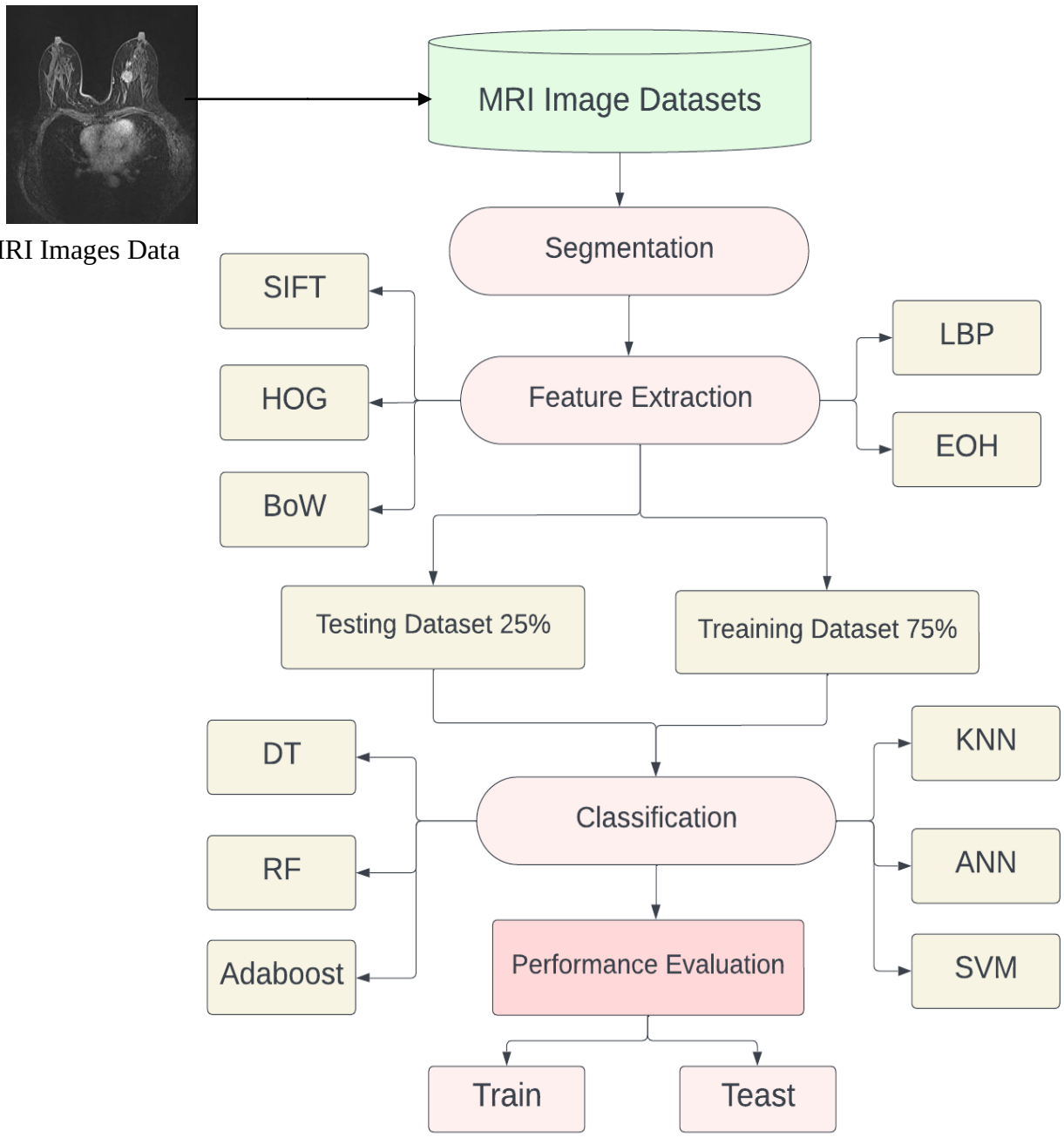

Figure 3.8 Proposed system diagram

3.4.1 Segmentation

The method proposed is used to segment MRI breast images. The segmentation algorithm provides a pixel-based strategy for enlarging regions that generate appropriate seeds and thresholds. Seeds are a crucial part of the initialization step in many segmentation techniques, helping to define the regions of interest and guide the subsequent image analysis process. Thresholding is a fundamental technique in image processing and segmentation, and it is commonly used to simplify complex images into regions of interest. This endeavor aims to extract binary black-and-white images from a grayscale image. Giving the value 0 (black) to every other pixel and 1 (white) to every pixel in the input image with a luminance more significant than the level produces grayscale original MRI breast scans. The upgraded image is more contrasted and more apparent than the original. The segmented image depicts the affected regions, condensing the image and eliminating superfluous elements. Following this section, has been transferred the data to the segment on feature extraction using multiple machine learning algorithms, as depicted in Figure 3. 9.

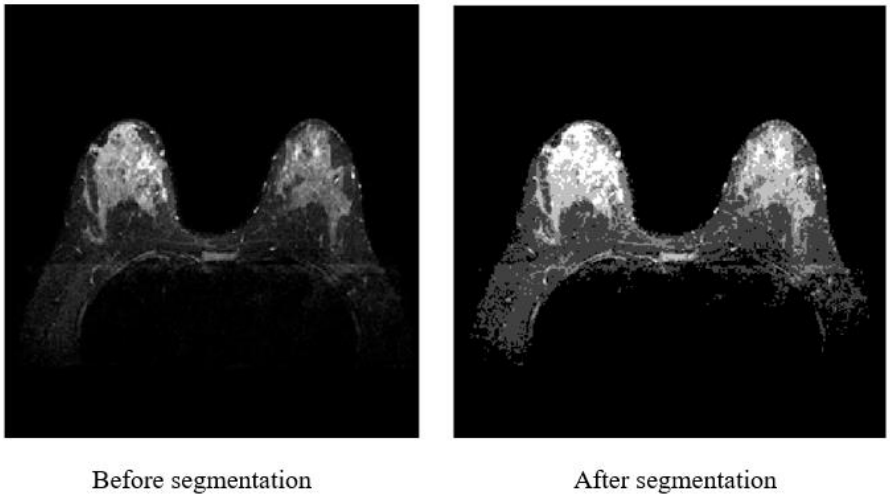

Figure 3. 9 Example of MRI image segmentation

3.4.2 Feature Extraction

Conventional breast MRIs are highly textured and complex in breast cancer images. Feature extraction is, therefore, essential for accurate breast cancer MRI image classification. In the classification approach, the characteristics of the images are combined based on specific criteria. The primary objective of feature extraction is to condense data while retaining the most relevant information. Diverse techniques have been devised to extract meaningful and distinguishing characteristics from data. This model's various feature extraction techniques to extract MRI image features are Scale-Invariant Feature Transform, Histogram of Oriented Gradients, Edge Oriented Histogram, Local Binary Patterns, and Bag of Words.

Utilizing feature extraction techniques for MRI breast cancer analysis, such as SIFT, HOG, EOH, LBP, and BoW, yields pertinent information from the images, including local structures, edges, and textures. Overall, feature extraction techniques are critical in MRI breast cancer analysis. These techniques can help radiologists and machine learning algorithms improve breast cancer detection, diagnosis, and monitoring by extracting relevant information from MRI images, as shown in Fig. 3. 10.

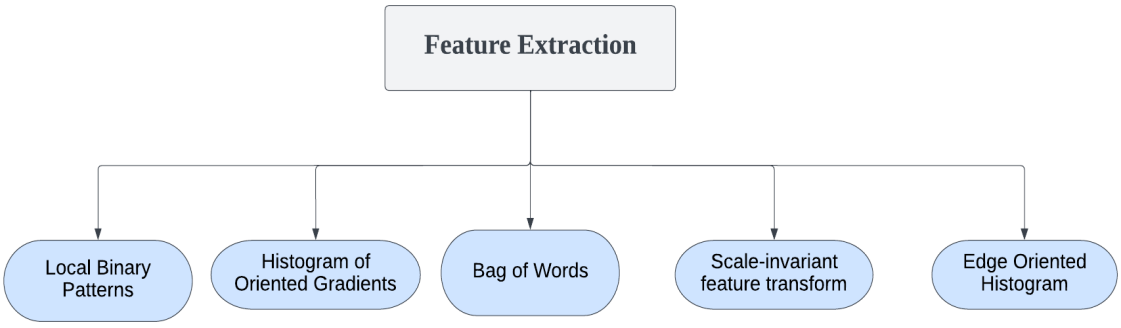

Figure 3. 10 Feature extraction using these methods

3.4.3 Classification Using Machine Learning Algorithms

In machine learning and pattern recognition, classification assigns input data elements to predetermined classes or categories. Due to the sporadic classification, multi-points have been employed to detect classifications in multiple breast regions that the conventional region-growing algorithm cannot determine. This study classified malignant and benign tumor cells using machine learning techniques. This research includes the parametric evaluation of six distinct machine-learning algorithms Many different machine-learning algorithms can be used for breast cancer classification as (k-Nearest Neighbor, Decision Tree, Random Forests, Artificial Neural Network, Support Vector Machine, and AdaBoost). The most appropriate algorithm will depend on the specific characteristics of the dataset and the desired performance metrics.

The optimal classification method for MRI breast cancer is determined by the unique datasets, the complexity of the task, and the available computational resources. Overall, machine learning techniques have the potential to significantly improve the detection, diagnosis, and monitoring of breast cancer. To identify breast MRI images for the detection and diagnosis of cancer, it is customary to experiment with various algorithms and modify their parameters to achieve maximum accuracy and robustness, as shown in Fig. 3. 11, the algorithms used in this research.

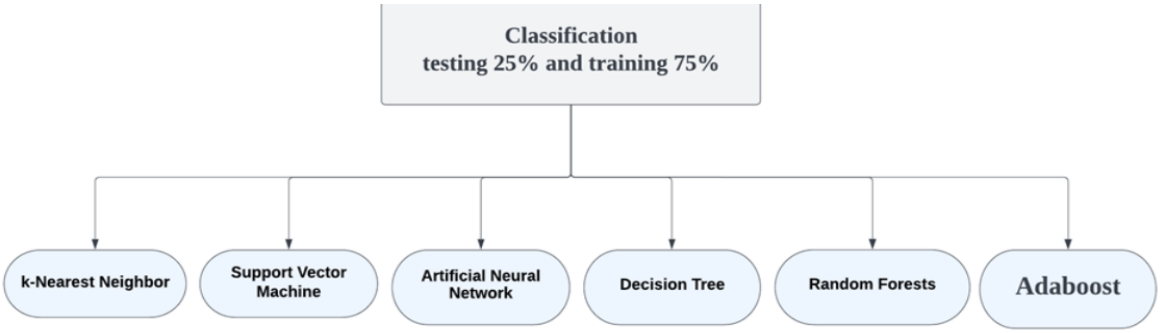

Figure 3. 11 Image classification using this algorithm

3.5 Deep Learning Models and Breast Cancer

Numerous prospective deep-learning computer vision models have recently demonstrated significant performance enhancements in CAD systems, particularly convolutional neural networks (CNN), transfer learning methods, and deep-learning-based object detection models. Several methodologies based on deep learning have been proposed for CAD systems. The conventional methodologies employed in the utilization of deep learning models for the categorization of breast cancer in mammography and MRI imaging:

1. Data Collection and Preprocessing: Collect large datasets, label them with class information, preprocess images, and apply data augmentation techniques for improved generalization and diversity.

2. Data Splitting: For deep learning model training, hyperparameter optimization, and performance evaluation on unseen data, divide the dataset into training, validation, and testing sets.

3. Model Selection: For mammography breast cancer and MRI image classification using deep learning, a suitable deep learning architecture was chosen utilizing convolutional neural networks for image analysis.

4. Model Architecture Design: Design deep learning model architecture by defining layers, activation functions, pooling layers, and output layers and experimenting for optimal performance.

5. Model Training: The training dataset was utilized to train the deep learning model. During training, the model adapts its weights and biases to reduce the classification error in the training data.

6. Model Evaluation: Evaluate the efficacy of a deep learning model using metrics such as accuracy, precision, recall, F1 score, and ROC-AUC as depicted in Figure 3. 12.

In order to mass identity, segment, and classify mammographic images with the least amount of human involvement, DL-designed CAD tools.

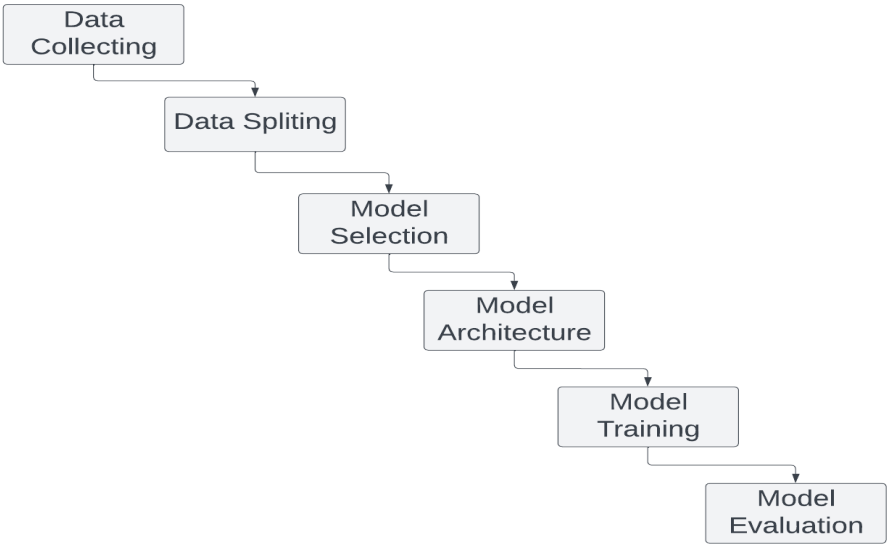

Figure 3. 12 Diagram for deep learning models

3.6 Proposed Method 2: Breast Tumor Recognition of Type and Size Using Deep Learning Models (BTRD)

The detection and diagnosis of breast cancer by CAD methods involve utilizing many techniques, including mammography. In breast cancer research, a CAD system was evaluated using an independent dataset; the results indicated that the system detects a high proportion of breast malignancies manifesting as tumors. In the past, detection, classification, and segmentation were applied to mammograms, MRIs, and other cancer screening methods. It was necessary to develop a more efficient and time-saving creative strategy to achieve comparable or even superior results to those of the past while gaining a competitive advantage.

The objective of this model is to develop and distinguish between normal, malignant, and benign tumors and classify breast density types based on mammograms. The initial step involves comparing right and left breast mammography using CNN. The second stage employs ResNet152V2 to distinguish between normal and abnormal breast mammography images and distinct types of breast density (A, B, C, and D). The third and final is using Mask R-CNN for classification between normal, malignant, and benign, and also have been working on extracting the size of the area of the tumor. The flowchart of our proposed system is shown in Fig. 3. 13. According to the study's findings, ResNet152V2 is a reliable model for identifying the kind of mammography and categorizing it as normal or abnormal.

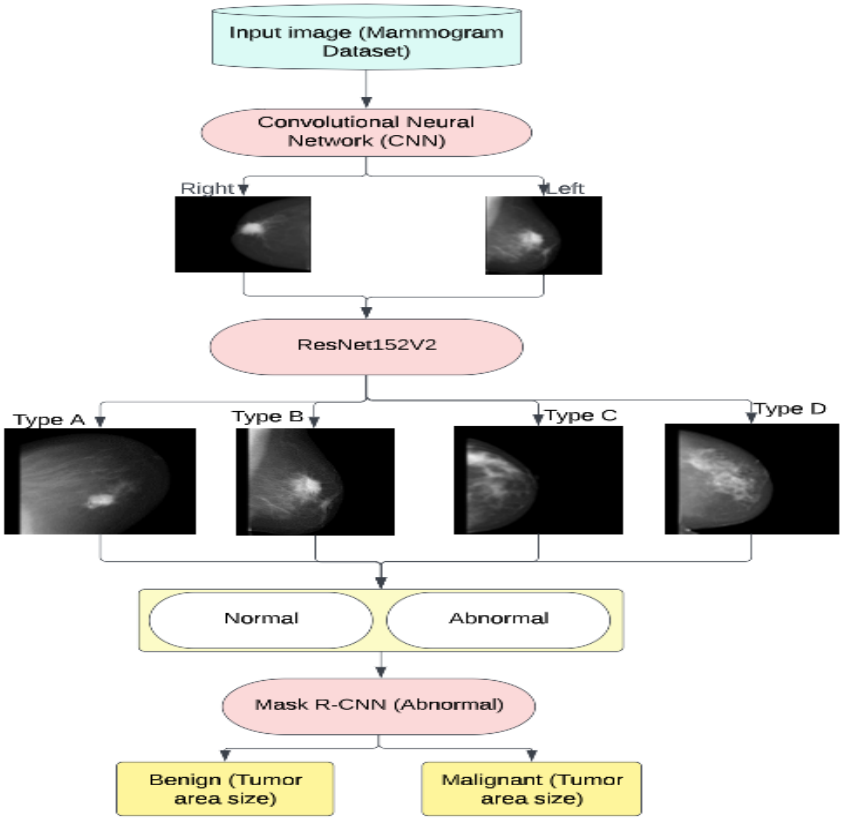

Figure 3. 13 Shows the detailed proposed model for mammograms (BTRD)

3.6.1 Proposed CNN Architecture

CNN's proposed architecture includes an input layer, multiple convolutional layers (C), max-pooling layers (M), and fully connected layers (F). It is a type of deep learning network that is particularly well-suited for image processing tasks. It uses a series of convolutional filters to extract features from the image. Each convolutional filter is designed to detect a specific feature type, such as edges, corners, or textures. Bypassing the image through a series of convolutional filters can produce a set of features representing the image at different levels of abstraction.

In this dissertation, the primary objective of the learning technique is to produce a small number of kernel matrices; the first inception of a convolutional neural network represents a sort of deep-learning technique. After resizing and reshaping an image, a preprocessing action has been proposed. CNN is designed to distinguish the images of right and left breast cancer. This process is carried out with various convolution layers to create a simple new model for CNN. It consists of eight layers and has a high level of accuracy as depicted in Figure 3. 14.

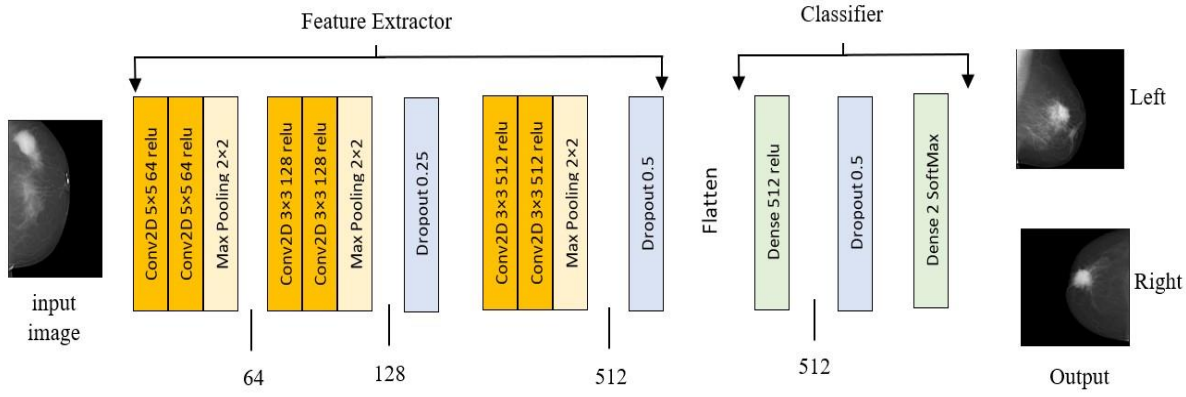

Figure 3. 14 Proposed convolutional neural network model

3.6.2 General Structure of Resnet152V2 Used for Breast Cancer Detection

ResNet-152V2 is a variant of ResNet (Residual Network), a prominent deep-learning model for image recognition tasks. The ResNet has several standard architectures, such as ResNet-50, ResNet-101, and ResNet-152, indicating several deep layers. These models can train the input based on their pre-trained initial weights. This approach accelerates the training and coverage to high accuracy. Each model architecture contains the original model followed by a reshape step, a flattened step, a first dense layer, a dropout layer, a second dense layer, and finally, an activation function that classifies the image as normal or abnormal, represented in Figure 3. 15. Also, this study, the ResNet152V2 architecture was employed to compare mammograms of four different density kinds (A, B, C, and D) based on the density observed in mammography. Breast density is classified into four categories, with A being the least dense and D being the densest. Denser breasts are more difficult to interpret on mammograms, as the dense tissue can mask the presence of tumors or other abnormalities, as illustrated in Figures 3. 16.

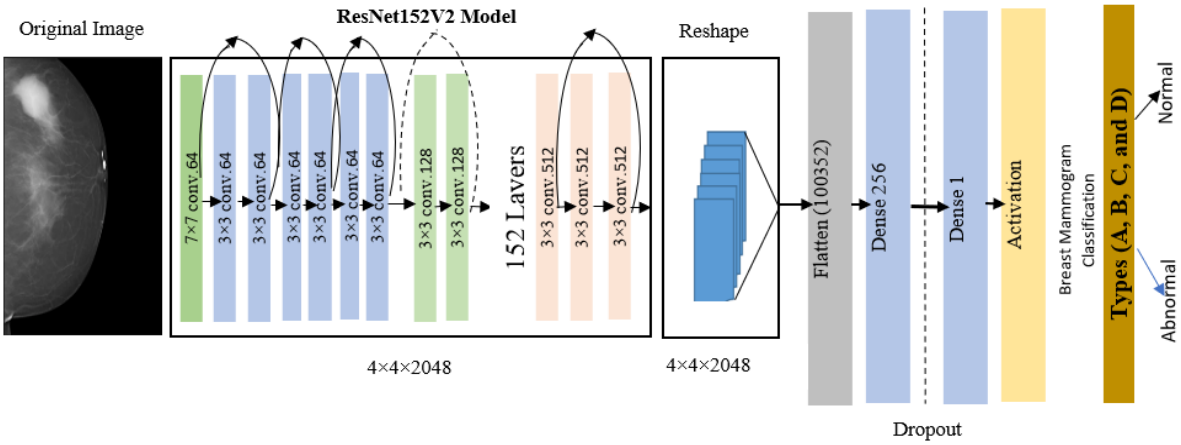

Figure 3. 15 The ResNet152V2 structure

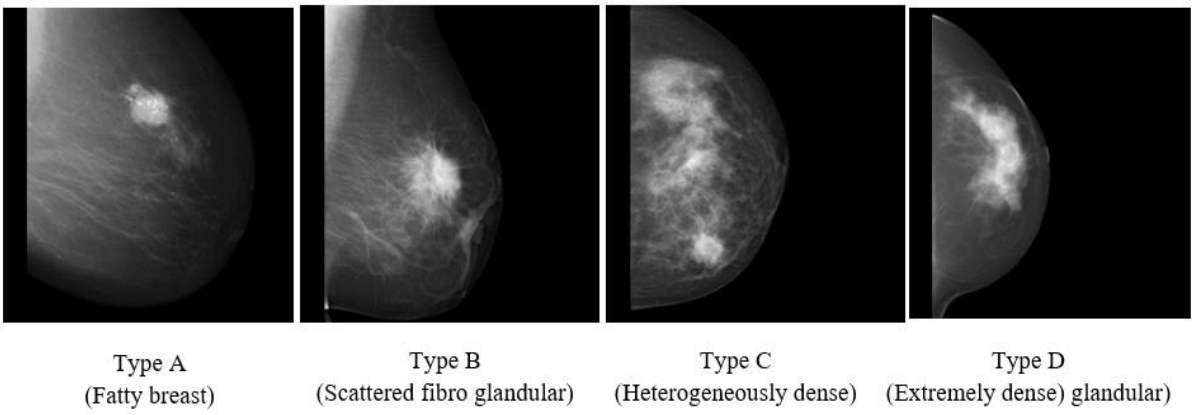

Figure 3. 16 Four kinds of breast density samples exist

3.6.3 Mask RCNN for Breast Tumor Detection

Mask RCNN is a standard deep-learning model utilized for segmentation tasks where the objective is to detect and segment multiple objects of interest within an image. It extends the faster R-CNN model, integrating object detection with region-based convolutional neural networks. Using mask R-CNN for object detection, this method identifies various items in an image and generates a boundary box that distinguishes between malignant and benign objects. Mask R-CNN includes the following components: a backbone, a region proposal network (RPN), a region of interest alignment layer (Roi Align), a bounding-box object detection head, and a mask generation head. The first four components comprise the Faster R-CNN model. This study employed mask RCNN to determine whether a tumor is malignant or benign. Trained Mask R-CNN on a dataset of images containing both malignant and benign tumors. The model learned to identify and segment tumors, as well as to distinguish between malignant and benign tumors. This model also used Mask R-CNN to calculate the size of the area of each tumor.

To do this, used the mask output by Mask R-CNN to count the number of pixels belonging to the tumor. Consequently, the overall structure is depicted in Fig. 3. 17.

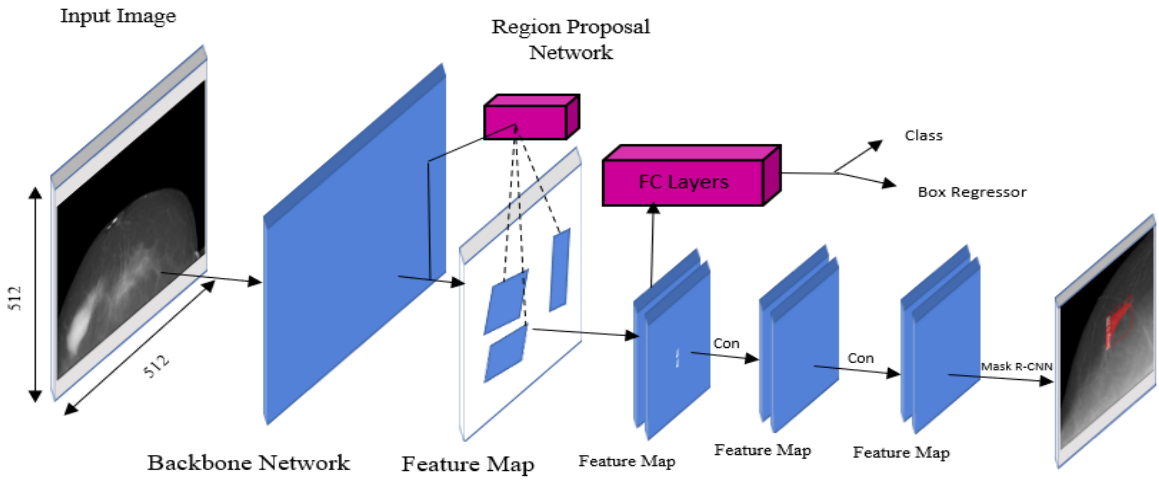

Figure 3. 17 Masking R-CNN architectures for breast mammography images

The term "region of interest" (ROI) in mammography refers to the specific spot within the image where a malignant tumor is identified. The ROI is typically identified by a radiologist who is reading the mammogram. The radiologist may use a variety of factors to identify the ROI, such as the presence of a mass, calcifications, or other abnormalities.

The ROI represented in Figure 3. 18 is distinct for each mammogram because the location and appearance of malignant tumors can vary widely. For example, a tumor may be located in the center of the breast or near the chest wall. It may be small and difficult to see, or it may be large and obvious. To assess the magnitude of the tumor's surface area, it is necessary to employ the RadiAnt program, which will be discussed in detail in the subsequent chapter, illustrated in Figure 3. 19.

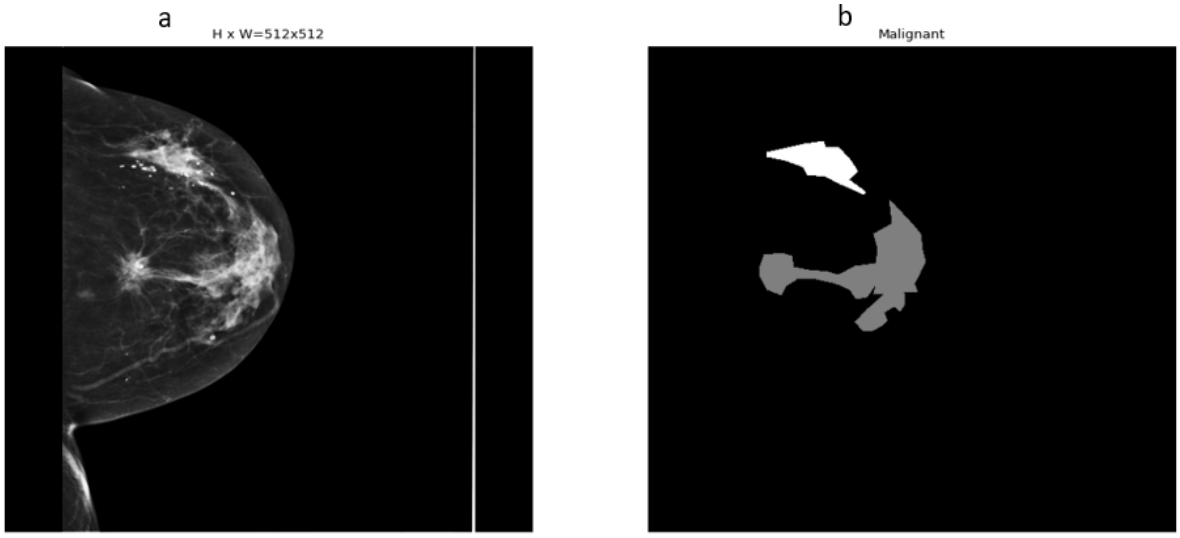

Figure 3. 18 Example of applying mammogram a. Breast mammogram image, b. The Mask R-CNN in the dataset is used to find the ROI

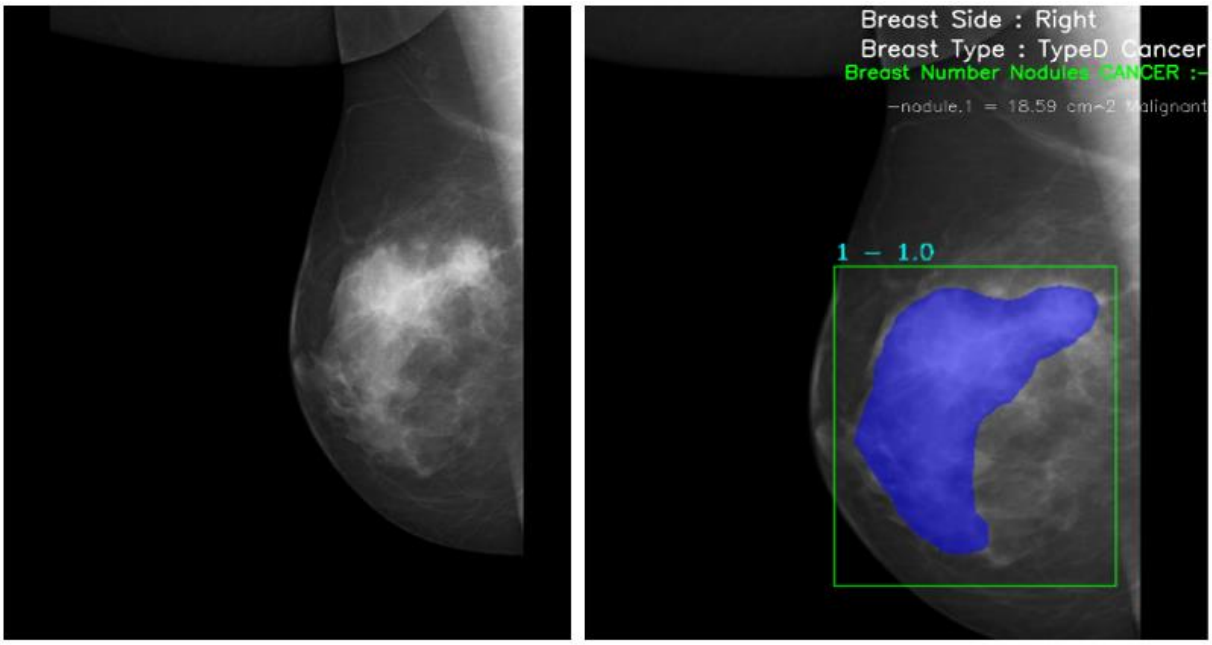

Figure 3. 19 Example breast cancer detection using Mask R-CNN

3.7 Proposed Method 3: Automated Detection of Breast Cancer for Mastectomy Using Deep Learning Models (ADBMD)

This section presents another proposed method for CAD systems in breast cancer MRI and DCE-MRI images. The ability to accurately interpret breast DCE-MRI images depends on several factors, including the visualization's quality, the doctor's level of skill, and the amount of time available for data analysis.

In these dissertations, how much one can distinguish between types of pre-NAC and post-NAC, especially between types of post-NAC, also depends on the type of breast cancer that can decide on mastectomy or WLE according to tissue size and tumor location. Researchers have used various image-processing techniques and segmentation algorithms to analyze samples and enhance visual accuracy to discover and interpret regions of interest. This model will focus on creating a system that goes through four stages, is the input dataset, and compares the normal and abnormal using EfficientNetV2L and the difference between the malignant and benign using Mask R-CNN. It also distinguishes between the right and left sides of the breast. If the patient is malignant, it will be decided to take a DCE-MRI image (pre-NAC and post-NAC). It should perform an MRI mainly after the fourth round of neoadjuvant chemotherapy to determine how the tumor responded to the treatment. After that, compare the types of post-NAC (neoadjuvant chemotherapy) by using Detectron2.

The acquired images obtained from magnetic resonance imaging and DCE-MRI are subjected to processing and afterward inputted into the breast cancer confirmation model to analyze and identify potentially malignant tumors. After this process, the data goes to the multidisciplinary team (MDT) of medical professionals, who collectively decide if the breast needs a mastectomy or wide local excision. The technique employed in this dissertation involves the utilization of Detectron2 with faster R-CNN to differentiate between a mastectomy and a

wide local excision. The main layout of the construction is illustrated in Figure 3. 20.

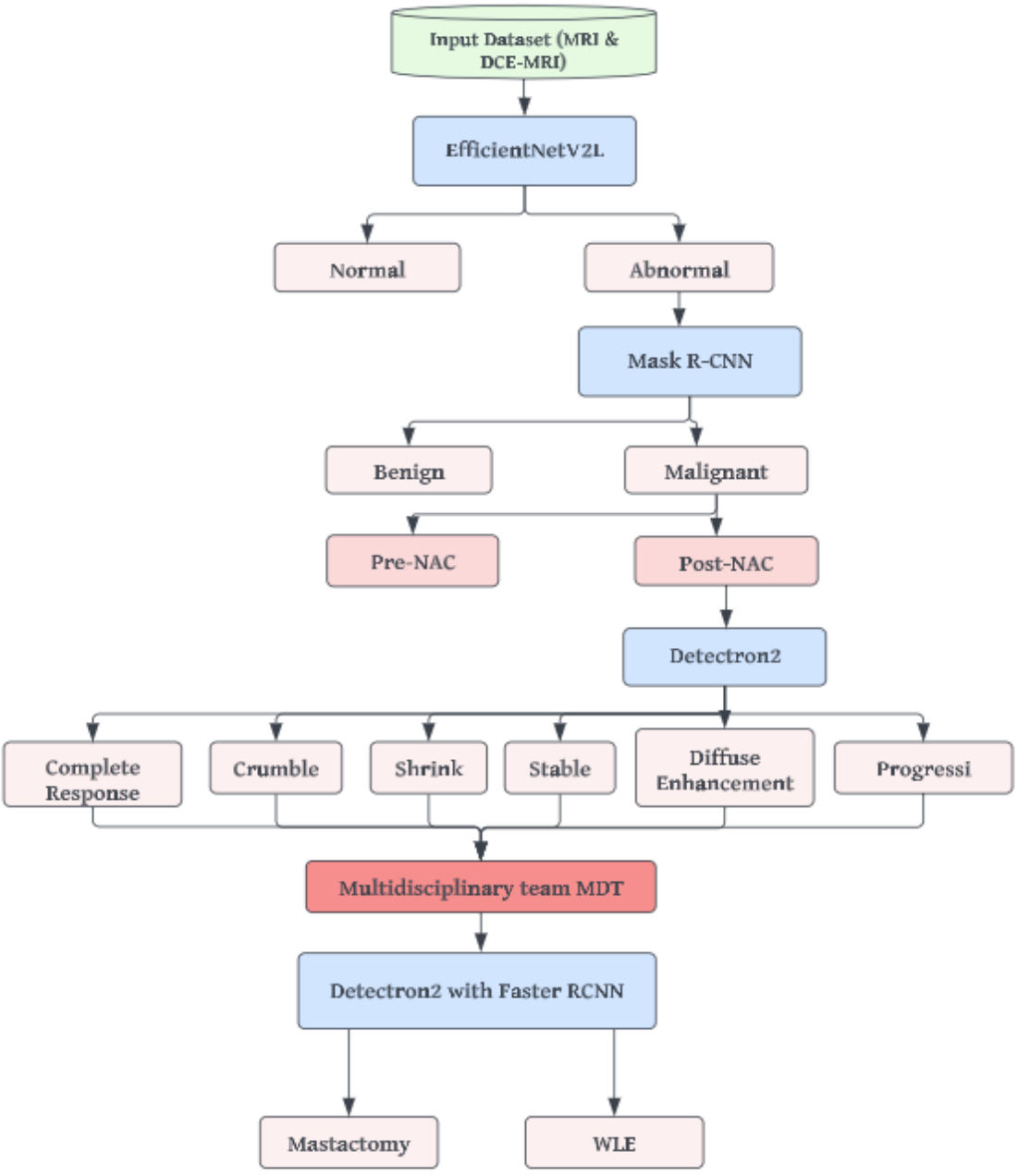

Figure 3. 20 Data flow diagram of the proposed adaptive MRI and DCE MRI images method (ADBMD)

3.7.1 Neoadjuvant Chemotherapy for Breast Cancer

Chemotherapy, or "chemo," is a medical procedure that uses drugs to slow or stop the development of breast cancer cells. Chemotherapy is considered a systemic therapy because it impacts the entire body and is used to treat breast cancer and other types of cancer.

Neoadjuvant therapy refers to treatment administered before breast surgery. The goal of neoadjuvant chemotherapy is to reduce the tumor so that it can be removed with less invasive surgery (M. S. Kim et al., 2020). Treatment with chemotherapy may last three to six months or longer. The patient must undergo an MRI before and after adjuvant therapy (pre- and post-NAC).

The assessment standards for the efficacy of malignancies have undergone numerous revisions with ongoing advances in therapy and cancer analysis. The collaboration resulted in the development of the Response Evaluation Criteria in Solid Tumors (RECIST), which is currently acknowledged by the cancer community. It provides objective criteria for determining whether a tumor vanishes, diminishes, remains stable, or grows. Complete response (CR), partial response (PR), stable disease (SD), and progressive disease (PD) are the terms used to describe these conditions. In Table 3. 2 of the RECIST standard, target lesions are quantifiable lesions used to compare efficacy before and after therapy. The following Equation 3.1 is used to identify post-NAC varieties:

$$\frac{\text{Area Post}-\text{NAC}}{\text{Area Pre}-\text{NAC}} \text{ X } 100 \quad \text{.....(3.1)}$$

Table 3. 2RECIST criteria for breast cancer tumor response

Objective Response	RECIST
Complete response (CR)	The tumor vanished entirely and persisted for four weeks.
Partial response (PR)	30% reduction of the target lesion is maintained for four weeks.
Stable disease (SD)	Alteration between PR and PD
Progressive disease (PD)	The longest diameter of the target lesion grew by more than 25%.

3.7.2. Multidisciplinary Team (MDT) for Breast Cancer

The neoadjuvant chemotherapy results are typically interpreted by a multidisciplinary team (MDT) of healthcare professionals, including oncologists, radiologists, pathologists, and surgeons. This MDT meeting aims to evaluate the response to neoadjuvant chemotherapy, adjust the treatment strategy if necessary, and decide on surgery or additional treatment. Multidisciplinary team (MDT) work has become less common for breast malignancies due to the complexity of diagnosis and treatment decisions. A multidisciplinary team's ability to handle tumors based on the results of post-neoadjuvant chemotherapy was essential to our effort (MDT). Then, the patient needs a mastectomy or wide local excision (WLE) (Brown et al., 2022).

This dissertation examines the evidence for the effectiveness of MDT for breast cancer. Distributing some forms to these teams and including essential questions about the patient (family history (15% of the family has cancer and 75% does not), type of cancer, immunohistochemistry (IHC) (70% ER-PR Positive her to positive, 20% ER-PR Positive her to negative, and 10% triple negative), or

immunohistochemistry, previous H of breast operation, and lactation (90% yes and 10% no)) as depicted in Figure 3. 21.

Through this form, histopathology has been able to construct a program that determines whether a patient should undergo a mastectomy or a wide local excision, in addition to evaluating their contribution to quality development.

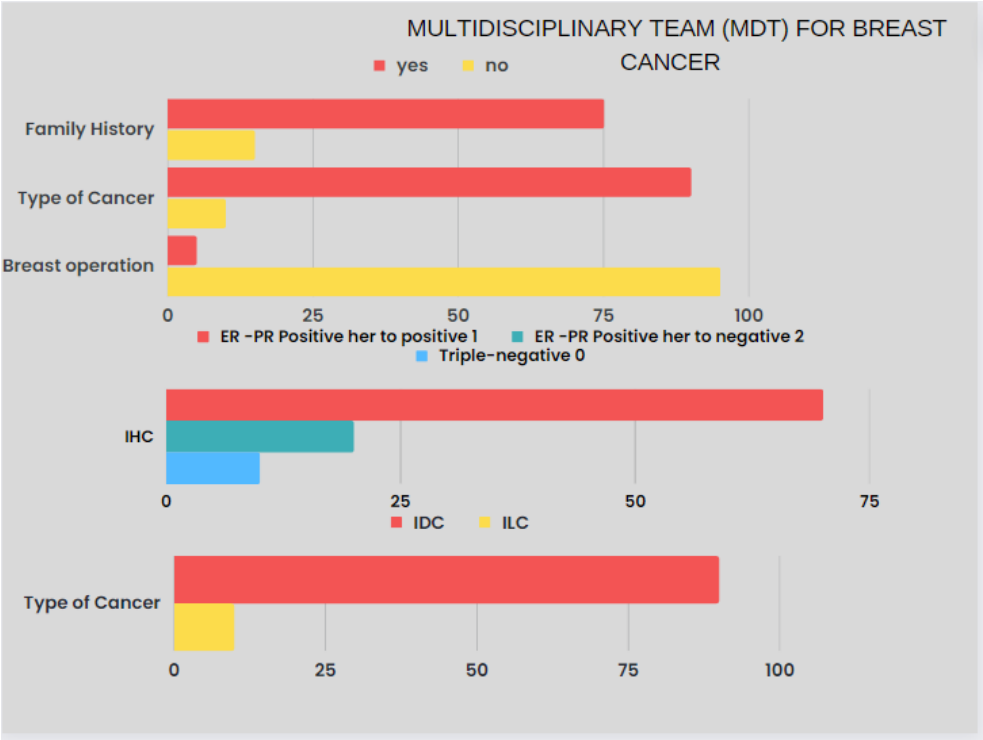

Figure 3. 21 Multidisciplinary teamwork (MDT) for breast cancer distribution of the two stages of mastectomy and WLE

3.7.3 General Structure of EfficientnetV2L is Used for Breast Cancer Classification

Google has recently introduced EfficientNetV2, a notable advancement over its predecessor, EfficientNet, in terms of training speed and a considerable

enhancement in accuracy. These models achieved a good balance between accuracy and model size, making them useful for a wide range of applications. EfficientNetV2L is a smaller and faster training system that seeks to provide a more efficient approach (Kumaraswamy et al., 2023). In addition, this work employs Attention (Att) and Feature Fusion (FF) techniques, which enhance the ability to represent features and the responsiveness of essential features. The entire structure of EfficientNetV2-L is presented in Table 3.3. EfficientNetV2 extensively employs the original fused MBConv and MBConv in its early layers. A smaller expansion ratio is preferred for MBConv as it generally results in lower memory access overhead. One of the strategies used in EfficientNetV2L in this study is the utilization of 3x3 kernels with reduced dimensions. Utilizing 3x3 kernels is relatively small and has fewer parameters compared to larger kernels like 5x5 or 7x7. This reduces the overall number of parameters in the model, making it more efficient and easier to train. This strategy helps achieve a balance between model efficiency and performance, making it a popular option for many computer vision applications. The component responsible for extracting picture characteristics remains unchanged, however, the ACON-C function has been substituted for the activation function in the dense layer.

Table 3. 3 Detailed Configuration of Efficientnetv2-L

Stage	Operator	Channels	Activation	Layers
0	Conv 3×3	24	SiLU	1
1	Fused- MBConv1, k3×3	32	SiLU	4
2	Fused- MBConv4, k3×3	32	SiLU	7
3	Fused- MBConv4, k3×3	64	SiLU	7
4	MBConv4, k3×3, SE0.25	96	SiLU/Sigmoid	10
5	MBConv6, k3×3, SE0.25	192	SiLU/Sigmoid	19
6	MBConv6, k3×3, SE0.25	224	SiLU/Sigmoid	25
7	Conv 1×1, BN	384	ACON-C	7
8	Pooling	1792		1
9	Dense	1792		1

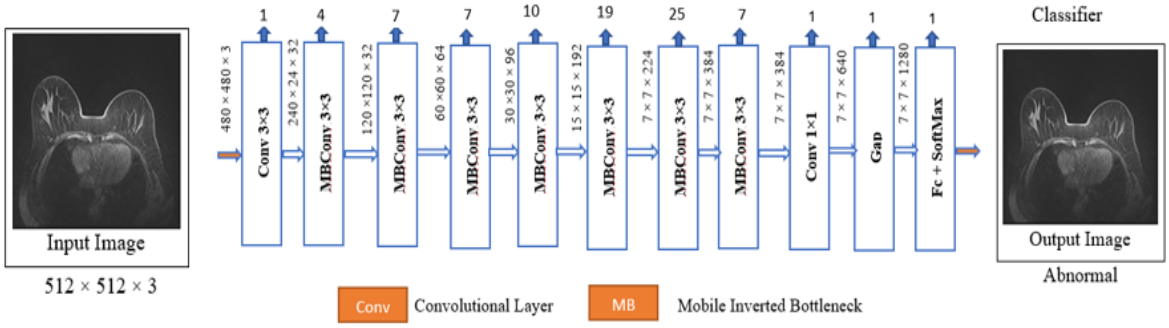

Figure 3. 22 The network architecture of EfficientNetV2-L

After the input data travels through the multi-layer network, it can produce a feature map with rich semantic information. Figure 3. 22 illustrates the structure of efficientNetV2-L, which consists of 84 layers and differentiates between normal and abnormal breast images. EfficientNetV2-L, a model derived from training-aware neural architecture search (NAS) and scaling techniques has superior training speed and parameter efficiency performance compared to previous models. Propose an enhanced methodology for progressive learning that incorporates adaptive adjustments to regularization and picture size. Research has shown that implementing this approach accelerates the training process and enhances precision.

3.7.4 The Mask RCNN for Breast Tumor Detection and Types of Malignant

Mask R-CNN is a powerful model for segmentation tasks, such as breast tumor identification, because it can identify and segment breast tumors in images, as well as provide bounding boxes and pixel-wise segmentation masks. Figure 3. 23 illustrates the network's architecture. Both faster R-CNN and mask R-CNN use

region proposal networks (RPNs) to classify and refine bounding boxes and extract features. Faster R-CNN employs ROI Pooler as a feature extraction method for quantifying each ROI region, followed by max pooling to address the issue of variable-scale ROI feature sizes.

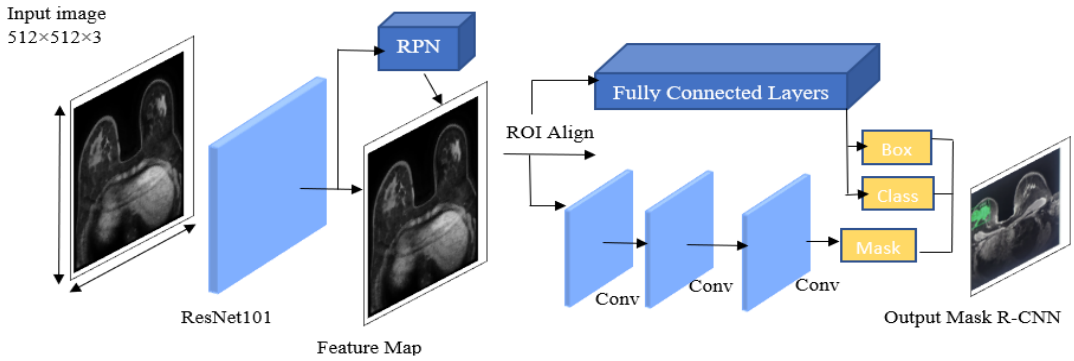

Figure 3. 23 The Mask R-CNN network architecture for compare between malignant and benign

This study employs the mask R-CNN model to distinguish between malignant and benign cases. Using the efficientNetV2L model, the image was inputted and compared between normal and abnormal conditions. If the image exhibits abnormalities, it undergoes the mask R-CNN method to discern any differences between the benign and malignant in Figure 3. 24. Then, the mask RCNN will compare the pre- and post-NAC if the image is malignant. Mask R-CNN is a prominent approach utilized for object detection and segmentation. The proposed method not only generates a bounding box around the target item but also performs pixel-level segmentation within the bounding box to determine whether each pixel belongs to the object.

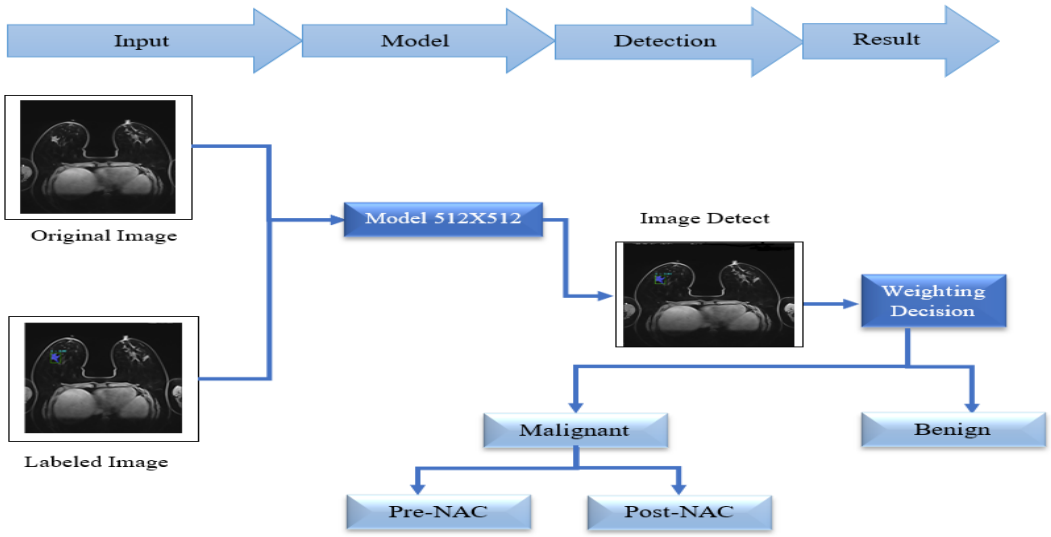

Figure 3. 24 Mask R-CNN for detecting between malignant and benign and types

3.7.5 The Detectron2 for Post-NAC Types Detection

The process of categorizing tumor responses in medical imaging after the delivery of neoadjuvant chemotherapy to a patient is widely referred to as post-neoadjuvant chemotherapy type detection. Neoadjuvant chemotherapy refers to the administration of chemotherapy to cancer patients before the commencement of the primary treatment, such as surgery, to reduce tumor size or improve the feasibility of the surgical intervention. The succeeding model was initialized after implementing the mask RCNN algorithm to distinguish between breast cancer images before and after neoadjuvant treatment. The trained model is subsequently employed with Detectron2 to perform a comparative examination of different post-neoadjuvant chemotherapy categories in DCE-MRI. In post-NAC it has been six types consisting of these (complete response, crumble, shrink, stable, diffuse enhancement, and progress); using this model, have been found these six species.

The methodology above is exclusively employed in the analysis of images about breast cancer-classified types of post-NAC, as depicted in Figure 3. 25.

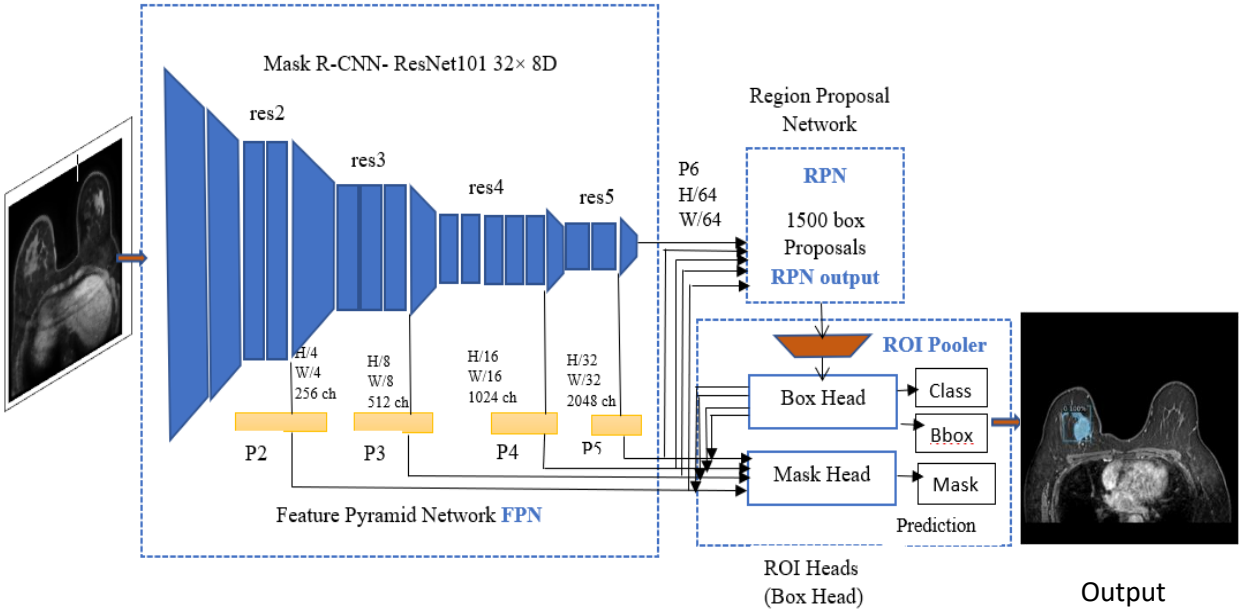

Figure 3. 25 The schematic architecture of Detectron2 used for type of Pre-NAC

3.7.6 The Detectron2 with Faster RCNN for WLE and Mastectomy's Breast Detection

The Detectron2 repository offers a wide range of pre-trained models for object identification. In this study, employed a model to perform fine-tuning on the dataset, a technique known as transfer learning. Figure 3. 26 illustrates utilizing Detectron2 with faster R-CNN to detect and classify breast regions in MRI images of wide local excision and mastectomy.

The utilization of Detectron2 with faster R-CNN presents a robust and effective approach for accurately and efficiently detecting the breast region in MRI images. By integrating the capabilities of faster R-CNN and the adaptability

offered by Detectron2, the generation of predictions can be enhanced in terms of accuracy. The utilization of the pre-trained mask R-CNN model is deemed suitable for this experiment due to its capability to anticipate bounding frames and masks for identified items.

The proposed method in the dissertation it is used to identify the difference between the right and left sides breast by analyzing the shape and appearance of the breast tissue in the MRI images.

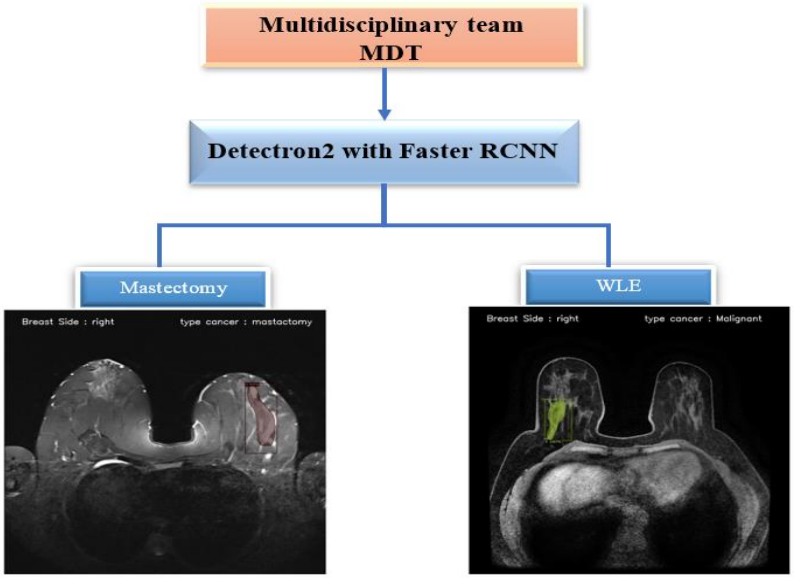

Figure 3. 26 The example used Detectron2 with Faster RCNN

3.8 Evaluation Criteria and Analyzing

The performance of machine learning algorithms is assessed using various evaluation metrics. While some algorithms excel on certain datasets or classes, others may struggle with different data or classes. This highlights the absence of a universally optimal algorithm. The primary purpose of evaluating a classification model is to accurately gauge its performance. Common evaluation methods

include the confusion matrix, accuracy, error rate, receiver-operating curve (ROC), area under the ROC curve (AUC), sensitivity, specificity, precision, and the F1-score.

3.8.1 Confusion Matrix

The confusion matrix serves as a detailed table that visualizes the classifier's effectiveness. In machine learning, the confusion matrix is often termed the error matrix. For image data, each pixel is classified as either positive or negative. Furthermore, the classification of a detected image area can be correct (true) or incorrect (false). As a result the decision will thus fall into one of four categories: True Positive (TP), True Negative (TN), False Positive (FP), or False Negative (FN) (FN). The right choice is represented by the diagonal of the confusion matrix.

The relation between positive class and negative class predictions can be depicted as a 2×2 confusion matrix in Table 3.4 that tabulates whether the obtained prediction falls into one of four categories.

Table 3. 4 Confusion matrix

Actual Class	**Predicted Class**	
	Positive	**Negative**
Positive	TP	FN
Negative	FP	TN

Accuracy: is the proportion of true positive and true negative divided by a total number of predictions. The best accuracy is 1, whereas the worst is 0. With the 2×2 confusion matrix, the formula of prediction accuracy is shown in Eq. 3.2.

$$\text{Accuracy} = \frac{TP+TN}{TP+TN+FP+FN} \quad \text{.....(3.2)}$$

3.8.2 Receiver Operating Characteristic (ROC)

The sensitivity and specificity for multiple values of a continuous test measure are combined to produce a receiver operating characteristic (ROC) curve. Charting sensitivity on the y-axis (TPR) versus 1-specificity on the x-axis (FPR) for each tabulated data yields the ROC curve. Figure 3. 27 demonstrates a typical ROC curve. The TPR is also known as the sensitivity or recall, and the FPR may be computed as the product of the specificity and the sensitivity. Any curve that is located above the diagonal line is indicative of a good classification model that is superior to random, but any curve that is located below the diagonal line indicates that the model is inferior to random.

A perfect binary classification model would provide a straight line from (0, 1) to (1, 1) as the output. This would indicate that the model has a sensitivity of 100% and a specificity of 100%.

The area under the ROC curve is referred to as the AUC and its value is always between 0 and 1. When examining binary classification models using the ROC curve approach, one might reach the conclusion that a greater AUC indicates a superior model. The area under the curve (AUC) for a random. (Namdar et al., 2021).

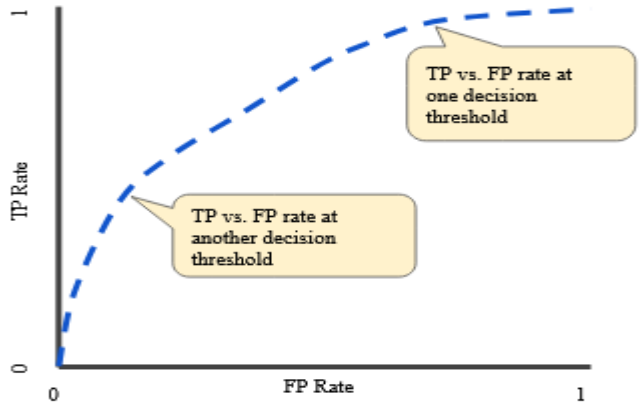

Figure 3. 27 The TP vs. FP rate at various categorization levels (Zhu, 2020).

Sensitivity (Recall): sensitivity refers to the model's capability to predicate the samples that belong to a class. The sensitivity (Recall or True positive rate) measures the proportion of positive examples that are correctly classified; its formula is in Eq. 3. 3.

$$\text{Sensitivity (Recall)} = \frac{\text{TP}}{\text{TP+FN}} \quad \ldots\ldots(3.3)$$

Precision (PR): precision is known as positive predictive value (PPV) that presents how the model predicts the correct class/pixel. It displays the correct proportion of models predicted positives; its formula is in Eq. 3.4.

$$\text{Precision (PR)} = \frac{\text{TP}}{\text{TP+FP}} \quad \ldots\ldots(3.4)$$

Specificity: specificity refers to the model's capability to mark that samples do not belong to this class. It measures the proportion of negative examples that correctly classified, and its formula is as in Eq. 3.5. The range of these parameters is from 0 to 1, when the values close to value 1, they are being more desirable.

$$\text{Specificity (SP)} = \frac{\text{TN}}{\text{TN+FP}} \quad \ldots\ldots(3.5)$$

F1 score: The F1 score represents the mathematical middle ground between accuracy and recall. It is a statistical measurement that is used in the process of rating performance. In other words, a score on the F1 scale ranges from 0 to 9, with 0 being the lowest possible score and 9 representing the best possible score. Therefore, this score takes both false positives and false negatives into account. The F1 score is defined as in Eq. 3.6.

$$\text{F-Score} = \frac{2\times\text{Percision}\times\text{Sensitivity}}{\text{Percision+Sensitivity}} \quad \ldots\ldots(3.6)$$

3.9 Summery

This dissertation presents a comparative analysis and two models, as detailed in the preceding sections. The exploration of machine learning algorithms commenced as the initial research direction. Feature extraction employing four distinct methods holds promise for improving the diagnosis of benign and malignant tumors using machine learning techniques. This study implemented six primary algorithms on three datasets. The subsequent chapter presents a comprehensive explanation of the results derived from the three datasets.

Model one (BTRD): This model unveils a holistic methodology for attaining optimal mammographic breast cancer diagnosis. This research stands out as the most effective solution against false-negative and false-positive predictions, despite requiring only minimal modifications to existing algorithms. With advancements in technology, incorporating additional refinements can propel this algorithm into a significantly more sophisticated tool for locating and eliminating cancer cells within the detected area.

Model two (ADBMD): This project seeks to develop a deep learning-powered system that can aid physicians in making diagnostic decisions. The model introduced here is a CAD system designed to detect breast malignancies in MRI and DCE-MRI images. To pinpoint the region of interest in a breast MRI image during the localization phase, an artificial segmentation technique based on local active outlines has been developed.

CHAPTER FOUR

4 RESULTS AND DISCUSSION

4.1 Introduction

This chapter presents the outcomes and performance assessments of all proposed methodologies which are presented in chapter three. Also, the techniques used for data augmentation are explained. In addition, a couple of different pieces of software have been used to guarantee accurate results, such as MATLAB which provides a large and diverse range of new functions related to the image processing field such as machine learning. Waikato Environment for Knowledge Analysis (WEKA 3.9.3) was perfect in preprocessing operations for datasets, testing the traditional machine learning algorithm, and selecting feature attributes of the datasets. Hence, this dissertation employed Python 3 and a GPU to conduct experiments and evaluate the influence of extracting various characteristics on the accuracy of the classification models developed. Additionally, RadiAnt software was used to execute the experiments and resize the images. Nevertheless, the early detection of mass abnormalities by screening mammography and MRI enables treatment and can even save a patient's life. The most significant aspect of the development of (CAD) systems is the automation of the early detection of breast cancer. The evaluation outcomes of the proposed models can be divided into three major sections: (1) Evaluation of machine learning algorithms; (2) breast tumor measurement identification; (3) automatic detection of breast cancer for mastectomy. In addition, various experiments are considered and carried out in three stages, and results are generated accordingly.

4.2 Implementation Environments

4.2.1 Tools for Modeling and Data Collection

Weka 3.9.6 (Bouckaert et al., 2013) is a robust data mining, machine learning, and visualization software for large datasets. The program's intuitive graphical interface enables non-technical users to investigate their data and rapidly generate insights. It supports algorithms such as decision trees, neural networks, SVMs, clustering methods, and association rule mining techniques, which can be used for classification, regression analysis, and predicting future trends in the analyzed data set. In addition, Weka provides various visualization options to help users gain a deeper comprehension of their dataset's structure or patterns, making it an indispensable tool for any organization seeking to make informed decisions based on its available datasets.

RadiAnt (DICOM, 2013) is a powerful and intuitive DICOM viewer program designed to meet the needs of medical professionals. It offers an easy-to-use user interface with various features, including advanced visualization tools, support for multiple modalities and image formats, comprehensive annotation capabilities, and integration with a Picture Archiving and Communication System (PACS) systems. RadiAnt's fast loading times and high-performance image processing algorithms can be used in clinical settings and research applications for efficient diagnosis or data analysis.

MATLAB 2021b is a programming software package scientists, engineers, and researchers use to analyze data. It offers an extensive library of functions for computer vision, deep learning, statistics, Fourier analysis, optimization, and more. With its intuitive Graphical User Interface (GUI), users can easily create scripts or programs in the MATLAB language that help automate complex tasks such as data processing or simulations. The program also includes interactive tools

for quickly creating graphs from any dataset with minimal effort required from the user.

Python 3.7 is a general-purpose programming language with a high level of abstraction. It has an easy-to-read syntax, making it suitable for both novice and experienced programmers. Due to the numerous packages and libraries it provides, it is a potent language in data science.

PyCharm is a specialized integrated development environment (IDE) for Python programming. It was developed by JetBrains, a software startup renowned for producing productivity-enhancing tools for developers. PyCharm provides comprehensive features and tools for Python application development, testing, and debugging. It is available in two editions: a free, open-source Community Edition and a for-profit Professional Edition with more advanced features.

Based on **Torch**, PyTorch is an open-source machine-learning application. This provides a dynamic and adaptable strategy for constructing and training neural networks. Tensor Flow version 1.15.0: This is a variant of the TensorFlow framework for deep learning. Tensors are multidimensional arrays with outstanding computational and graphical capabilities.

Several other libraries have been used in this dissertation, such as Keras V.2.2.5, Numpy V.1.21.6, Anaconda any version, Open CV V.4.1.1.26, Scikit Image V.0.16.1, Matploit lib V.3.5.3, and Imagug V.0.4.0.

4.2.2 Preprocessing Datasets

Chapter Three shows that different breast cancer MRI images and mammography datasets have been used and collected. Due to hardware limitations and the proposed research methods, all images in the databases were resized to different dimensions, and different preprocessing operations were applied. In the

project or study involving image data, certain adjustments were made to the images for practical and methodological reasons. In the context of image processing and machine learning, hardware limitations could refer to constraints in terms of memory, processing power, or the capabilities of the imaging equipment (e.g., MRI equipment or scanners). These limitations can make working with images in their original, high-resolution formats challenging. These modifications were made to overcome practical challenges and ensure that the research could be conducted effectively, even though they may introduce variations and alterations to the image data. The preprocessing techniques applied to datasets depended on the models used in these methods. The main techniques used in the training datasets were the following:

1- Increasing brightness or contrast (randomly chosen).

2- Decreasing brightness or contrast (randomly chosen).

3- Noise reduction.

4- Image resizing.

A sample chosen at random or method is one in which all of the variables have an equal chance of being selected. Randomness is frequently added to algorithms to improve their modeling and robustness. The above preprocessing techniques are reasonable for the data collection setup. However, it is worth mentioning that each breast cancer image collected and augmented for each model and method differed depending on the problem. Adopting various image processing techniques encourages researchers to develop new datasets and methods to generate variations of samples from existing dataset samples, such as the data augmentation technique described in the following section. Table 4. 1 depicts the characteristics of all datasets utilized in this dissertation.

Table 4. 1 Datasets used in this dissertation and their purposes

Dataset	Total No. of Images	Type of Purposed
Erbil and Sulaymaniyah Breast MRI	920	Classification of tumor type
ACRIN-Contralateral-Breast-MRI	1280	Classification of tumor type
Breast Cancer MRI	400	Classification of tumor type
Mammography	510	Detection and Classification of tumor type
DCE-MRI	800	Detection and Classification of tumor type

4.2.4 Experimental Setup

The experiments have been conducted by splitting the dataset into training and testing. The training dataset is used to train an algorithm for machine learning. During training, the algorithm learns to recognize data patterns and modifies internal parameters to minimize error. The more diverse and representative the training dataset, the greater the algorithm's ability to generalize to new, untested data.

Each database was divided into three subsets: training, validating, and testing. In other datasets, 80% of the data was used for training, 10% for testing, and 10% for validation. The acquisition of a dedicated dataset for breast cancer detection entails the following two components:

(1) Images of breast cancer typically refer to a dataset or a compilation of medical images acquired from patients' breasts using MRI and mammography

technology. These images are compiled to assist with breast cancer detection, diagnosis, and monitoring.

(2) Image processing: The images are annotated with the VGG Image Annotator (VIA) application tool, labeled, and separated into training and evaluation sets. The specific stages of this procedure are described below.

First, the folder "dataset" is created, followed by the subfolders "train" and "val" for training samples and test samples, respectively. The images in each mask RCNN and detectron2 folder correspond to a JavaScript Object Notation (JSON) format labeled by VIA annotation software. The interface for labeling is depicted in Figure 4. 1.

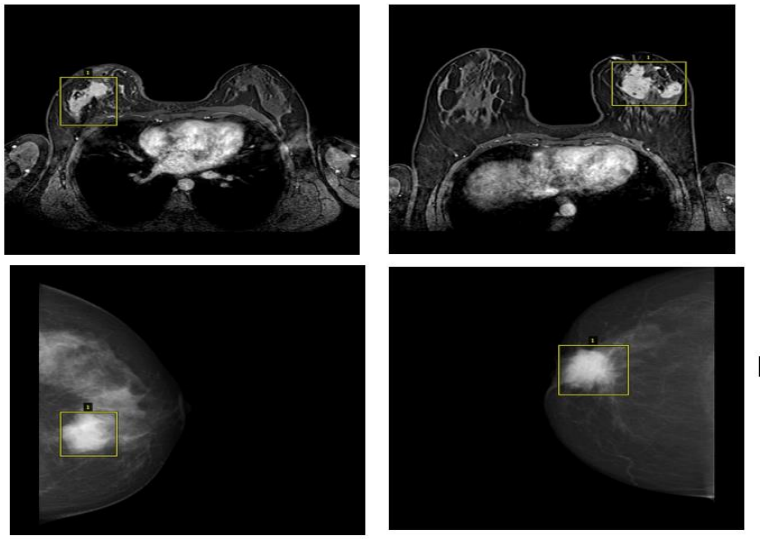

Figure 4. 1 Sample using VIA labeled breast cancer images

4.3 Evaluation Results of the Proposed Models

Evaluation of proposed models in research is essential for determining their efficacy and comparing them to existing models or standards. The evaluation

results shed light on the performance of the proposed model in terms of precision, recall, F1 score, and other relevant metrics.

This thesis presents three models for segmenting mammograms and detecting breast cancer using MRI. The first model is founded on the performance evaluation of machine learning algorithms for breast cancer recognition. On mammograms, the second model entails identifying breast tumor type and size. Based on MRI images, the third paradigm is the automated detection of breast cancer for mastectomy.

4.3.1 First Experiment: Evaluation Results of Breast Cancer Recognition Using Traditional Machine Learning

Initially, the proposed method incorporated machine learning techniques that are now extensively employed in breast cancer classification. This study investigated machine learning techniques to diagnose BC using MRI images. chapter three provides additional information on the model's design and how it was proposed. The subsequent sections describe the implementation and evaluation of the model. Our breast cancer dataset was previously preprocessed for the training phase. The study utilizes MRI images as input preprocesses, isolates features (Sift, HOG, LBP, BoW, and EOH), and employs diverse classifying algorithms (KNN, decision tree (DT), Naive Bayes, ANN, SVM, RF, and AdaBoost). Breast cancer MRI images from Erbil and Sulaymaniyah Hospitals have been used to evaluate the efficacy of breast cancer regions using datasets such as (the ACRIN-Contralateral-Breast-MRI) and (the Breast Cancer MRI dataset).

4.3.1.1 The Datasets Used

The proposed system utilized three datasets, two datasets are public, and the third one is private. The three datasets have been comprehensively elucidated in the preceding sections, emphasizing the number of images and various significant details about each dataset. The files have been scaled using the RadiAnt tool, a widely utilized medical program across multiple healthcare facilities. The dimensions of each image are 512 by 512, a size that has been determined to be optimal for displaying cancer images based on previous research findings. Furthermore, two additional software have been employed. The initial software utilized for the outcomes and characteristics is MATLAB 2021b. The second tool, Weka, is used for classification purposes. Table 4. 2 presents the methodology employed for selecting and allocating samples from the three datasets used to implement these methods.

Table 4. 2 The mechanism for distributing and choosing samples from datasets

No. of Selected Dataset	**Normal**	**Training**		**Testing**	
1280 images selected randomly	80	900		300	
		Benign	**Malignant**	**Benign**	**Malignant**
		300	600	120	150
400 images selected randomly	50	225		75	
		Benign	**Malignant**	**Benign**	**Malignant**
		20	205	30	45
920 images selected randomly	70	640		210	
		Benign	**Malignant**	**Benign**	**Malignant**
		100	540	90	120

4.3.1.2 Results and Evaluation

The efficacy of the suggested methodology is evaluated using authentic MRI images of patients diagnosed with breast cancer. The three datasets consist of volume MRI images of patients categorized as benign, malignant, or normal. Five feature extraction methods and six classification algorithms were evaluated on three datasets, employing preprocessing techniques for image scaling. The results indicate that using the aforementioned methodologies and algorithms in conjunction with this model is an appropriate combination. Also, found that in this model, the best method and the best algorithms. The HOG method achieved the highest performance in conjunction with ANN for classification across three datasets. Specifically, a classification accuracy of 94% was attained for the Erbil and Suleimani breast cancer datasets. For the second dataset, BC MRI, the BoW method combined with ANN achieved a classification accuracy of 96%, while the Naïve Bayes method achieved 97% accuracy. Lastly, for the third dataset, ACRIN-Contralateral-Breast-MRI, the BoW method, in combination with Adaboost, achieved a classification accuracy of 99%, and the HOG method, in conjunction with ANN, achieved 98% accuracy. The effectiveness of the methods and classifiers is evident in the results presented in Table A.1 and Figures A.1, A.2, and A.3.

The sets are divided into training and testing parts in Tables A. 2, A. 3, and A. 4. This dissertation used a 75/25 split for training and testing. This means that 75% of the data was used for training, and 25% of the data was used for testing. This is a common split ratio for training and testing sets. There are multiple ways to divide a dataset into training and test sets. One of the methods employed here is the division of datasets, which is random splitting. This method randomly divides the dataset into training and test sets.

It's a straightforward approach and is often used when there are no specific considerations for data distribution or order. Although tables display the results, as shown below and the results in the table are improved or clearer.

The algorithms' accuracy, precision, sensitivity, and f-score must be assessed to determine optimal classification accuracy. The bag of words model, SIFT descriptors, and HOG approaches outperform other breast cancer image classification methods. After carefully evaluating our models, the Artificial Neural Network, Support Vector Machine, and AdaBoost algorithms performed best. These algorithms outperform all others with 96% sensitivity and 97% precision. In summary, artificial neural networks, support vector machines, and AdaBoost machines have shown higher accuracy and precision in breast cancer prediction and detection. This study's findings apply only to the three datasets. This constraint highlights the need for further research to use these methods in more databases.

4.3.2 Second Experiment: Recognition of Breast Tumor Type and Size on Mammograms using Deep learning models

In this model, a method is proposed for the classification, segmentation, measurement of tumor size and classification of breast varieties. Chapter 3 provides additional information regarding the model's design and how it was proposed. In this chapter, described the model's implementation and evaluation. Our preprocessed breast cancer dataset was previously compiled for training purposes.

ResNet152V2 is an additional classification model used to determine whether a breast type is normal or cancerous. Using ResNet152V2, the system could compare categories with an overall accuracy of 100 percent. Using Mask R-CNN, its ability to detect masses accurately differentiates benign from malignant

tumors with 98% accuracy. Mask R-CNN is a deep learning algorithm that can detect multiple objects in an image and generate a mask around each object using the instance segmentation process. Mask R-CNN extends Faster R-CNN by adding a branch for predicting object masks in addition to the existing branches for bounding box detection and classification.

4.3.2.1 Datasets Used in These Models

The evaluation of the proposed model is conducted using a dataset including 510 mammography images. To enhance the categorization process, the dataset was partitioned into subsets based on the distinction between images depicting the left and right breast. The mammographic pictures included in this investigation were sourced from the ZIHE collection, curated specifically for research endeavors. Chapter three provides a comprehensive explanation of the original dimensions of all the color photographs. Ideally, it is advantageous to correct the photos before commencing the processing phase. Table 4. 3 presents a visual representation of the distribution of the dataset under examination.

Table 4. 3 Mammography dataset description that is collected of (Zhen Erbil Hospital)

Mammography dataset number	**Benign**		**Malignant**	**Normal**
510	210		178	122
Character of background tissue composition	Fatty Type (A)	Fibro Glandular Type (B)	Heterogeneously Type (C)	Extremely Dense Type (D)
	128	154	158	70

4.3.2.2 Preprocessing Datasets

Pre-processing is the process of preparing data for analysis or machine learning. It involves converting unstructured data into a format that can be readily analyzed or utilized to train a machine-learning model. The primary objective of this study is to develop a model that can distinguish between normal, malignant, and benign tumors and classify breast density types varieties based on mammograms. The proposed architecture is divided into three phases. Beginning with the collection of the dataset as described above, the dataset then went through three stages.

1. The Data Augmentation Algorithm (DAA) is a technique that uses machine learning and computer vision to enlarge datasets. This is particularly essential when working with small amounts of data, as it can help improve the performance and generalizability of machine learning models. A set of transformations can be applied to the training data in this work. In this model, we employ flip, a frequent form of data augmentation.

There are two significant varieties of flips: vertical (y-axis) and horizontal (x-axis). Used a single X-axis type, and each image in the collection is vertically mirrored. This means the left side of the image becomes the right side, and vice versa. The intricate data augmentation algorithm is depicted in Figure 4. 2. As a result, an input image will yield two images.

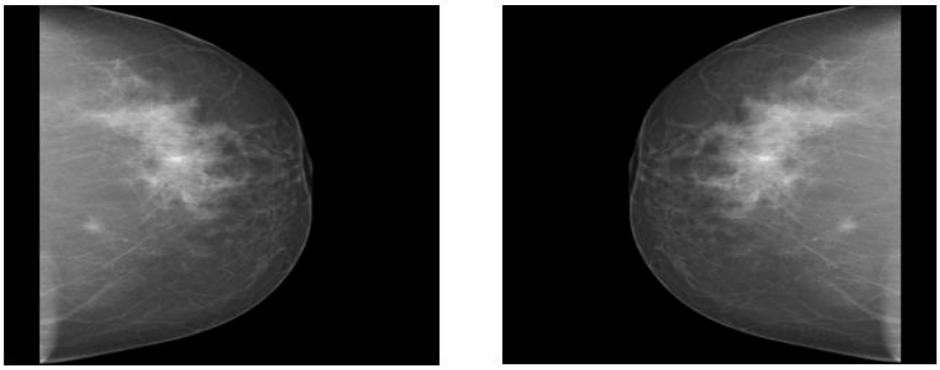

Figure 4. 2 Rotating images around the x-axis

2. Data Resizing: Data downsizing is an important step in preparing input data for machine learning algorithms. It comprises eliminating or reducing redundant data from the dataset. This is done to improve the overall performance of the machine learning model by optimizing computational efficiency. This step helps eliminate redundancy in the input data by ensuring that all input images have the exact dimensions. This, in turn, reduces the computational complexity of the network, as you do not have to deal with images of varying sizes during training and inference. It also simplifies the neural network architecture design, as the input layer's dimensions are fixed. This is made feasible by the Python/Keras preprocessing library. After experimenting with various image dimensions, have been settled on 512 by 512 pixels, which reduces the image dimensions by 48 by 48 pixels-preserving image legibility while effectively utilizing computational complexity.

3. Data Reshaping: is a fundamental preprocessing step in machine learning and deep learning workflows. It involves changing the shape or dimensions of your data to make it suitable for input into a particular algorithm or

model. This stage modifies the ResNet-152V2 input layer to accommodate the input geometry of our preprocessed dataset ($ImgWidth$ = 48, $ImgHeight$ = 48, $NoChannels$ = 1) grayscale images. This is accomplished with the aid of the Python/ Keras preprocessing library.

4.3.2.3 Experimental Tools

Python was used to carry out these labor experiments. Python is the finest programming language for deep learning, data science, and machine learning and is widely used in these fields. Anaconda is a scientific Python and programming language distribution.

Tensor Flow version 1.15.0 is a free and open-source machine learning software library. It can be used for various tasks, but the training and inference of deep neural networks are its primary focus. The open-source software library Keras, version 2.2.5, provides a Python interface for artificial neural networks. Keras serves as the TensorFlow library's interface. OpenCV (Open-Source Computer Vision Library) is a collection of programming functions geared primarily toward real-time computer vision.

PyCharm is an integrated development environment (IDE) utilized in computer programming, specifically for Python. Table 4. 4 displays the hyperparameters for the Mask R-CNN framework based on TensorFlow.

Table 4. 4 TensorFlow-based Mask R-CNN

Batch_Size	1
Detection_Max_Instances	100
Detection_Min_Confidence	0.9
Gpu_Count	1
Images_Per_Gpu	2
Learning_Rate	0.001
Num_Classes	3
Steps_Per_Epoch	100
Weight_Decay	0.0001
Validation_Steps	50
Use_Mini_Mask	True

This means that the model will process 100 batches of training images per epoch. The batch size is specified as 1, so each batch will contain 1 image. The model will use a total of 100 * 1 = 100 images per epoch. However, it is important to note that this is just the number of images that the model will process during training. The actual number of images that the model needs to see in order to learn to detect objects accurately will vary depending on the specific dataset and model architecture being used.

4.3.2.4 Experimental Setup

The data set was divided into three sections: an 80% training set for model optimization outcomes, a 10% testing data set for model evaluation and recording of testing outcomes, and a 10% validation dataset for model optimization. Initially, using the mammography images and precise positioning images provided by the

doctor, clusters of classification points will be learned, separated from non-clusters, and the CNN model is trained. CNN then separated the images of the right and left breasts using the model. The system utilizes the ResNet152V2 model to extract cluster characteristics. The model is then applied to Mask R-CNN to classify clusters as benign or malignant and to determine tumor size. For each experimental batch size = 1 and epochs = 60, they have been adapted to the optimized Mask R-CNN parameters. Each experiment's results and testing will be discussed in depth.

4.3.2.5 Result and Discussion

In this work, first, features have been selected from the dataset has been collected in the hospital. In general, the system consists of three models for breast mammogram images. That is three feature-selection algorithms, namely, CNN, ResNet152V2, and Mask R-CNN. Table 4. 5 depicts the cluster classification performance of a convolutional neural network. Table 4. 6 depicts the classification performance of breast density types using the ResNet152V2 algorithm with a 98% accuracy rate. The accuracy of Mask R-CNN's breast cancer detection performance is 97% as shown in Table 4. 7. The precision, specificity, and sensitivity of our suggested methods are also approximately 98% percent, 99% and 97% respectively. This proves the reliability of our investigation. Four methods are used to evaluate the models: accuracy (AC), precision (PR), sensitivity (SE), F-Score (FS), and specificity (SP), where TP denotes true positive, TN denotes true negative, FP denotes false positive, and FN denotes false negative.as

Table 4. 5 Breast cancer classification performance of CNN for right and left

Method	Testing performance				
	Sensitivity	**Precision**	**Specificity**	**F-Score**	**Accuracy**
Right	98.3%	97.4%	97.3%	97.3%	98.5%
Left	97.3%	98.6%	98.3%	97.6%	97.3%

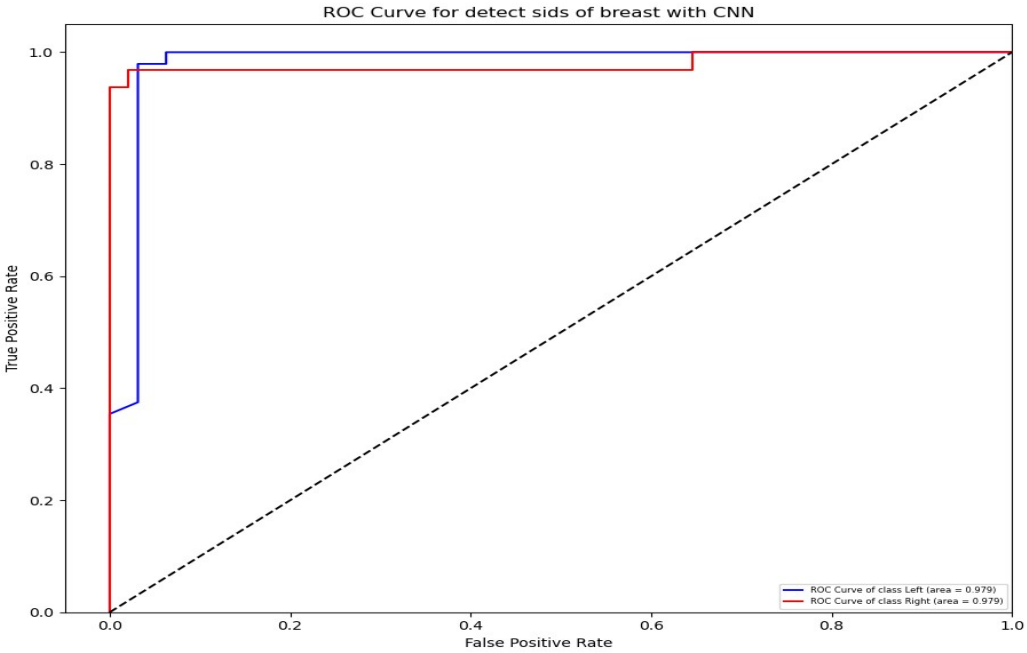

Figure 4. 3 CNN ROC for breast right and left

Figure 4. 3 depicts the utilization of a convolutional neural network (CNN) that underwent training employing an input image of dimensions 512-by-512 pixels. The ROC curve illustrates a potential trade-off between accuracy and error rates for the specified class and provides a summary value (0 to 1). It is an analysis of the entire data set, including comparisons between the right and left breast,

using CNN; the Roc curve of class left =0.979, Roc curve of class right =0.979, and the area under the curve (AUC) = 0.979; total predict image process time duration was 2.26 seconds.

1. ROC for RestNet152V2

The presented Table 4. 6 displays the outcomes obtained from the application of RestNet152V2 on the dataset under examination. The table also highlights the disparities observed among the several types (A, B, C, and D) of breasts, indicating whether each type is classified as normal or abnormal.

Table 4. 6 Breast density type classification performance ResNet152V2

Method		**Testing performance**				
		Sensitivity	**Precision**	**Specificity**	**F-Score**	**Accuracy**
Type A	Abnormal	96.3%	100%	100%	98.1%	98.1%
	Normal	100%	100%	100%	100%	100%
Type B	Abnormal	92.5%	100%	100%	93.9%	93.9%
	Normal	100%	93.8%	96%	94.3%	94.3%
Type C	Abnormal	100%	94.0%	96%	91.3%	91.3%
	Normal	100%	96.0%	97%	98.0%	98.0%
Type D	Abnormal	100%	100%	100%	100%	100%
	Normal	100%	95.7%	96%	97.8%	97.8%

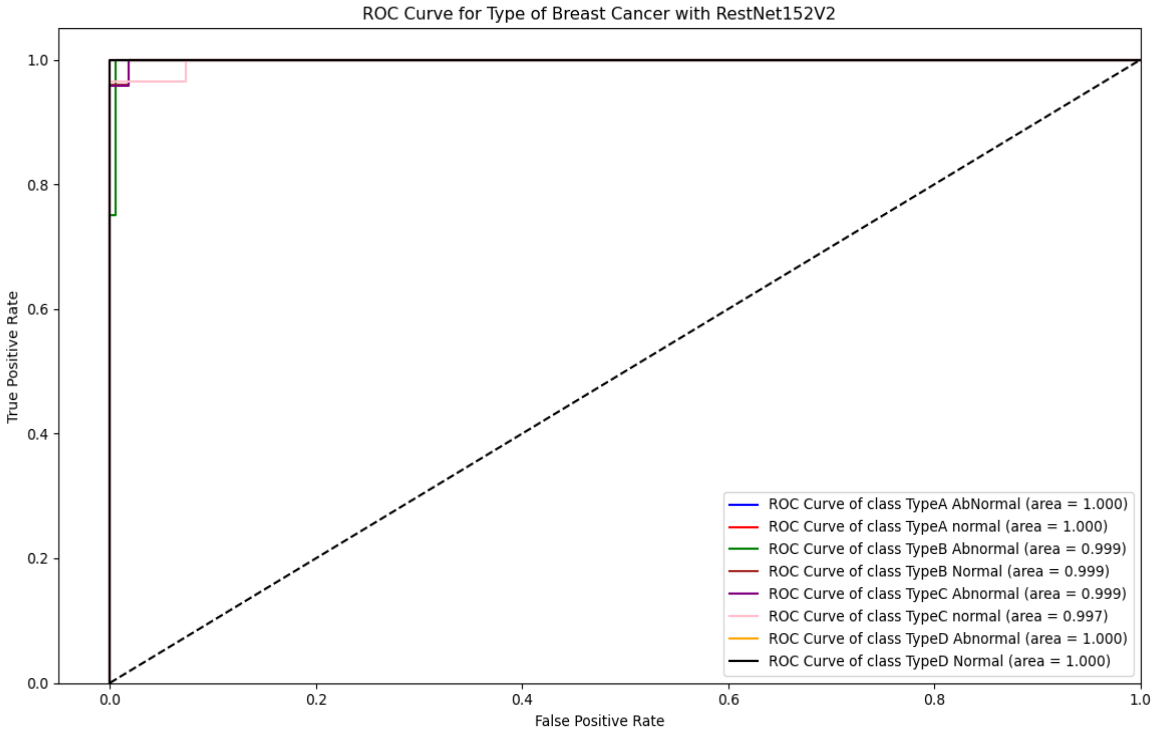

Figure 4. 4 ResNet152V2 ROC for breast types

Figure 4. 4 presents the analysis results encompassing the whole data set, which encompasses various breast types and distinguishes between normal and abnormal findings on a mammography image. The receiver operating characteristic (ROC) curve for class type A, encompassing both normal and abnormal instances, has an area under the curve (AUC) of 1.000. Similarly, class type B has an AUC of 0.999, class type C has an AUC of 0.998, and class type D has an AUC of 1.000. The overall time duration of the prediction image processing amounted to 0.01 seconds.

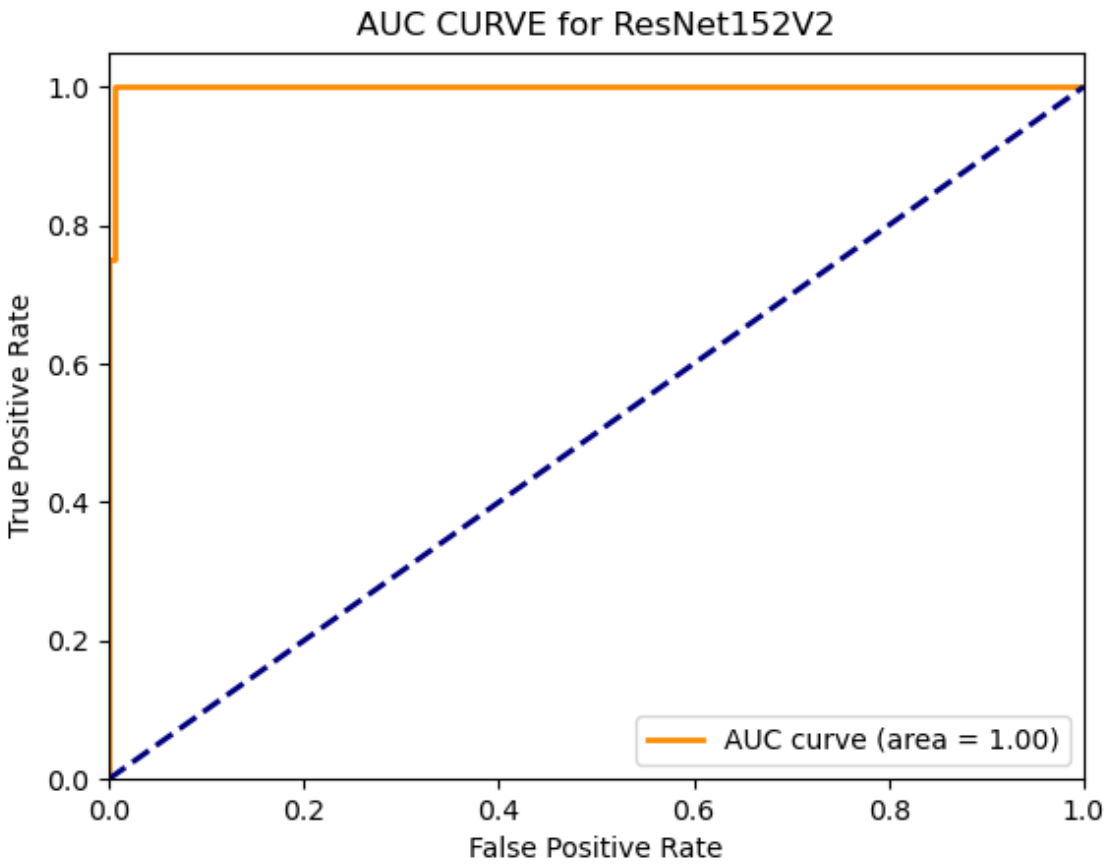

Figure 4. 5 Area Under the Curve (area= 1.000) by using ResNet152V2

Figures 4. 5 display graphs depicting the area under curves (AUC) of the true positive rate (TPR) against the false positive rate (FPR). It is evident from the figure that the proposed model exhibited superior performance compared to all other experimental methodologies, achieving an AUC of 1 for the specific breast type.

2. ROC Mask RCNN

Table 4. 7 presents the assessment results of Mask R-CNN on the designated test dataset, specifically for the classification of malignant and benign cancer

kinds. The table provides a breakdown of the evaluation performance for each method (AC, FS, SE, PR, and SP), with detailed explanations.

Table 4. 7 Breast cancer classification performance of Mask R-CNN

Mask R-CNN	**Testing performance**				
	Sensitivity	**Precision**	**Specificity**	**F-Score**	**Accuracy**
Malignant	96.6%	98.7%	96.4%	97.6%	96.5%
Benign	96.4%	92.0%	96.6%	94.1%	96.5%

Subsequently, the Mask RCNN algorithm was employed to determine the size of the tumor region. Radiologists in the field of radiology employ the RadiAnt DICOM Viewer program to determine the size of an area in an image. It is established that every 790 pixels in the image corresponds to a length of 1 cm. The size of the tumor area, denoted as illustrated in equation 4.1, is determined using this conversion factor, as shown in Fig. 4. 6. Subsequently, the Mask R-CNN technique is employed to identify the region of interest (ROI) for each image.

$$\text{Area tumor} = \frac{area\ Mask}{790\ pixel} \quad \text{.....(4.1)}$$

In RadiAnt:

$2.5cm^2$ =1976 pixel.

1cm= 1976/2.5= 790 pixel.

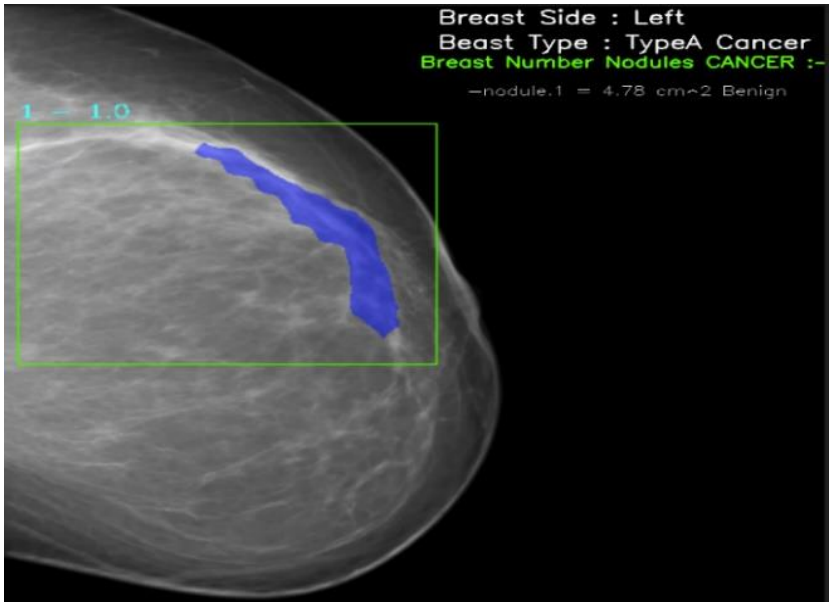

Figure 4. 6 Example the area tumor size

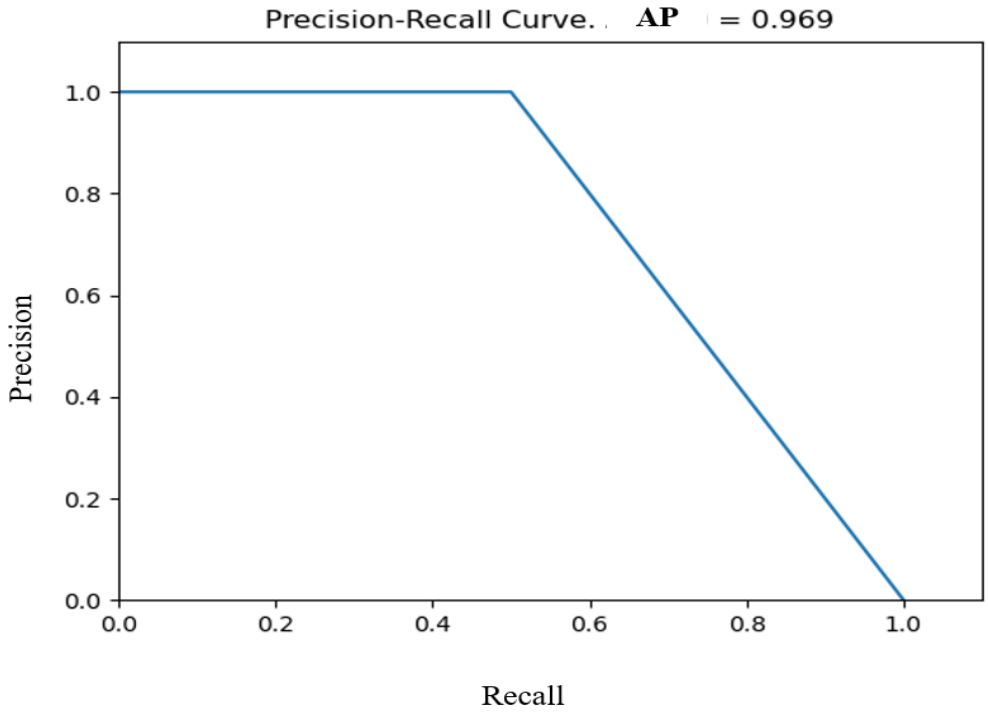

Figure 4. 7 The precision-recall curve of Mask R-CNN at AP = 0.969 in the training set

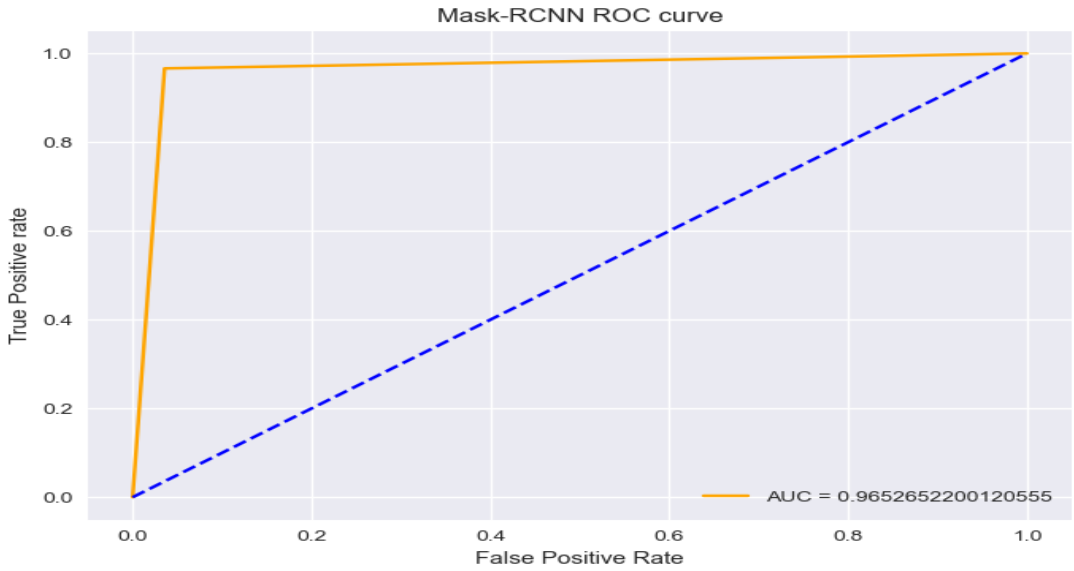

Figure 4. 8 Area Under the Curve (area= 0.965) by using Mask R-CNN

Figures 4. 7 and 4. 8 depict the Precision-Recall outcome obtained from the use of the mask RCNN detector on the test dataset. The Mask RCNN model has demonstrated exceptional performance in accurately detecting and classifying various types and sizes of breast cancer tumors. The precision confidence of the model exceeded 96%, as depicted in the figures presented.

Table 4. 8 Distribution of each type of breast image in training, validation and test set

	Type A	**Type B**	**Type C**	**Type D**
Training	120	100	111	93
Validation	10	10	11	12
Testing	10	10	11	12

The aforementioned Table 4. 8 presents data pertraining to the distributions of mammography images for breast cancer. In order to obtain precise and current statistics regarding the distribution of breast image categories within a certain dataset, it is imperative to elucidate the distinctions between various forms of breasts.

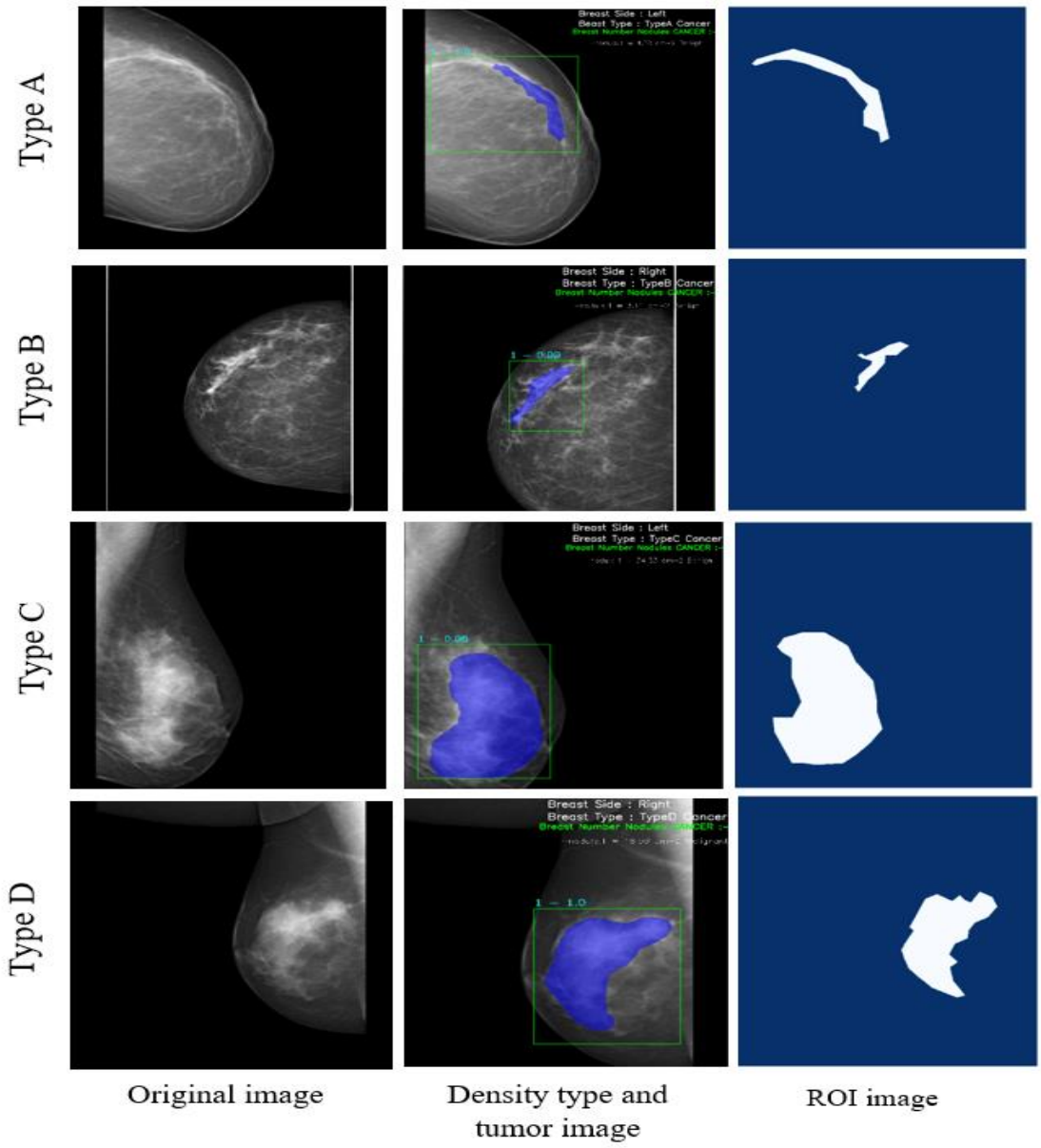

Figure 4. 9 Examples of breast density type to cancer area detection based on the algorithms

In the given dataset, Figure 4.9 illustrates each row corresponds to a specific density category, while each column represents the resulting image output using a particular preprocessing technique. The initial column depicted the original images, while the second and third columns depicted the images subsequent to the application of adjustments to the region of interest (ROI) and density type, as well as the tumor image, through the utilization of Mask R-CNN.

4.3.2.6 Experimental Results Analysis

This study employs original and annotated breast mammography images in the training procedure. In addition, have been set epochs = 50 to train the model by modifying multiple hyperparameters for optimal performance. A low error rate indicates that the model's performance is satisfactory.

The loss versus epoch score is depicted in Figure 4. 10 for this process. The plot for the accuracy metric compares the training accuracy and assessment accuracy achieved during training. The graph demonstrates that both accuracy curves rise continuously as training progresses, with a higher ceiling level for training accuracy, which for ResNet152V2 was not reached until 50 epochs were completed. After 70 epochs, the average assessment accuracy was found to be 97.5%, with training and validation accuracy levels ranging from 98% to 99.9%.

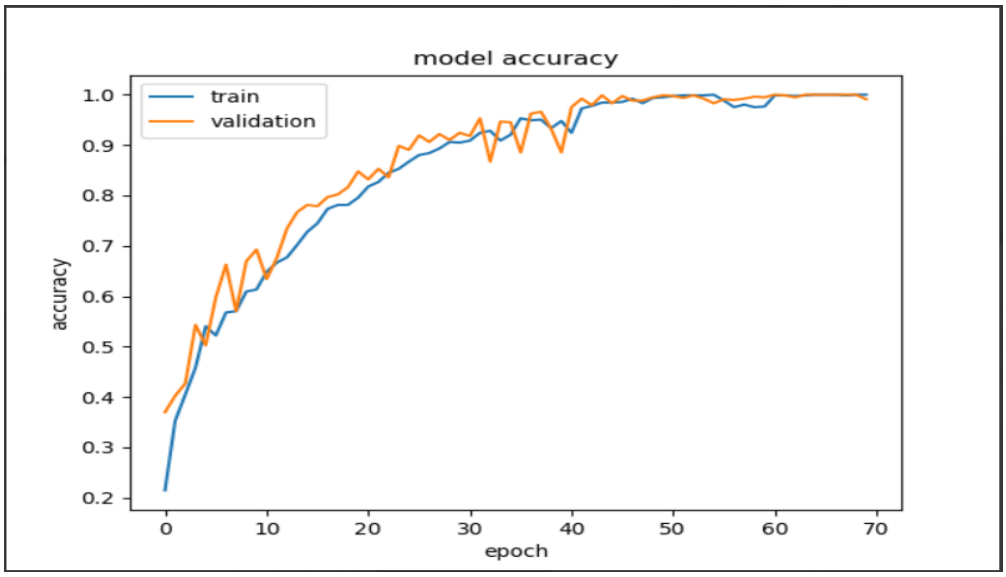

Figure 4. 10 Training/Validation Accuracies vs. number of epochs (ResNet152V2)

In addition, Figure 4. 11 illustrates CNN's accuracy as determined during training and validation. Both accuracy curves rise gradually as training progresses, with a higher ceiling level for training accuracy, which CNN did not attain until 10 epochs had passed. After 50 epochs, the average assessment accuracy was 99%, whereas the training and validation accuracy levels fluctuated between 98% and 99.8%.

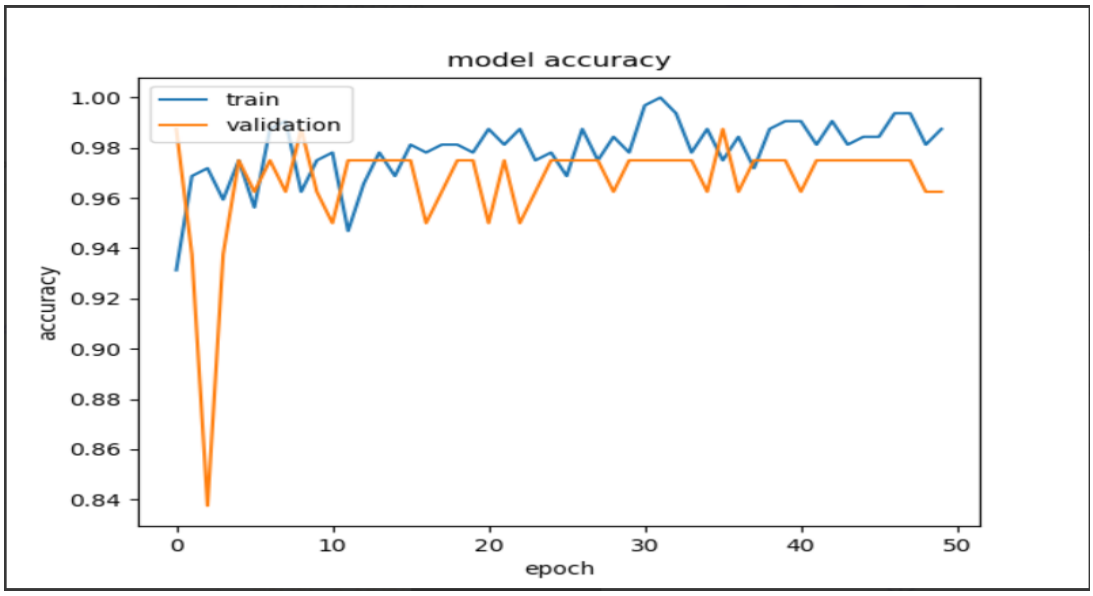

Figure 4. 11 Training/Validation Accuracies vs. number of epochs (CNN)

Fig. 4. 12 indicates that the loss function at epoch 0 is 2, while the loss result at epoch 50 is 0.4. These results indicate that an increase in epochs may result in a modest loss score. Based on the results of the training phase, our proposed model is capable of detecting breast cancer in the testing phase with strong detection outcomes. According to the graph, both accuracy trajectories improve continuously as training progresses, with the training accuracy reaching a maximum of approximately 100% after only 50 epochs. After 50 epochs, the testing accuracy fluctuated between 98% and 96.8%, but the aggregate testing

accuracy was 98%. The testing procedure produces the expected output and detects the output of the model.

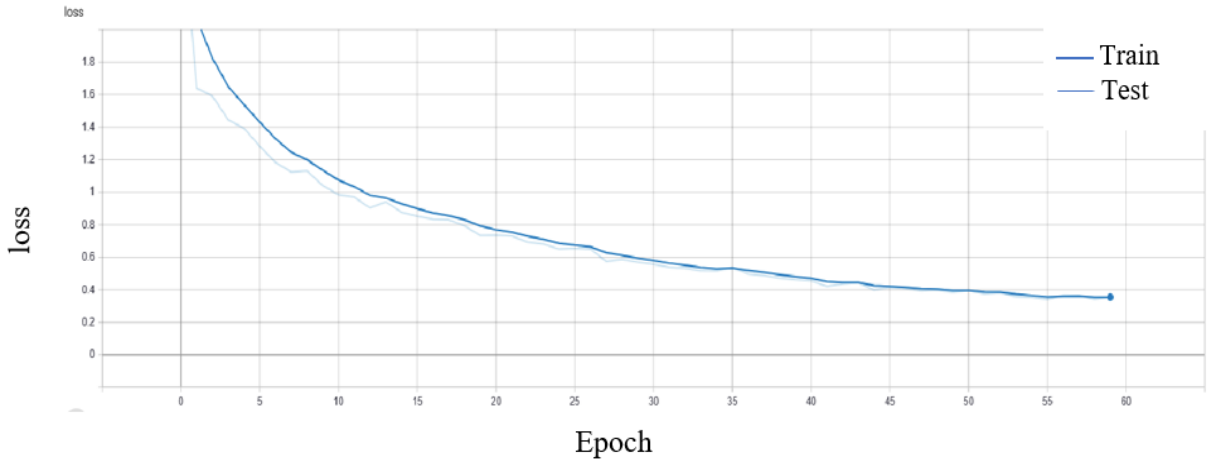

Figure 4. 12 Training/testing losses for the proposed detection system vs. number of epochs

4.3.2.7 Comparing the Proposed Method with the Other Models

In order to make a comparison between the model with the best-achieved result in this work and the state-of-the-art studies, have been presented a number of previous works that used different datasets. A comparison of mammogram detection algorithms for breast cancer based on data collected at an Erbil hospital Every mammogram can detect breast cancer, but the locations, types, and shapes of the lesions vary. All samples were arbitrarily divided into training sets, test sets, and validation sets. Comparing the performance of the Mask R-CNN algorithm to that of other algorithms for the detection of breast cancer reveals that it achieves significant results. The proposed architecture in this dissertation was much better, and it achieved a comparable result to the work but using our own dataset. The findings for comparison with those of other investigations are presented in Tables

4.14. Nevertheless, there is a significant difference between our proposed model and the pre-trained model in terms of the complexity of the model.

Table 4. 9 Phase-comparison between the suggested approach with other previously released breast mass detection and categorization approaches

Author(s)	Methodology	Dataset	Proposed method	Accuracy
(Raza & Syed, 2021b)	Mask RCNN	DICOM data	Cancerous tumors for classification and segmentation.	85%
(Hsieh et al., 2020)	VGG16, Mask R-CNN, Inception V3	Collected dataset from hospital of Chung-Shan Medical University	Tumor classification and segmentation.	87%, 89% and 90%
(Chiao et al., 2019)	Mask R-CNN	Collected the primary ultrasound images with biopsy histological and diagnostic reports from China	The method provides a comprehensive and non-invasive way to detect and classify breast lesions.	85%
(Soltani et al., 2021)	Mask R-CNN	INbreast dataset	Automatic breast mass segmentation method based on the Mask RCNN model of deep learning using detectron2.	95.8%
Our proposed	CNN, ResNet152V2, Mask R-CNN	Collected the primary mammogram images diagnostic report from Erbil	Breast cancer detection, classification, segmentation, size of the tumor, and types of breast.	98.3%, 100% and 98%

The comparative analysis of the proposed dissertation methodology has been conducted in relation to the existing state of the study. Table 4.10 presents a comparison between the planned work and previously published studies. A comparative study has been conducted, examining the utilization of several approaches in a DL model, the comparison of breast type density, the total number of cases included in the experiment, the accuracy, and the coefficient.

Table 4. 10 Accuracy of different breast density types classifications in terms of their best results

Author(s)	Model	No. of Image	No. of Density	Accuracy
(Mohamed et al., 2018)	Deep Learning (CNN)	500	BI-RADS II and BI-RADS III	94%
(Gandomkar et al., 2019)	Deep Learning (InceptionV3)	150	Dense and Fatty	92%
(Saffari et al., 2020)	Deep Learning (CNN)	410	4 Classes	98.75%
(Lopez-Almazan et al., 2022)	Deep Learning (CNN)	892	BI-RADS 1 and BI-RADS 4	85%
Our proposed	Deep Learning (ResNet152V2)	510	Breast Type (A, B, C, and D)	100%

4.3.3 Third Experiment: Automatic Breast Cancer for Mastectomy Detection Using Deep Learning Models with MRI Images

This study used magnetic resonance imaging (MRI) to detect breast cancer. After neoadjuvant chemotherapy (NAC), an MRI, called DCE-MRI, is taken

again. In Chapter 3, a comprehensive analysis is presented about the design and methodologies employed in the model. Before training, the breast cancer dataset in this study underwent preprocessing.

The model uses Mask R-CNN and Detectron2 deep learning methods to detect multiple things in one image. Instance segmentation generates a mask around each recognized object in these algorithms.

Another model for comparing normal and atypical breasts is EfficientNetV2L. This study uses the Mask R-CNN algorithm to distinguish malignant and benign tumors pre- and post-NAC and separate between right and left breasts. The study also compares post-NAC tumor types using Detectron2. After the Multidisciplinary Team (MDT) decided if the breast needed a mastectomy or WLE, used Detectron2 with Faster R-CNN for this dissertation. EfficientNetV2L accurately identified normal and abnormal breast states 100% of the time. Mask R-CNN can distinguish benign and malignant tumors with 97% accuracy.

4.3.3.1 The Datasets that were Used in the Proposed Algorithm

Further analysis is conducted to investigate the distribution of samples in the dataset, aiming to gain a more comprehensive image of both malignant and benign occurrences. Based on the statistical data, it can be shown that within the given sample of 145 patients, corresponding to 2175 images, a substantial majority of 65% received a cancer diagnosis. Additionally, a smaller subgroup of 20% had mastectomy as a treatment option. Furthermore, the dataset encompasses a proportion of 35% benign occurrences. In this model, worked on the 1700 images, which were chosen randomly. Table 4.11 presents a visual representation of the sample distribution within the dataset.

Table 4- 11 MRI and DCE-MRI images dataset description

MRI and DCE-MRI Datasets	**Benign**	**Malignant**	**Normal**
1700	300	1330	70
Abnormality of Malignant (2260)	**Pre-NAC**	**Post-NAC**	
	1330	930	
Post-NAC (930)	**WLE**	**Mastectomy**	
	530	400	

4.3.3.2 Implementing the Proposed Algorithm and the Results

Experiments in this paper employed Python 3. The data set was divided into three sections: a 70% training set for refining the model's results, a 20% validation set, and a 10% testing set for evaluating the models and recording testing results. Using the code provided in Table 4.12, the combined versions of the Mask R-CNN model and EfficientNetV2L were implemented. This code permits the integration of both algorithms, capitalizing on their respective advantages and augmenting the model's overall performance. Combining these two versions allows for more precise and efficient object detection and classification results (because both algorithms work on different versions).

Table 4. 12 EfficinetNetV2L connected with other versions

EfficinetNetV2L
class efficient: def __init__(self): sys.path.insert(1, os.path.abspath('./efficientnetv2/somepath/tensorflow/2.10.0')) # print(os.path.abspath('./efficientnetv2/somepath/tensorflow/2.10.0')) import tensorflow as tf print(tf.__version__) # print('wait to load efficientv2l.model') self.model = tf.keras.models.load_model('./efficientv2l.model') self.CATEGORIES = ["Normal", "AbNormal"] def prepare(self, input_image): image_resize = cv2.resize(input_image, (480, 480)) new_image = image_resize.reshape (-1, 480, 480, 3) new_image = np.array(new_image) return new_image **'-1'.** the size of this dimension will be calculated automatically to ensure the total number of elements remains the same.

The settings of the improved Detectron2 have been adjusted for each experimental batch size of 1 and iteration count of 5000. This algorithm utilizes Detecrtron2 models, specifically Mask R-CNN. The detailed analysis of training outcomes and the subsequent validation or testing of each test will be thoroughly discussed, as outlined in Table 4.13.

Table 4. 13 Implement details of this work from Mask R-CNN and Detectron2

Name	Value
Initial learning rate	1e-3
Optimizer	Adam
Image size	1024*1024
Epochs	80 (Mask RCNN)
Iteration	5000 (Detectron2)
Batch size	1
GPU information	RTX 2060 (6 GB)

4.3.3.3 Result and Discussion

his work's primary learning technique objective is to produce several models. The accuracy, specificity, and sensitivity calculated for the confusion matrix throughout the testing presented in this paper serve as the evaluation metrics for the four models comprising this system. All of the information shown in the tables and figures is explained below.

Table 4.14 demonstrates that the efficientNetV2L achieves the highest accuracy on the training and testing datasets. This algorithm distinguished between normal and abnormal breasts with a 95.00% accuracy rate. Using efficientNetV2L yields the highest sensitivity results, with a score of 96.0%. The highest specificity is achieved with an efficientNetV2L efficiency of 96.00%.

Table 4. 14 The performance of applying regular DL models using efficinetNetV2L

Approach	Models		Training performance				Testing Performance			
			AC	PR	SE	FM	AC	PR	SE	FM
Deep Learning	Efficient NetV2L	Normal	100%	100%	100%	100%	95%	96%	96%	95%
		Abnormal	100%	100%	100%	100%	95%	94%	96%	94%

Figure 4.13 depicts the ROC curve for breast cancer MRI images. The ROC curve indicates TPR and FPR at various network edge parameters. This diagram illustrates how the proposed efficientNetv2L obtained a classification accuracy of 100% for two classes: normal and abnormal datasets.

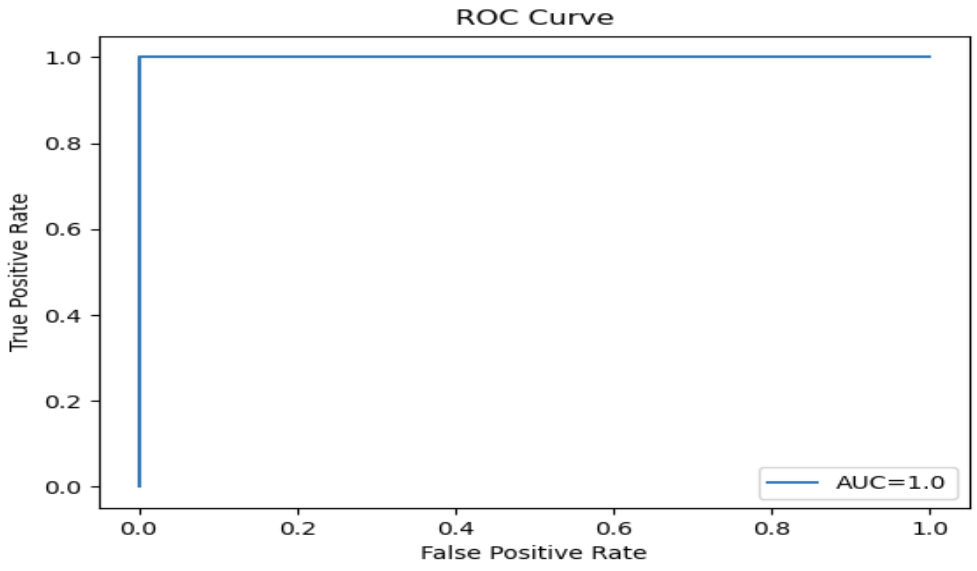

Figure 4. 13 ROC Curve (area= 1.0) by using efficientNetv2L

Table 4. 15 demonstrates that the Mask RCNN algorithm distinguishes between malignant and benign breasts with the highest degree of precision using the datasets for which it was applied. If the breast is malignant, compared it to pre-NAC or post-NAC using this algorithm, also used to compare between right and left breast. Using mask RCNN, the highest sensitivity accuracy of 90.00% is attained at 97.00% and 93.03%. The highest level of specificity is achieved with a mask of 97.00%.

Table 4. 15 The performance of applying regular DL models using Mask R-CNN.

Approach	**Models**			**Training performance**				**Testing Performance**			
				AC	PR	SE	FM	AC	PR	SE	FM
Deep Learning	Mask R-CNN	Benign		90%	80%	97%	88%	87%	74%	99%	85%
		Malignant	Pre-NAC	97%	98%	97%	98%	97%	99%	97%	98%
			Post-NAC	93%	96%	91%	94%	89%	98%	87%	92%

Figure 4.14 depicts the ROC curve of our model and its relationship between TPR and FPR. The ROC curve is a threshold-independent metric that demonstrates classification accuracy. The area under the ROC curve (AUC) is a crucial indicator of the classifier's accuracy. Our model's AUC is 0.978, which is very close to 1, indicating that it is an effective classifier.

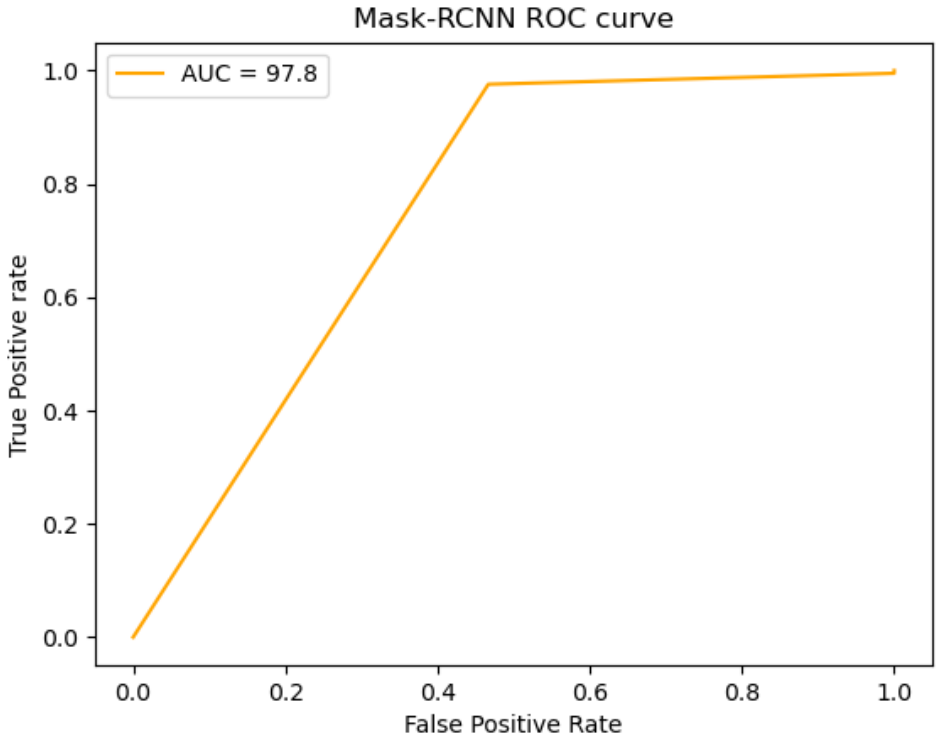

Figure 4. 14 Area Under the Curve (area= 0.978) by using Mask R-CNN for pre and post-NAC

4.3.3.4 Implementation of the Detectron2

After Detectron2's installation was successful, used its pre-trained models to train our dataset and have since used them to work with Faster R-CNN, Mask R-CNN, and Detectron2. To rank the outcomes of each model, the average accuracy (AP) measure was used to rate the results of each model. The AP and average recall (AR) assignments in Detectron2 are famous metrics for measuring the accuracy of object detectors. Average Precision (AP) evaluates object detection accuracy by analyzing the balance between true positives and false positives at varying confidence thresholds. On the other hand, average Recall (AR)

emphasizes the model's ability to detect as many ground truth objects as feasible across all recall levels. Both metrics help evaluate the overall performance of an object detection model in Detectron2 because they shed light on various aspects of the model's precision and completeness. To calculate AP using Detectron2, you can use the COCO Evaluator class. This class provides several methods for evaluating the performance of object detection models on the COCO dataset. As demonstrated with an example, it is difficult but is relatively straightforward. However, a quick review of precision, recall, and IoU is shown in Fig. 4.15.

Average Precision (AP):	
AP	% AP at IoU =.50: .05: .95(Primary challenge metric)
$AP^{Iou} = .50$	% AP at IoU =.50 (PASCAL VOC metric)
$AP^{Iou} = .75$	% AP at IoU =.75 (Strict metric)
AP Across Scales:	
AP^{small}	% AP for small objects: area $<32^2$
AP^{medium}	% AP for medium objects: $32^2 <$ area $< 96^2$
AP^{large}	% AP for large objects: area $> 96^2$
Average Recall (AR):	
$AR^{max=1}$	% AR given 1 detection per image
$AR^{max=10}$	% AR given 10 detections per image
$AR^{max=100}$	% AR given 100 detections per image
AR Across Scales:	
AR^{small}	% AR for small objects: area $< 32^2$
AR^{medium}	% AR for medium objects: $32^2 <$ area $< 96^2$
AR^{large}	% AR for large objects: area $> 96^2$

Figure 4. 15 Average Precision and Recall measures

In COCO, there are more small objects than large objects. Things are divided into three categories based on size: small (area < 32^2), 34% are medium (32^2 < area < 96^2), and 24% are massive (area > 96^2) (Ahmad & Mouiad, 2021). The area is measured as the number of pixels in the segmentation mask. The average precision large (APL) result in Table 4-21 is indicated as "not a number" (nan) due to the algorithm's failure to meet the criterion, which necessitates a value smaller than < 962. They achieved the best results according to the outcomes, rendering them superior to earlier models.

The first dataset yielded the subsequent results. Tables 4.16 and 4.17 display the metrics of the model developed using the MRI breast image and DCE-MRI datasets for the unseen testing subset. Display the results of the trained models using the average point box and the largest dataset. According to the results, they had the best outcomes, rendering them superior to earlier models.

Table 4. 16 The results of the Segmentation on the dataset using Faster-RCNN

Networks		**AP**	**AP50**	**AP75**	**APS**	**APM**	**APL**
Faster_ RCNN _R_101 FPN_3X	Box	74.4%	87.2%	85.4%	61.4%	85.1%	nan
	Mask	63.8%	87.2%	85.4%	54.8%	73.3%	nan

Table 4. 17 The results of the Segmentation on the dataset using Mask-RCNN.

Networks		**AP**	**AP50**	**AP75**	**APS**	**APM**	**APL**
Mask_ RCNN _R_101 FPN_3X	Box	46.6%	59.1%	56.3%	33.7%	53.7%	61.7%
	Mask	22.2%	43.0%	19.7%	15.5%	26.7%	35.0%

1. Detectron2

As previously stated, the dissertation divided the images and their respective kinds into separate training and validation sets. The comparison of tumor DCE-MRI images between different pre-NAC types is shown in Fig. 4.16, which shows breast MRI scans of various malignant tumors (a–f) before utilizing

Detectron2. The original reference image is on the left side of the photo, and the pre-NAC kinds, following the application of the algorithm for detection, are shown on the right side. The result is shown in Table 4.18.

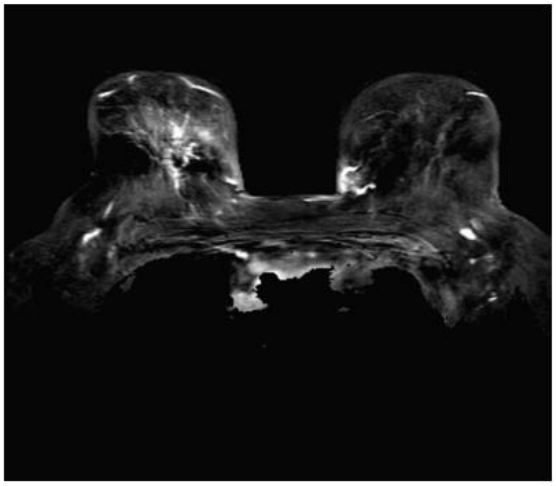

a. Breast MRI image

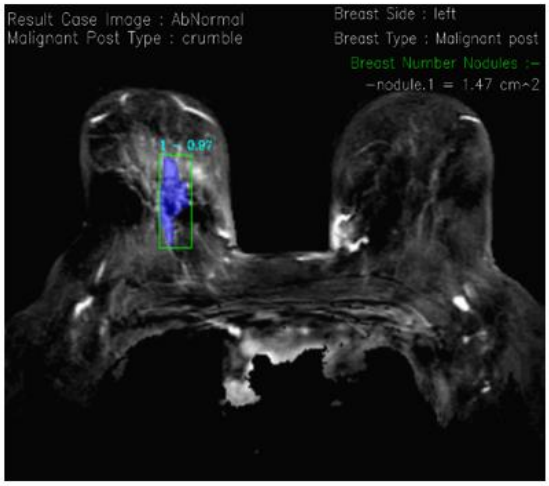

Type = Crumble (left side)

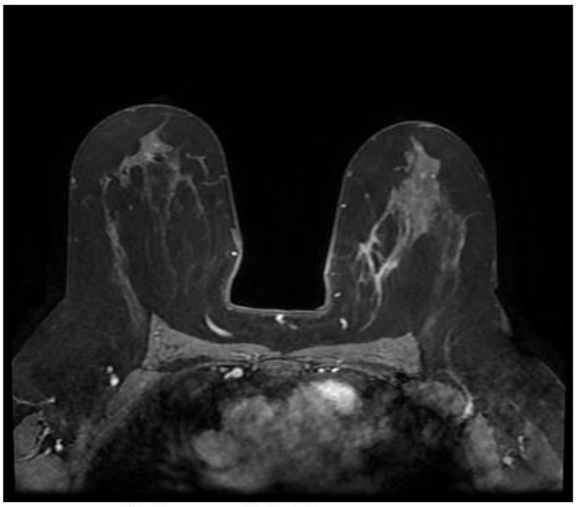

b. Breast MRI image

Type = Shrink (right side)

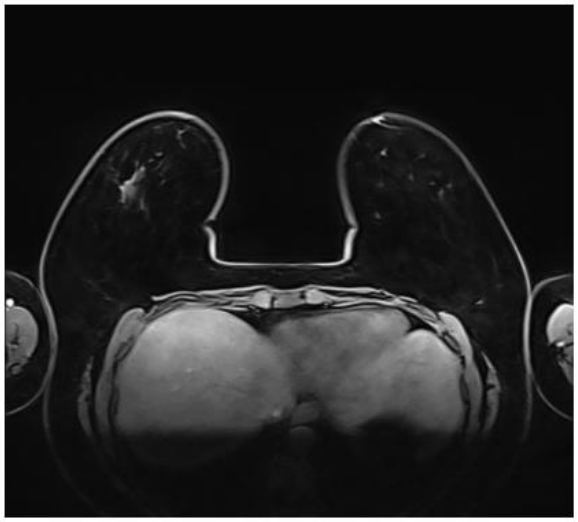

c. Breast MRI image

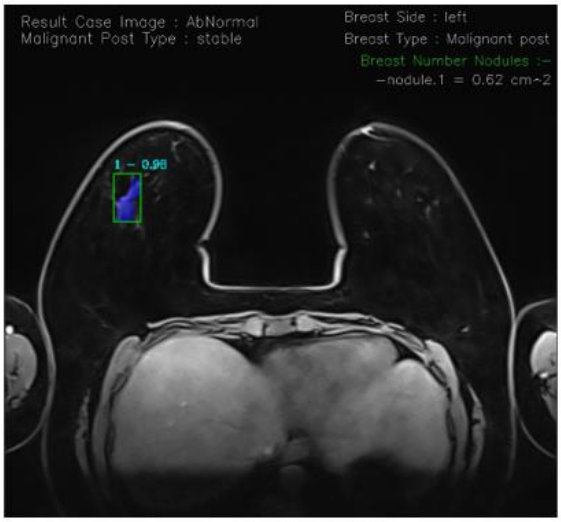

Type = Stable (left side)

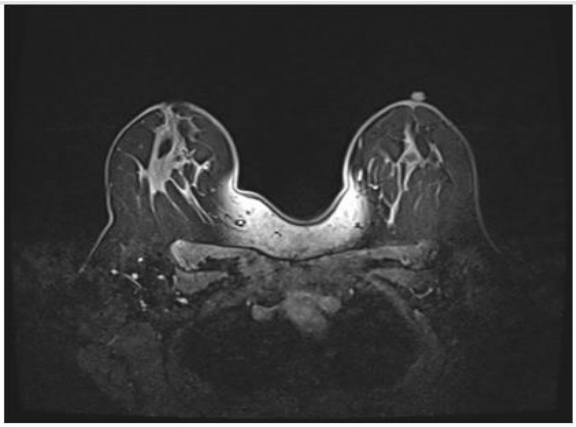

d. Breast MRI image

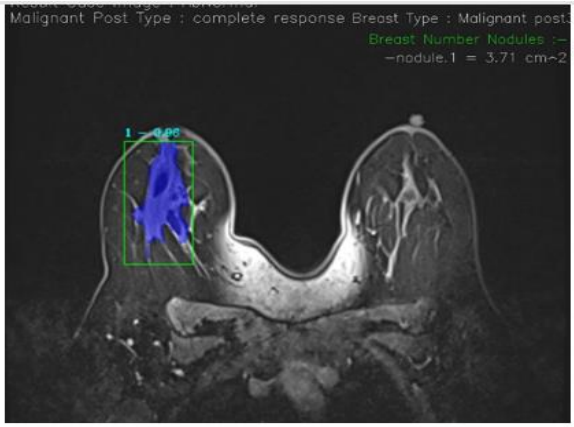

Type = Complete response (left side)

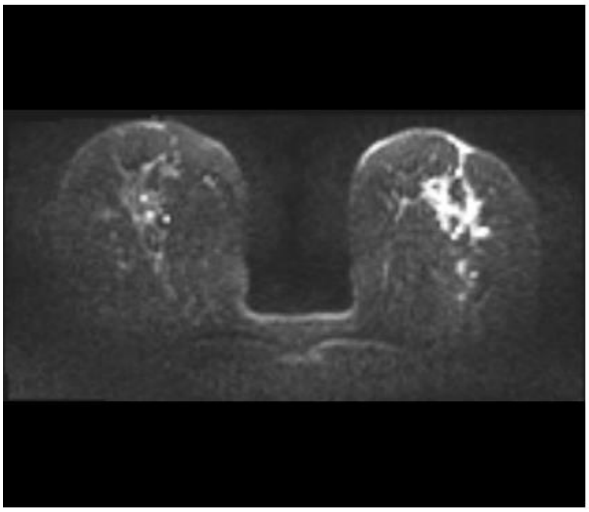

e. Breast MRI image

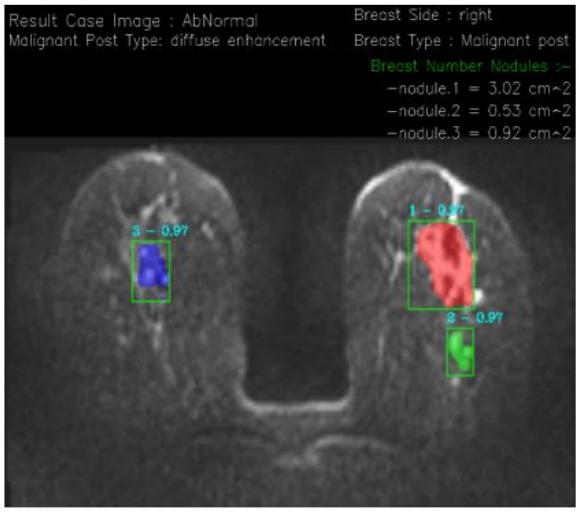

Type = Diffuse enhancement (both)

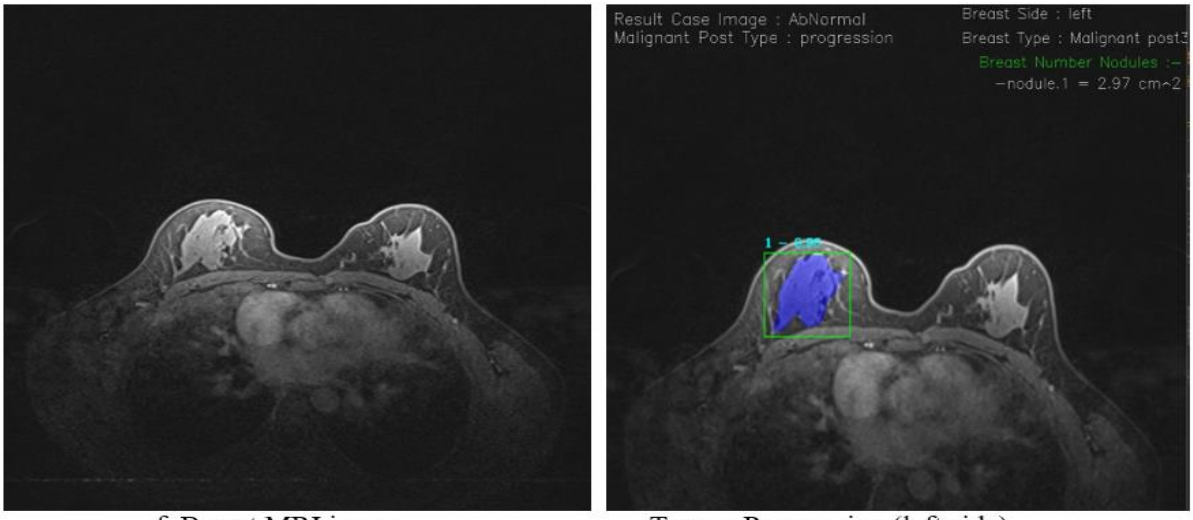

f. Breast MRI image Type = Progression (left side)

Figure 4. 16 Example of tumor types post-NAC images.

Table 4. 18 Performance of the Detectron2 (Mask R-CNN) on the training dataset using a different combination of the batch size, optimizer, and loss function

Model name	**Batch Size**	**Optimizer**	**Loss Function**	**Types**	**Metrics**			
					Pression	Recall	Accuracy	F1-score
Detectron2 (ResNet 101) Mask R-CNN	1	Adam	DCE+L1	Complete Response	93%	100%	97%	97%
				Crumble	100%	100%	100%	100%
				Diffuse enhancement	100%	100%	100%	100%
				Progression	100%	100%	100%	100%
				Shrink	96%	93%	95%	95%
				Stable	100%	100%	100%	100%

The micro, macro, and weighted averages, along with the F1-Score, are presented in Tables 4. 19 and 4. 20, respectively, for the dataset. Both tables and classes have F1-Scores of 98% and 99%, respectively. As a consequence, the percentages of false positives and false negatives are quite low, indicating that the model successfully classifies the correct class.

Table 4. 19 The Micro, Macro, and Weighted Average (Detectron2 with Mask R-CNN)

Label	**Testing Performance**			
	Pression	**Recall**	**Accuracy**	**F1-score**
Micro Average	98%	98%	98%	98%
Macro Average	98%	99%	99%	99%
Weighted Average	98%	98%	98%	98%

2. Detectron2 with Faster RCNN

Figure 4. 17 explains how Detectron2 and Faster R-CNN were integrated into the proposed MRI breast cancer image to determine that this patient requires a mastectomy, denoted in brown. Also, see Figure 4. 18. After applying Detectron2 and Faster R-CNN to MRI breast cancer images, it is also explained that this patient requires a wide local excision, denoted in green shown in Table 4. 20.

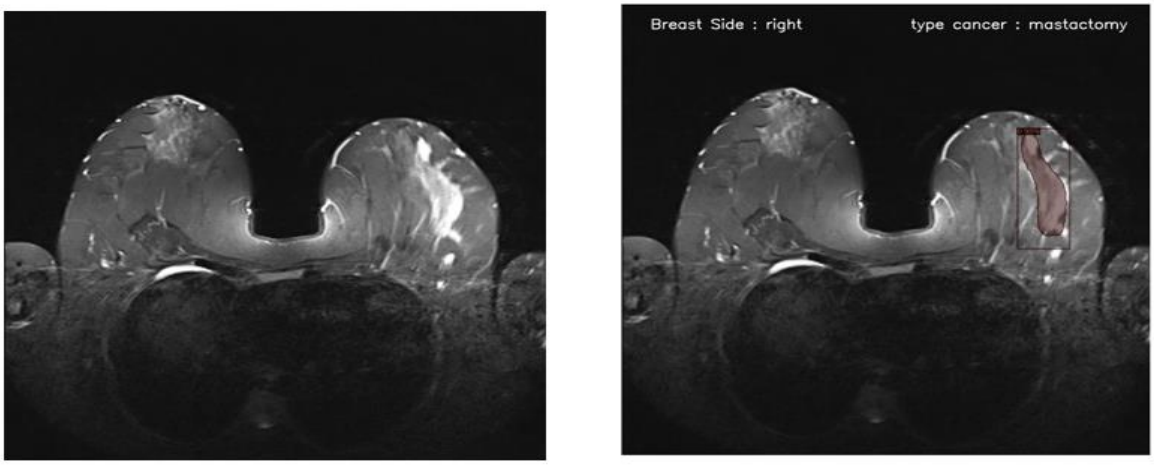

a. Breast MRI image

b. Mastectomy

Figure 4. 17 Detection results were obtained using thresholding

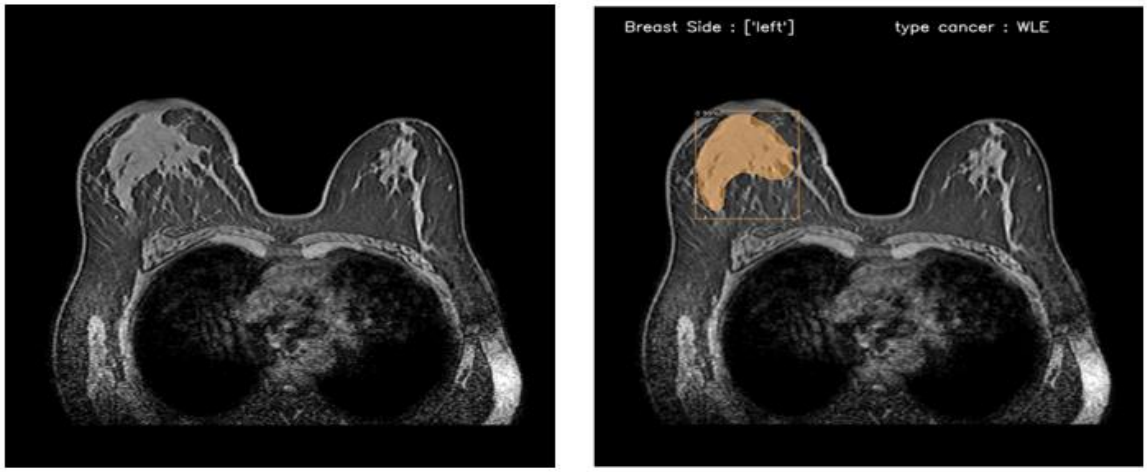

a. Breast MRI image

b. Malignant (WLE)

Figure 4. 18 Segmentation results were obtained using thresholding.

Table 4. 20 Performance of the Detectron2 (Faster R-CNN) on the training dataset using a different combination of the batch size, optimizer, and loss function

Model name	**Batch Size**	**Optimizer**	**Loss Function**	**Types**	**Metrics**			
					Pression	Recall	Accuracy	F1-score
Detectron2 (ResNet101) Faster R-CNN	1	Adam	DCE+L1	Mastectomy	93%	86%	86%	86%
				WLE	90%	80%	81%	81%

The dataset's micro, macro, and weighted averages, as well as its F1-Score, are displayed in Tables 4. 21. The F1-Score is 0.83 and 0.86 for both tables and classes, respectively. As both the number of false positives and false negatives are moderate, this indicates that the model is effectively classifying the correct category.

Table 4. 21 The Micro, Macro, and Weighted Average (Detectron2 with Faster R-CNN)

Label	**Pression**	**Recall**	**Accuracy**	**F1-score**
Micro Average	86%	80%	83%	83%
Macro Average	92%	72%	81%	79%
Weighted Average	87%	80%	83%	83%

4.3.3.5 Loss Results.

Figure 4.19 depicts the loss graphs of the suggested model during the training phase of the Detectron2 with Mask RCNN model. After each period of training, the training and validation losses were determined. As the training process progresses, the value of training loss decreases rapidly, followed by validation loss. Figure 15 depicts the X axis as 5000 iterations and the Y axis as cross-entropy loss. After multiple epochs, the validation loss begins to increase while the training loss continues to decrease, indicating model overfitting. This period was selected as the most recent one that did not overfit. During the training period, the loss function decreases monotonically after 2000 iterations, whereas the validation loss is evident after 4000 iterations. The stabilization of losses at the end of training indicates that the proposed model learns and segments without overfitting.

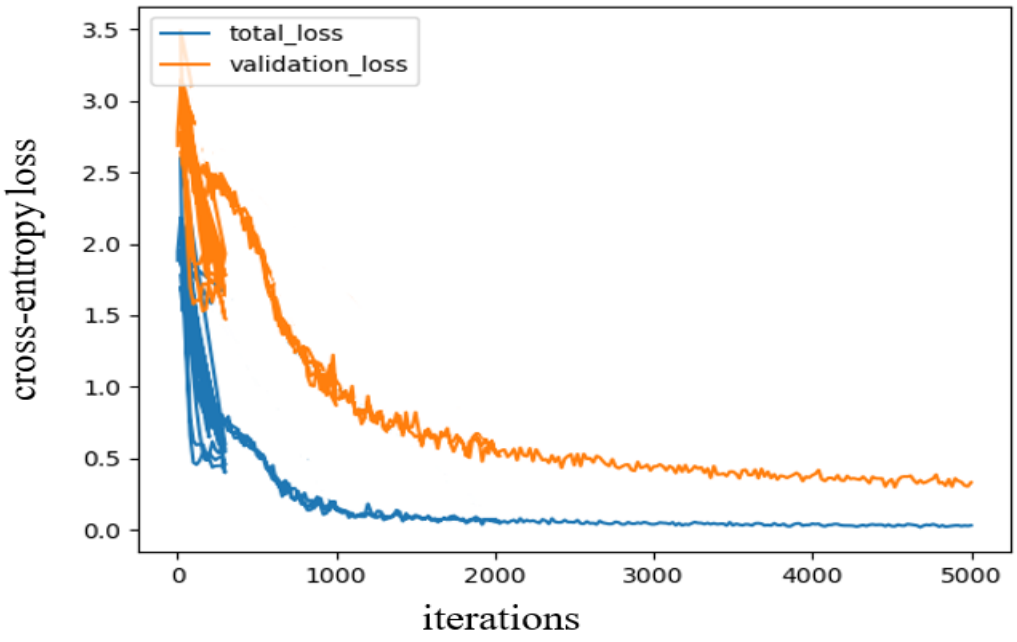

Figure 4. 19 Training loss and validation loss curves of Detectron2 with Mask R-CNN for breast cancer MRI images

Figure 4. 20 depicts, in contrast, the training loss curve of efficientV2-L after 50 iterations. During the early training rounds, it is possible to observe a rapid decrease in accuracy losses, which started to stabilize after approximately 40 epochs. This indicates that the model matched the characteristics of the dataset well throughout the entire training process. In theory, the efficient V2-L model offers the highest performance because it obtains the lowest loss value compared to the mask RCNN model.

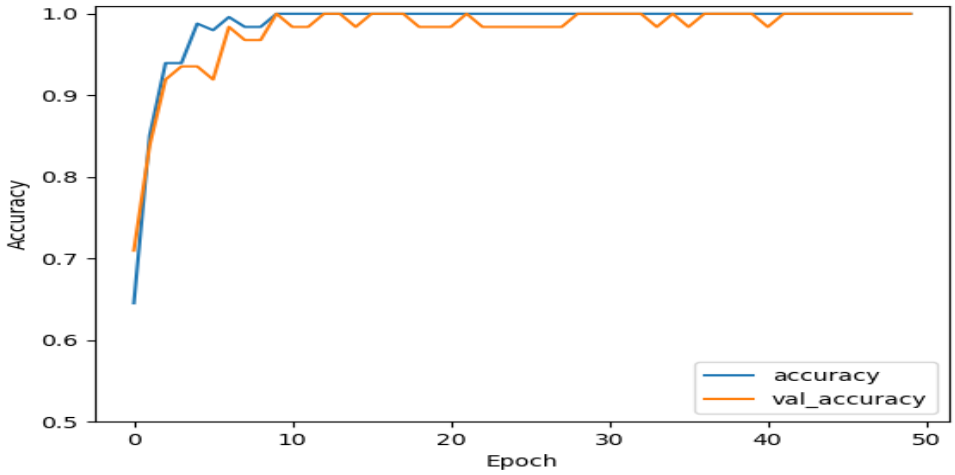

Figure 4. 20 Validation and accuracy loss curve for efficientV2-L

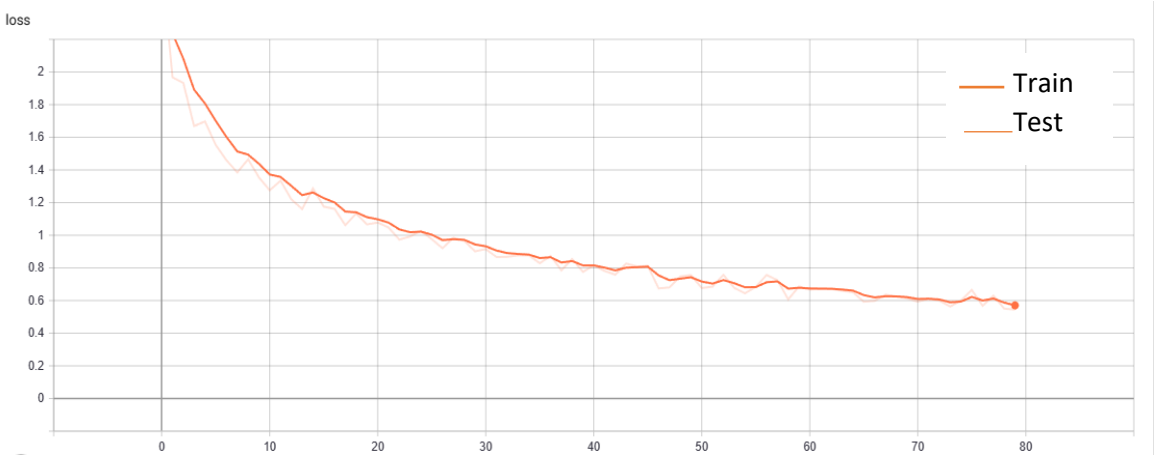

Figure 4. 21 Loss Function of breast cancer type (malignant and Benign) Mask RCNN

Due to the considerable volume of data and extensive computational demands associated with deep learning algorithms, employed transfer learning as a strategy and leveraged pre-learned weights that were first trained. In Figure 4.21, the loss function employed in the Mask RCNN model is depicted, specifically in the context of breast cancer classification.

4.3.3.6 Initially using YOLO Rather than Mask RCNN.

In this study, the YOLOV7 model was initially employed for the detection of malignant and benign breast images, as well as the identification of pre-neoadjuvant chemotherapy (NAC) and post-NAC conditions in cases of malignancy. However, the outcome is unsatisfactory as YOLOV7 is primarily designed for detecting large objects rather than small ones, as shown in Table 4-22. Therefore, have been opted to utilize Mask RCNN instead. During that particular period, there was only this particular version however, the issue has since been resolved by the implementation of YOLOV8.

Table 4. 22 The effectiveness of implementing YOLOV7

Class	Labels	precision	Recall	mAP@.50	mAP@.50:.95
All	430	0.395	0.646	0.413	0.251
Left	121	0.488	0.992	0.515	0.383
Malignant Pre-NAC	44	0.363	0.545	0.464	0.216
Malignant post-NAC	62	0.409	0.323	0.248	0.108
Right	124	0.5	0.992	0.591	0.458

A higher mAP@.50 and mAP@.50:.95 score generally means that the object detection model is operating more effectively. It's crucial to remember that the two measures are assessing distinct things. The model's capacity to detect items at a single IoU threshold is measured by mAP@.50, whilst its ability to detect objects across a range of IoU thresholds is measured by mAP@.50:.95.

4.3.3.7 Comparing the Proposed Algorithm with the Existing Works.

In order to make a comparison between the model with the best-achieved result in this work and other model, have been presented a number of previous works that were applied to the same dataset, which is DCE-MRI breast cancer.

The comparison of the models is based on the algorithms implemented and the datasets utilized. The findings are presented in Table 4.23 for the purpose of comparison with the findings of other investigations. In this table, has only mention the type of dataset used for what purpose because this type of dataset has not been used for what have been done.

Table 4. 23 Phase comparison between the using dataset DCE-MRI image approach with other previously released used about what

Author(s)	Dataset	Methodology	Proposed method	Accuracy
(Benjelloun et al., 2018)	DCE-MRI	Deep Learning	segmentation of breast tumors	76.14%
(Maicas et al., 2017)	DCE-MRI	globally optimal inference in a continuous space (GOCS)	segmentation	77%

(J. Zhou et al., 2020)	DCE-MRI	ResNet50	3D tumor segmentation	89%
(Hu et al., 2021)	4D DCE-MRI	CNN architecture	Classification lesions	91%
(Sutton et al., 2020)	MRI post-NAC	Recursive Feature Elimination Random Forest (RFE-RF)	complete response	94%
(Choi et al., 2020)	DCE-PET/MRI	CNN	deep learning model can predict pathological responses to NAC in patients with advanced breast cancer	80%
(Conte et al., 2020)	DCE–MRI image	CNN	discrimination between in situ and infiltrating tumors	75%
(Li et al., 2022)	DCE–MRI image	CNN	Prediction for Distant Metastasis breast	80%
(Ye et al., 2022)	DCE–MRI image	deep transfer learning	process images, and then, the features of breast cancer	70%
(Militello et al., 2022)	DCE–MRI image	Fuzzy C-Means (sFCM)	segment masses on dynamic contrast-enhanced (DCE) MRI of the breast	93%
Proposed approach	MRI and DCE–MRI image	Mask R-CNN Detectron2	Types of Post-NAC and mastectomy or WLE	97% 97% and 93 %

4.4 Advantages and Limitations of the Proposed Method (BTRD).

Although our proposed method poses good results for cancer detection in mammograms, this work has some pros and cons. In this section, discussed the advantages and limitations of our proposed method. The core advantages of this current research work are as follows:

1. Created a model for breast cancer classification from mammograms that combines the principles of deep learning and optimization algorithms.

2. Introduced an attention mechanism on a deep CNN-based transfer learning model, with ResNet152V2, and fine-tune it to extract deep features from the input images to classify breast density images and classify between them.

3. Used Mask R-CNN, an extension of faster R-CNN, which combines object identification and segmentation for high accuracy. The technology can accurately identify and localize items, which may help detect tumors or anomalies in breast cancer images.

4. When evaluating the different datasets, have attained attain state-of-the-art classification accuracy, high precision, and recall values of the original feature set against the other models.

5. The instance-level segmentation of mask R-CNN makes ROI analysis easier. This segmentation allows radiologists and researchers to examine distinct regions in breast cancer images, helping them understand irregularities.

The limitations of this research work are described as follows:

1. The collected breast cancer images are manually categorized, which is time-consuming and might be prone to errors.

2. It is normal for breast cancer detection and recognition systems to identify cancer in breast image analysis incorrectly. Applying image preprocessing steps such as conversion, scaling, and rotation could exacerbate the issue.

3. Similar to other deep learning models, mask R-CNN requires significant annotated training data to perform well. Collecting and annotating medical images for breast cancer analysis can be time-consuming and require specialized knowledge.

4. The architecture of Mask R-CNN is complex, requiring significant computational resources and training time. This may limit its applicability in specific situations, especially if you have limited computing resources.

5. Time complexity is a factor has been need to emphasize more in the future.

4. 5 Advantages and Limitations of the Proposed Method (ADBMD)

Although our proposed method achieves excellent results for cancer detection in MRI and DCE-MRI images, this work has some pros and cons. This section discusses the pros and cons of our proposed method. The core advantages of this current research work are as follows:

1. Created a model for breast cancer classification from breast MRI and DCE-MRI images that combine the principles of deep learning and optimization algorithms.

2. Introduced the Detectron2 classifier, which is used in our approach because of its high accuracy for detecting the type of post-NAC, and have been used Detectron2 with faster RCNN to detect between mastectomy and WLE.

3. Introduced an attention mechanism that can identify the difference between the right and left sides breast. These differences between the right and

left sides breast are important to consider when diagnosing and treating breast cancer. For example, radiologists may pay more attention to the right side breast when reading mammograms, and surgeons may remove more lymph nodes from under the right arm when performing a mastectomy.

Even though the proposed study demonstrated the potential of using deep learning models for detecting, classifying, and segmenting breast cancer, the suggested approach presents some limitations.

1. The initialization in the optimization algorithm is random. So, it may sacrifice some accuracy and convergence time results.

2. The main limitation is the instantaneity, where the most time-consuming stage is the classifier's training. The slow convergence of the boosting algorithm, especially between (efficientNetV2-L and mask RCNN) and high-dimensional features, is the cause of this limitation.

4.6 Summery

The main goal of this dissertation is to further medical imaging research. Presenting a framework that incorporates deep learning models, image processing, and machine learning algorithms. The proposed architecture improves breast cancer detection accuracy and efficiency. Deep learning models for anomalous tissue detection efficiently categorize and distinguish malignant and benign images in the dataset, promoting prompt identification and improved outcomes.

This study provides three models, the first of which employs machine learning to detect breast cancer. This model has two layers. Feature extraction using multiple methods is one method. The next step is algorithm-based classification.

Mammogram analysis helps identify and characterize breast tumor types and sizes. After distinguishing the four mammography classifications (A, B, C, and D), the healthy and abnormal breast regions are identified and isolated from the mammogram images, and tumor dimensions are determined.

Another application is automated breast cancer detection for mastectomy or substantial local excision. This study will distinguish between normal and abnormal circumstances and malignant (before or post-neoadjuvant treatment) and benign tumors. Comparisons between mastectomy and WLE. The first model after comparison between models, found that ANN, SVM, and AdaBoost achieved a higher efficiency of 96%, and Precision of 97%, and outperformed all others. The second model results are promising, with a 99.3% CNN, 100% ResNet152V2, and 98% Mask R-CNN overall accuracy. The third model results show the accuracy rates for EfficientNetV2L, Mask R-CNN, Detectron2 with Mask R-CNN, Detectron2, and Faster RCNN were respectively 99%, 100%, 98.6%, and 97.7.

CHAPTER FIVE

5 CONCLUSIONS AND FUTURE WORK

5.1 Conclusions

Early disease detection allows surgery, chemotherapy, and radiation therapy to begin quickly, improving treatment outcomes.

Researchers have developed computer-aided detection (CAD) systems that use machine learning (ML) algorithms to analyze mammography and identify potential abnormalities in order to circumvent this limitation. These CAD systems help radiologists make more precise diagnoses by highlighting suspicious areas that the human eye may have overlooked.

Computer-aided detection and diagnosis systems have substantially increased the sensitivity and specificity of breast cancer detection, thereby decreasing the likelihood of false negative and false positive mammogram readings. The model results have led to the following conclusions:

In the first experimental work it is demonstrated that feature selection and feature extraction using five methods (Sift, HOG, LBP, BoW, and EOH) can enhance the performance evaluation diagnosis when machine learning techniques are employed. On the three breast cancer datasets, seven algorithms were utilized in this research: SVM, k-NN, RF, AdaBoost, ANN, and decision trees. It has been attempted to compare the efficacy and performance of these algorithms in terms of accuracy, precision, sensitivity, and specificity in order to identify the algorithm with the highest classification precision. Using the BoW model for breast cancer image classification tasks with SIFT descriptors and HOG methods yielded the best results. After a thorough comparison of our models, discovered that ANN,

SVM, and AdaBoost outperformed all others with an efficiency of 96% and a precision of 97%. These models have demonstrated their efficacy in predicting and diagnosing breast cancer and have obtained the best performance in terms of precision and accuracy. Therefore, it is necessary to consider future work and apply the same algorithms and methods to other databases in order to confirm the results derived from this database.

In the second experimental model, a comprehensive methodology for optimal mammographic breast cancer diagnosis was presented. The methodology for this study consists of the three phases described above: The first stage used CNN to compare right and left breasts; the result was 99.3%; the second stage used ResNet152V2 to distinguish between the four categories of breasts and to compare normal and abnormal breast cancer; the result was 100%. In the third and final stage, if the breast cancer was abnormal, it was sent to the Mask R-CNN for comparison between malignant and benign, determining the extent of the tumor, with a 98% success rate.

The dissertation concludes that ResNet152V2 is a reasonable model for detecting the density type of mammogram and classifying it. EfficientNetV2, which is a big improvement over EfficientNet in terms of training speed and a decent improvement in terms of accuracy. According to these two radiology physicians who have observed the model, they provide full support for the model.

Finally, the third model for breast tumor detection in MRI and DCE-MRI images is introduced. To locate the region of interest in a breast MRI image during the localization phase, an artificial segmentation technique dependent on local active contours has been developed. It includes the four components enumerated above. In this research, the accuracy rates for EfficientNetV2L, Mask R-CNN, Detectron2 with Mask R-CNN, Detectron2, and Faster RCNN were 99.9%, 100%, 98.6%, and 97.7%, respectively. Mask RCNN is a good tool for detecting and

recognizing breast cancer in these methods. Mask R-CNN has been shown to be highly effective in breast cancer detection due to its accuracy in object detection as well as its ability to perform segmentation and detect regions of the tumor.

Detectron2 offers various image preprocessing capabilities, such as resizing, normalization, and cropping, which can help ensure that the input images are properly prepared for object detection. As the results show, the use of this algorithm gave us reliable results with the support of both doctors, and the results are 100% complete.

5.2 Future Work

In the future, multiple suggestions can be considered to enhance the proposed algorithms. This dissertation investigated deep convolutional neural networks in an effort to identify applicable approaches in this field.

As technology advances in the future, this algorithm can be enhanced to provide a significantly more sophisticated solution for locating and eradicating cancer cells in the detected area by incorporating a few additional developments. In future research, if a type C or D breast cancer mammogram patient requires an MRI image to compare the two images (MRI and mammogram) to extract the tumor, what is the difference between the two images? Doctors have difficulty with varieties C and D due to their high density.

The models could be improved by incorporating additional data and machine learning models to compare types of mastectomy, WLE, and metastasis varieties. This enhances the presentation and dependability of the framework. By submitting MRI data, the machine learning framework may assist the general public in determining the likelihood of malignancy in adult patients.

Overall, it is essential to continue working on the proposed system to improve and aid breast cancer research by developing algorithms that can assist specialists and reduce their examination time and subjectivity. Thus, the strategy yielded encouraging results and is suitable for further development in the classification and identification of lesions.

REFERENCE

Abas, S. M. (2022). *Diseases Diagnosis Using Machine Learning of Medical Images*. *December*.

Abbas, Q. (2016). DeepCAD: A computer-aided diagnosis system for mammographic masses using deep invariant features. *Computers*, *5*(4). https://doi.org/10.3390/computers5040028

Abdel Rahman, A. S., Belhaouari, S. B., Bouzerdoum, A., Baali, H., Alam, T., & Eldaraa, A. M. (2020). Breast Mass Tumor Classification using Deep Learning. *2020 IEEE International Conference on Informatics, IoT, and Enabling Technologies, ICIoT 2020*, 271–276. https://doi.org/10.1109/ICIoT48696.2020.9089535

Abdelbaki, A. (2019). *ConvNet Features for Lifelong Place Recognition and Pose Estimation in Visual SLAM by*. *March 2018*. https://doi.org/10.13140/RG.2.2.10816.89607

Acharya, S., Alsadoon, A., Prasad, P. W. C., Abdullah, S., & Deva, A. (2020). Deep convolutional network for breast cancer classification: enhanced loss function (ELF). *Journal of Supercomputing*, *76*(11), 8548–8565. https://doi.org/10.1007/s11227-020-03157-6

Adel, E., Elmogy, M., & Elbakry, H. (2014). Image Stitching based on Feature Extraction Techniques: A Survey. *International Journal of Computer Applications*, *99*(6), 1–8. https://doi.org/10.5120/17374-7818

Adusei, E. (2020). *Circulating Cell-Free DNA as a Blood Biomarker in Monitoring Response to Chemotherapy in Breast Cancer*. *10476157*.

Ahmad, S., & Mouiad, A. (2021). *Comparative Study : 2D object Detection & inferencing using Detectron2 2D object Detection & inferencing using Detectron2 : comparative study Abstract : A*ugust, 0–5.

Ahmed, L., Iqbal, M. M., Aldabbas, H., Khalid, S., Saleem, Y., & Saeed, S. (2020). Images data practices for Semantic Segmentation of Breast Cancer using Deep Neural Network. *Journal of Ambient Intelligence and Humanized Computing*, *0123456789*. https://doi.org/10.1007/s12652-020-01680-1

Al-Haija, Q. A., & Manasra, G. F. (2020). Development of Breast Cancer Detection Model Using Transfer Learning of Residual Neural Network (ResNet-50). *American Journal of Science & Engineering*, *1*(3), 30–39. https://doi.org/10.15864/ajse.1304

Al-masni, M. A., Al-antari, M. A., Park, J. M., Gi, G., Kim, T. Y., Rivera, P., Valarezo, E., Choi, M. T., Han, S. M., & Kim, T. S. (2018). Simultaneous detection and classification of breast masses in digital mammograms via a deep learning YOLO-based CAD system. *Computer Methods and Programs in Biomedicine*, *157*, 85–94. https://doi.org/10.1016/j.cmpb.2018.01.017

Alzubaidi, L., Zhang, J., Humaidi, A. J., Al-Dujaili, A., Duan, Y., Al-Shamma, O., Santamaría, J., Fadhel, M. A., Al-Amidie, M., & Farhan, L. (2021). Review of deep learning: concepts, CNN architectures, challenges, applications, future directions. In *Journal of Big Data* (Vol. 8, Issue 1). Springer International Publishing. https://doi.org/10.1186/s40537-021-00444-8

American Cancer Society. (2022). Breast Cancer What is breast cancer ? *American Cancer Society. Cancer Facts and Figures Atlanta, Ga: American Cancer Society*, 1–19. http://www.cancer.org/cancer/breast-cancer/about/what-is-breast-cancer.html

Arafa, A., El-Sokary, N., Asad, A., & Hefny, H. (2019). Computer-Aided Detection System for Breast Cancer Based on GMM and SVM. *Arab Journal of Nuclear Sciences and Applications*, *52*(2), 142–150. https://doi.org/10.21608/ajnsa.2019.7274.1170

Atrey, K., Sharma, Y., Bodhey, N. K., & Singh, B. K. (2019). Breast cancer prediction using dominance-based feature filtering approach: A comparative investigation in machine learning archetype. *Brazilian Archives of Biology and Technology*, *62*, 1–15. https://doi.org/10.1590/1678-4324-2019180486

Bakheet, S., & Al-Hamadi, A. (2021). A framework for instantaneous driver drowsiness detection based on improved HOG features and naïve bayesian classification. *Brain Sciences*, *11*(2), 1–15. https://doi.org/10.3390/brainsci11020240

Bardou, D., Zhang, K., & Ahmad, S. M. (2018). *Classification of Breast Cancer Based on Histology Images Using Convolutional Neural Networks*. *XX*(c). https://doi.org/10.1109/ACCESS.2018.2831280

Benhassine, N. E., Boukaache, A., & Boudjehem, D. (2020). A NEW CAD SYSTEM for BREAST CANCER CLASSIFICATION USING DISCRIMINATION POWER ANALYSIS of WAVELET'S COEFFICIENTS and SUPPORT VECTOR MACHINE. *Journal of Mechanics in Medicine and Biology*, *20*(6), 1–14. https://doi.org/10.1142/S0219519420500360

Benjelloun, M., El Adoui, M., Larhmam, M. A., & Mahmoudi, S. A. (2018). Automated Breast Tumor Segmentation in DCE-MRI Using Deep Learning. *2018 4th International Conference on Cloud Computing Technologies and Applications, Cloudtech 2018*, 1–6. https://doi.org/10.1109/CloudTech.2018.8713352

Bharat, A., Pooja, N., & Reddy, R. A. (2018). Using Machine Learning algorithms for breast cancer risk prediction and diagnosis. *2018 IEEE 3rd International Conference on Circuits, Control, Communication and Computing, I4C 2018*, *x*, 1–4. https://doi.org/10.1109/CIMCA.2018.8739696

Bhatti, H. M. A., Li, J., Siddeeq, S., Rehman, A., & Manzoor, A. (2020). Multi-

detection and Segmentation of Breast Lesions Based on Mask RCNN-FPN. *Proceedings - 2020 IEEE International Conference on Bioinformatics and Biomedicine, BIBM 2020*, 2698–2704. https://doi.org/10.1109/BIBM49941.2020.9313170

Bilal, M., Maqsood, M., Yasmin, S., Hasan, N. U., & Rho, S. (2022). A transfer learning-based efficient spatiotemporal human action recognition framework for long and overlapping action classes. In *Journal of Supercomputing* (Vol. 78, Issue 2). Springer US. https://doi.org/10.1007/s11227-021-03957-4

Bouckaert, R. R., Frank, E., Hall, M., Kirkby, R., Reutemann, P., Seewald, A., & Scuse, D. (2013). *WEKA Manual Version 3-6-9*.

Brown, G. T. F., Bekker, H. L., & Young, A. L. (2022). Quality and efficacy of Multidisciplinary Team (MDT) quality assessment tools and discussion checklists: a systematic review. *BMC Cancer*, *22*(1), 1–10. https://doi.org/10.1186/s12885-022-09369-8

Burbank, F. (2006). Breast interventional devices: how they evolve and define new subspecialities. *Breast Cancer Research*, *8*(S1). https://doi.org/10.1186/bcr1416

Byra, M., Galperin, M., Ojeda-Fournier, H., Olson, L., O'Boyle, M., Comstock, C., & Andre, M. (2019). Breast mass classification in sonography with transfer learning using a deep convolutional neural network and color conversion. *Medical Physics*, *46*(2), 746–755. https://doi.org/10.1002/mp.13361

Cai, H., Huang, Q., Rong, W., Song, Y., Li, J., Wang, J., Chen, J., & Li, L. (2019). Breast Microcalcification Diagnosis Using Deep Convolutional Neural Network from Digital Mammograms. *Computational and Mathematical Methods in Medicine, 2019*. https://doi.org/10.1155/2019/2717454

Cai, L., Wang, X., Wang, Y., Guo, Y., Yu, J., & Wang, Y. (2015). Robust phase-

based texture descriptor for classification of breast ultrasound images. *BioMedical Engineering Online*, *14*(1), 1. https://doi.org/10.1186/s12938-015-0022-8

Cai, N., Chen, H., Li, Y., Peng, Y., & Li, J. (2021). Adaptive Weighting Landmark-Based Group-Wise Registration on Lung DCE-MRI Images. *IEEE Transactions on Medical Imaging*, *40*(2), 673–687. https://doi.org/10.1109/TMI.2020.3035292

Chaurasia, V., Pal, S., & Tiwari, B. B. (2018). Prediction of benign and malignant breast cancer using data mining techniques. *Journal of Algorithms and Computational Technology*, *12*(2), 119–126. https://doi.org/10.1177/1748301818756225

Chen, L., Li, S., Bai, Q., Yang, J., Jiang, S., & Miao, Y. (2021). Review of image classification algorithms based on convolutional neural networks. *Remote Sensing*, *13*(22), 1–51. https://doi.org/10.3390/rs13224712

Chiao, J. Y., Chen, K. Y., Ken Ying-Kai Liao, Hsieh, P. H., Zhang, G., & Huang, T. C. (2019). Detection and classification the breast tumors using mask R-CNN on sonograms. *Medicine (United States)*, *98*(19), 1–5. https://doi.org/10.1097/MD.0000000000015200

Choi, J. H., Kim, H. A., Kim, W., Lim, I., Lee, I., Byun, B. H., Noh, W. C., Seong, M. K., Lee, S. S., Kim, B. Il, Choi, C. W., Lim, S. M., & Woo, S. K. (2020). Early prediction of neoadjuvant chemotherapy response for advanced breast cancer using PET/MRI image deep learning. *Scientific Reports*, *10*(1), 1–11. https://doi.org/10.1038/s41598-020-77875-5

Conte, L., Tafuri, B., Portaluri, M., Galiano, A., Maggiulli, E., & De Nunzio, G. (2020). Breast cancer mass detection in dce-mri using deep-learning features followed by discrimination of infiltrative vs. in situ carcinoma through a machine-learning approach. *Applied Sciences (Switzerland)*, *10*(17).

https://doi.org/10.3390/app10176109

Conti, A., Duggento, A., Indovina, I., Guerrisi, M., & Toschi, N. (2021). Radiomics in breast cancer classification and prediction. *Seminars in Cancer Biology*, *72*(April), 238–250. https://doi.org/10.1016/j.semcancer.2020.04.002

Dargan, S., Kumar, M., Ayyagari, M. R., & Kumar, G. (2020). A Survey of Deep Learning and Its Applications: A New Paradigm to Machine Learning. *Archives of Computational Methods in Engineering*, *27*(4), 1071–1092. https://doi.org/10.1007/s11831-019-09344-w

Dawoud, B. M., Darweesh, A. N., Hefeda, M. M., Kamal, R. M., & Younis, R. L. (2022). Diagnostic value of contrast-enhanced mammography in the characterization of breast asymmetry. *Egyptian Journal of Radiology and Nuclear Medicine*, *53*(1). https://doi.org/10.1186/s43055-022-00943-5

De Filippis, R., Carbone, E. A., Gaetano, R., Bruni, A., Pugliese, V., Segura-Garcia, C., & De Fazio, P. (2019). Machine learning techniques in a structural and functional MRI diagnostic approach in schizophrenia: A systematic review. *Neuropsychiatric Disease and Treatment*, *15*, 1605–1627. https://doi.org/10.2147/NDT.S202418

De Freitas Oliveira Baffa, M., & Grassano Lattari, L. (2019). Convolutional Neural Networks for Static and Dynamic Breast Infrared Imaging Classification. *Proceedings - 31st Conference on Graphics, Patterns and Images, SIBGRAPI 2018*, 174–181. https://doi.org/10.1109/SIBGRAPI.2018.00029

de Lima, S. M. L., da Silva-Filho, A. G., & dos Santos, W. P. (2016). Detection and classification of masses in mammographic images in a multi-kernel approach. *Computer Methods and Programs in Biomedicine*, *134*, 11–29. https://doi.org/10.1016/j.cmpb.2016.04.029

De Lima, S. M. L., Da Silva-Filho, A. G., & Dos Santos, W. P. (2014). A methodology for classification of lesions in mammographies using zernike moments, ELM and SVM neural networks in a multi-kernel approach. *Conference Proceedings - IEEE International Conference on Systems, Man and Cybernetics*, *2014-Janua*(January), 988–991. https://doi.org/10.1109/SMC.2014.6974041

Desai, M., & Shah, M. (2021). An anatomization on breast cancer detection and diagnosis employing multi-layer perceptron neural network (MLP) and Convolutional neural network (CNN). *Clinical EHealth*, *4*(2021), 1–11. https://doi.org/10.1016/j.ceh.2020.11.002

Di Micco, R., O'Connell, R. L., Barry, P. A., Roche, N., MacNeill, F. A., & Rusby, J. E. (2017). Standard wide local excision or bilateral reduction mammoplasty in large-breasted women with small tumours: Surgical and patient-reported outcomes. *European Journal of Surgical Oncology*, *43*(4), 636–641. https://doi.org/10.1016/j.ejso.2016.10.027

DICOM. (2013). *RadiAnt DICOM Viewer User manual*. 1–93. http://www.radiantviewer.com

Esgario, J. G. M., & Krohling, R. A. (2022). *Beyond Visual Image: Automated Diagnosis of Pigmented Skin Lesions Combining Clinical Image Features with Patient Data*. *1987*. https://arxiv.org/abs/2201.10650v1

Feng, H., Cao, J., Wang, H., Xie, Y., Yang, D., Feng, J., & Chen, B. (2020). A knowledge-driven feature learning and integration method for breast cancer diagnosis on multi-sequence MRI. *Magnetic Resonance Imaging*, *69*, 40–48. https://doi.org/10.1016/j.mri.2020.03.001

Feng, J., & Jiang, J. (2022). Deep Learning-Based Chest CT Image Features in Diagnosis of Lung Cancer. *Computational and Mathematical Methods in Medicine*, *2022*. https://doi.org/10.1155/2022/4153211

Feng, Y., Zhang, L., & Yi, Z. (2018). Breast cancer cell nuclei classification in histopathology images using deep neural networks. *International Journal of Computer Assisted Radiology and Surgery*, *13*(2), 179–191. https://doi.org/10.1007/s11548-017-1663-9

Flavahan, W. A., Gaskell, E., & Bernstein, B. E. (2017). Epigenetic plasticity and the hallmarks of cancer. *Science*, *357*(6348). https://doi.org/10.1126/science.aal2380

Gandomkar, Z., Suleiman, M. E., Demchig, D., Brennan, P. C., & McEntee, M. F. (2019). *BI-RADS density categorization using deep neural networks*. *March 2019*, 22. https://doi.org/10.1117/12.2513185

García Marcos, E. (2018). *Glandular tissue pattern analysis through multimodal MRI-mammography registration*. https://widgets.ebscohost.com/prod/customerspecific/ns000545/customproxy.php?url=https://search.ebscohost.com/login.aspx?direct=true&db=edstdx&AN=edstdx.10803.585969&amp%0Alang=pt-pt&site=eds-live&scope=site

Girshick, R. (2015). Fast R-CNN. *Proceedings of the IEEE International Conference on Computer Vision*, *2015 Inter*, 1440–1448. https://doi.org/10.1109/ICCV.2015.169

Girshick, R., Donahue, J., Darrell, T., & Malik, J. (2014). Rich feature hierarchies for accurate object detection and semantic segmentation. *Proceedings of the IEEE Computer Society Conference on Computer Vision and Pattern Recognition*, 580–587. https://doi.org/10.1109/CVPR.2014.81

Goh, Y., Chan, C. W., Pillay, P., Lee, H. S., Pan, H. Ben, Hung, B. H., Quek, S. T., & Chou, C. P. (2021). Architecture distortion score (ADS) in malignancy risk stratification of architecture distortion on contrast-enhanced digital mammography. *European Radiology*, *31*(5), 2657–2666. https://doi.org/10.1007/s00330-020-07395-3

Gonzalez, S., Arellano, C., & Tapia, J. E. (2019). Deepblueberry: Quantification of Blueberries in the Wild Using Instance Segmentation. *IEEE Access*, *7*(1), 105776–105788. https://doi.org/10.1109/ACCESS.2019.2933062

Goorts, B., Dreuning, K. M. A., Houwers, J. B., Kooreman, L. F. S., Boerma, E. J. G., Mann, R. M., Lobbes, M. B. I., & Smidt, M. L. (2018). MRI-based response patterns during neoadjuvant chemotherapy can predict pathological (complete) response in patients with breast cancer. *Breast Cancer Research*, *20*(1), 1–10. https://doi.org/10.1186/s13058-018-0950-x

Hassan, E., & Talaa, N. E. F. M. (2022). *Review : Mask R - CNN Models*. *3*(1), 1–10.

Hazra, A., Kumar, S., & Gupta, A. (2016). Study and Analysis of Breast Cancer Cell Detection using Naïve Bayes, SVM and Ensemble Algorithms. *International Journal of Computer Applications*, *145*(2), 39–45. https://doi.org/10.5120/ijca2016910595

Henriksen, E. L., Carlsen, J. F., Vejborg, I. M. M., Nielsen, M. B., & Lauridsen, C. A. (2019). The efficacy of using computer-aided detection (CAD) for detection of breast cancer in mammography screening: a systematic review. *Acta Radiologica*, *60*(1), 13–18. https://doi.org/10.1177/0284185118770917

Hirra, I., Ahmad, M., Hussain, A., Ashraf, M. U., Saeed, I. A., Qadri, S. F., Alghamdi, A. M., & Alfakeeh, A. S. (2021). Breast Cancer Classification from Histopathological Images Using Patch-Based Deep Learning Modeling. *IEEE Access*, *9*, 24273–24287. https://doi.org/10.1109/ACCESS.2021.3056516

Hossam, A., Harb, H. M., & Abd El Kader, H. M. (2018). Automatic Image Segmentation Method for Breast Cancer Analysis Using Thermography. *JES. Journal of Engineering Sciences*, *46*(1), 12–32. https://doi.org/10.21608/jesaun.2017.114377

Houssein, E. H., Emam, M. M., Ali, A. A., & Suganthan, P. N. (2021). Deep and machine learning techniques for medical imaging-based breast cancer: A comprehensive review. *Expert Systems with Applications*, *167*, 114161. https://doi.org/10.1016/j.eswa.2020.114161

Howard, A. G., Zhu, M., Chen, B., Kalenichenko, D., Wang, W., Weyand, T., Andreetto, M., & Adam, H. (2017). *MobileNets: Efficient Convolutional Neural Networks for Mobile Vision Applications*. *October*. http://arxiv.org/abs/1704.04861

Hsieh, Y. C., Chin, C. L., Wei, C. S., Chen, I. M., Yeh, P. Y., & Tseng, R. J. (2020). Combining VGG16, Mask R-CNN and Inception V3 to identify the benign and malignant of breast microcalcification clusters. *2020 International Conference on Fuzzy Theory and Its Applications, IFUZZY 2020*, 1–4. https://doi.org/10.1109/iFUZZY50310.2020.9297809

Hu, Q., Whitney, H. M., Li, H., Ji, Y., Liu, P., & Giger, M. L. (2021). Improved classification of benign and malignant breast lesions using deep feature maximum intensity projection mri in breast cancer diagnosis using dynamic contrast-enhanced mri. *Radiology: Artificial Intelligence*, *3*(3). https://doi.org/10.1148/ryai.2021200159

Huang, Y., Chen, W., Zhang, X., He, S., Shao, N., Shi, H., Lin, Z., Wu, X., Li, T., Lin, H., & Lin, Y. (2021). Prediction of Tumor Shrinkage Pattern to Neoadjuvant Chemotherapy Using a Multiparametric MRI-Based Machine Learning Model in Patients With Breast Cancer. *Frontiers in Bioengineering and Biotechnology*, *9*(July), 1–15. https://doi.org/10.3389/fbioe.2021.662749

Hubert-moy, L., Guyot, A., Lennon, M., & Hubert-moy, L. (2021). *Objective comparison of relief visualization techniques with deep CNN for archaeology Journal of Archaeological Science : Reports Objective comparison of relief visualization techniques with deep CNN for archaeology*. Journal of

Archaeological Science: Reports; Elsevier Ltd. https://doi.org/10.1016/j.jasrep.2021.103027

Islam, M. N., Mahmud, T., Khan, N. I., Mustafina, S. N., & Islam, A. K. M. N. (2021). Exploring Machine Learning Algorithms to Find the Best Features for Predicting Modes of Childbirth. *IEEE Access*, *9*(February), 1680–1692. https://doi.org/10.1109/ACCESS.2020.3045469

Ismail, N. S., & Sovuthy, C. (2019). Breast Cancer Detection Based on Deep Learning Technique. *2019 International UNIMAS STEM 12th Engineering Conference, EnCon 2019 - Proceedings*, 89–92. https://doi.org/10.1109/EnCon.2019.8861256

Jiang, H., & Learned-Miller, E. (2017). Face Detection with the Faster R-CNN. *Proceedings - 12th IEEE International Conference on Automatic Face and Gesture Recognition, FG 2017 - 1st International Workshop on Adaptive Shot Learning for Gesture Understanding and Production, ASL4GUP 2017, Biometrics in the Wild, Bwild 2017, Heteroge*, 650–657. https://doi.org/10.1109/FG.2017.82

Jiang, L. (2013). *Association between use of specialized diagnostic assessment units and the diagnostic interval in Ontario breast cancer patients*.

Jones, E. F., Hathi, D. K., Freimanis, R., Mukhtar, R. A., Chien, A. J., Esserman, L. J., Van'T Veer, L. J., Joe, B. N., & Hylton, N. M. (2020). Current landscape of breast cancer imaging and potential quantitative imaging markers of response in er-positive breast cancers treated with neoadjuvant therapy. *Cancers*, *12*(6), 1–24. https://doi.org/10.3390/cancers12061511

Kadhim, R. R., & Kamil, M. Y. (2022). Evaluation of Machine Learning Models for Breast Cancer Diagnosis Via Histogram of Oriented Gradients Method and Histopathology Images. *International Journal on Recent and Innovation Trends in Computing and Communication*, *10*(4), 36–42.

https://doi.org/10.17762/ijritcc.v10i4.5532

Khalil, R., Osman, N. M., Chalabi, N., & Abdel Ghany, E. (2020). Unenhanced breast MRI: could it replace dynamic breast MRI in detecting and characterizing breast lesions? *Egyptian Journal of Radiology and Nuclear Medicine*, *51*(1). https://doi.org/10.1186/s43055-019-0103-y

Khourdifi, Y., & Bahaj, M. (2019). Applying best machine learning algorithms for breast cancer prediction and classification. *2018 International Conference on Electronics, Control, Optimization and Computer Science, ICECOCS 2018*, 1–5. https://doi.org/10.1109/ICECOCS.2018.8610632

Khuriwal, N., & Mishra, N. (2018). Breast Cancer Diagnosis Using Deep Learning Algorithm. *Proceedings - IEEE 2018 International Conference on Advances in Computing, Communication Control and Networking, ICACCCN 2018*, 98–103. https://doi.org/10.1109/ICACCCN.2018.8748777

Kim, C. M., Park, R. C., & Hong, E. J. (2020). Breast mass classification using eLFA algorithm based on CRNN deep learning model. *IEEE Access*, *8*, 197312–197323. https://doi.org/10.1109/ACCESS.2020.3034914

Kim, D. Y., Lee, S. J., Kim, E. K., Kang, E., Heo, C. Y., Jeong, J. H., Myung, Y., Kim, I. A., & Jang, B. S. (2022). Feasibility of anomaly score detected with deep learning in irradiated breast cancer patients with reconstruction. *Npj Digital Medicine*, *5*(1), 1–7. https://doi.org/10.1038/s41746-022-00671-0

Kim, M. S., Park, H. Y., Kho, B. G., Park, C. K., Oh, I. J., Kim, Y. C., Kim, S., Yun, J. S., Song, S. Y., Na, K. J., Jeong, J. U., Yoon, M. S., Ahn, S. J., Yoo, S. W., Kang, S. R., Kwon, S. Y., Bom, H. S., Jang, W. Y., Kim, I. Y., … Choi, Y. D. (2020). Artificial intelligence and lung cancer treatment decision: Agreement with recommendation of multidisciplinary tumor board. *Translational Lung Cancer Research*, *9*(3), 507–514. https://doi.org/10.21037/tlcr.2020.04.11

Kim, Y., Sim, S. H., Park, B., Chae, I. H., Han, J. H., Jung, S. Y., Lee, S., Kwon, Y., Park, I. H., Ko, K., Lee, C. W., Lee, K. S., Kang, H. S., & Lee, E. S. (2021). Criteria for identifying residual tumours after neoadjuvant chemotherapy of breast cancers: a magnetic resonance imaging study. *Scientific Reports*, *11*(1), 1–10. https://doi.org/10.1038/s41598-020-79743-8

Kumaraswamy, E., Kumar, S., & Sharma, M. (2023). An Invasive Ductal Carcinomas Breast Cancer Grade Classification Using an Ensemble of Convolutional Neural Networks. *Diagnostics*, *13*(11). https://doi.org/10.3390/diagnostics13111977

Kumeda, B., Fengli, Z., Oluwasanmi, A., Owusu, F., Assefa, M., & Amenu, T. (2019). Vehicle Accident and Traffic Classification Using Deep Convolutional Neural Networks. *2019 16th International Computer Conference on Wavelet Active Media Technology and Information Processing, ICCWAMTIP 2019, August 2020*, 323–328. https://doi.org/10.1109/ICCWAMTIP47768.2019.9067530

Latif, J., Xiao, C., Imran, A., & Tu, S. (2019). Medical imaging using machine learning and deep learning algorithms: A review. *2019 2nd International Conference on Computing, Mathematics and Engineering Technologies, ICoMET 2019*, 1–5. https://doi.org/10.1109/ICOMET.2019.8673502

Leithner, D., Wengert, G. J., Helbich, T. H., Thakur, S., Ochoa-Albiztegui, R. E., Morris, E. A., & Pinker, K. (2018). Clinical role of breast MRI now and going forward. *Clinical Radiology*, *73*(8), 700–714. https://doi.org/10.1016/j.crad.2017.10.021

Lenc, L., & Kr, P. (2014). *TWO-STEP SUPERVISED CONFIDENCE MEASURE FOR AUTOMATIC FACE RECOGNITION Dept . of Computer Science & Engineering Faculty of Applied Sciences University of West Bohemia Plzeˇn , Czech Republic New Technologies for the Information Society Faculty of*

Applied . 1–6.

Li, L., Tian, H., Zhang, B., Wang, W., & Li, B. (2022). Prediction for Distant Metastasis of Breast Cancer Using Dynamic Contrast-Enhanced Magnetic Resonance Imaging Images under Deep Learning. *Computational Intelligence and Neuroscience*, *2022*. https://doi.org/10.1155/2022/6126061

Loizidou, K., Skouroumouni, G., Pitris, C., & Nikolaou, C. (2021). Digital subtraction of temporally sequential mammograms for improved detection and classification of microcalcifications. *European Radiology Experimental*, *5*(1). https://doi.org/10.1186/s41747-021-00238-w

Lopez-Almazan, H., Javier Pérez-Benito, F., Larroza, A., Perez-Cortes, J. C., Pollan, M., Perez-Gomez, B., Salas Trejo, D., Casals, M., & Llobet, R. (2022). A deep learning framework to classify breast density with noisy labels regularization. *Computer Methods and Programs in Biomedicine*, *221*, 106885. https://doi.org/10.1016/j.cmpb.2022.106885

Lu, H. C., Loh, E. W., & Huang, S. C. (2019). The Classification of Mammogram Using Convolutional Neural Network with Specific Image Preprocessing for Breast Cancer Detection. *2019 2nd International Conference on Artificial Intelligence and Big Data, ICAIBD 2019*, 9–12. https://doi.org/10.1109/ICAIBD.2019.8837000

Magboo, V. P. C., & Magboo, M. S. (2021). Machine learning classifiers on breast cancer recurrences. *Procedia Computer Science*, *192*, 2742–2752. https://doi.org/10.1016/j.procs.2021.09.044

Mahmood, T., Li, J., Pei, Y., Akhtar, F., Ur Rehman, M., & Wasti, S. H. (2022). Breast lesions classifications of mammographic images using a deep convolutional neural network-based approach. *PLoS ONE*, *17*(1 January), 1–25. https://doi.org/10.1371/journal.pone.0263126

Maicas, G., Carneiro, G., & Bradley, A. P. (2017). Globally optimal breast mass

segmentation from DCE-MRI using deep semantic segmentation as shape prior. *Proceedings - International Symposium on Biomedical Imaging*, 305–309. https://doi.org/10.1109/ISBI.2017.7950525

Makone, A. 2020. (2020). *Faster RCNN. Faster than fast | by Ashutosh Makone | Medium*. https://ashutoshmakone.medium.com/faster-rcnn-502e4a2e1ec6

Mendel, K., Li, H., Sheth, D., & Giger, M. (2019). Transfer Learning From Convolutional Neural Networks for Computer-Aided Diagnosis: A Comparison of Digital Breast Tomosynthesis and Full-Field Digital Mammography. *Academic Radiology*, *26*(6), 735–743. https://doi.org/10.1016/j.acra.2018.06.019

Michael, E., Ma, H., Li, H., Kulwa, F., & Li, J. (2021). Breast Cancer Segmentation Methods: Current Status and Future Potentials. *BioMed Research International, 2021*. https://doi.org/10.1155/2021/9962109

Militello, C., Rundo, L., Dimarco, M., Orlando, A., Conti, V., Woitek, R., D'Angelo, I., Bartolotta, T. V., & Russo, G. (2022). Semi-automated and interactive segmentation of contrast-enhancing masses on breast DCE-MRI using spatial fuzzy clustering. *Biomedical Signal Processing and Control, 71*(PA), 103113. https://doi.org/10.1016/j.bspc.2021.103113

Min, H., Wilson, D., Huang, Y., Liu, S., Crozier, S., Bradley, A. P., & Chandra, S. S. (2020). Fully Automatic Computer-aided Mass Detection and Segmentation via Pseudo-color Mammograms and Mask R-CNN. *Proceedings - International Symposium on Biomedical Imaging, 2020-April*, 1111–1115. https://doi.org/10.1109/ISBI45749.2020.9098732

Mohamed, A. A., Berg, W. A., Peng, H., Luo, Y., Jankowitz, R. C., & Wu, S. (2018). A deep learning method for classifying mammographic breast density categories. *Medical Physics*, *45*(1), 314–321. https://doi.org/10.1002/mp.12683

Moy, L., Yassin, N. I. R., Omran, S., El Houby, E. M. F., Allam, H., Sharma, S., Deshpande, S., Cai, H., Huang, Q., Rong, W., Song, Y., Li, J., Wang, J. J., Chen, J., Li, L., Lee, C., McCaskill-Stevens, W., Loizidou, K., Skouroumouni, G., … Cömert, Z. (2020). Breast cancer diagnosis using a multi-verse optimizer-based gradient boosting decision tree. *IEEE Access*, *5*(1), 1–23. https://doi.org/10.1155/2019/2717454

Mu'jizah, H., & Novitasari, D. C. R. (2021). Comparison of the histogram of oriented gradient, GLCM, and shape feature extraction methods for breast cancer classification using SVM. *Jurnal Teknologi Dan Sistem Komputer*, *9*(3), 150–156. https://doi.org/10.14710/jtsiskom.2021.14104

Murtaza, G., Shuib, L., Abdul Wahab, A. W., Mujtaba, G., Mujtaba, G., Nweke, H. F., Al-garadi, M. A., Zulfiqar, F., Raza, G., & Azmi, N. A. (2020). Deep learning-based breast cancer classification through medical imaging modalities: state of the art and research challenges. *Artificial Intelligence Review*, *53*(3), 1655–1720. https://doi.org/10.1007/s10462-019-09716-5

Naji, M. A., Filali, S. El, Bouhlal, M., Benlahmar, E. H., Abdelouhahid, R. A., & Debauche, O. (2021). Breast Cancer Prediction and Diagnosis through a New Approach based on Majority Voting Ensemble Classifier. *Procedia Computer Science*, *191*, 481–486. https://doi.org/10.1016/j.procs.2021.07.061

Namdar, K., Haider, M. A., & Khalvati, F. (2021). A Modified AUC for Training Convolutional Neural Networks: Taking Confidence Into Account. *Frontiers in Artificial Intelligence*, *4*(November), 1–12. https://doi.org/10.3389/frai.2021.582928

Naresh, S., & Vani, S. (2015). Breast Cancer Detection using Local Binary Patterns. *International Journal of Computer Applications*, *123*(16), 6–9. https://doi.org/10.5120/ijca2015905726

Nayak, D. R., Padhy, N., Mallick, P. K., Zymbler, M., & Kumar, S. (2022). Brain

Tumor Classification Using Dense Efficient-Net. *Axioms*, *11*(1). https://doi.org/10.3390/axioms11010034

Obaid, O. I., Mohammed, M. A., Abd Ghani, M. K., Mostafa, S. A., & Al-Dhief, F. T. (2018). Evaluating the performance of machine learning techniques in the classification of Wisconsin Breast Cancer. *International Journal of Engineering and Technology(UAE)*, *7*(4.36 Special Issue 36), 160–166. https://doi.org/10.14419/ijet.v7i4.36.23737

Omondiagbe, D. A., Veeramani, S., & Sidhu, A. S. (2019). Machine Learning Classification Techniques for Breast Cancer Diagnosis. *IOP Conference Series: Materials Science and Engineering*, *495*(1). https://doi.org/10.1088/1757-899X/495/1/012033

Pei, L., Xu, J., & Cai, J. (2018). An image retrieval algorithm based on semantic self-feedback mechanism. *Advances in Intelligent Systems and Computing*, *686*(4), 295–301. https://doi.org/10.1007/978-3-319-69096-4_41

Pham, V., Pham, C., & Dang, T. (2020). Road Damage Detection and Classification with Detectron2 and Faster R-CNN. *Proceedings - 2020 IEEE International Conference on Big Data, Big Data 2020*, 5592–5601. https://doi.org/10.1109/BigData50022.2020.9378027

Pomponiu, V., Hariharan, H., Zheng, B., & Gur, D. (2014). *Improving Breast Mass Detection using Histogram of Oriented Gradients*. *9035*, 1–6. https://doi.org/10.1117/12.2044281

Pratiwi, A. D., & Sari, I. P. (2022). Robust Breast cancer Detection using Faster R-CNN Algoritma. *International Journal of Informatics and Computation*, *4*(1), 43. https://doi.org/10.35842/ijicom.v4i1.49

Praveen, S. P., Srinivasu, P. N., Shafi, J., Wozniak, M., & Ijaz, M. F. (2022). ResNet-32 and FastAI for diagnoses of ductal carcinoma from 2D tissue slides. *Scientific Reports*, *12*(1), 1–16. https://doi.org/10.1038/s41598-022-

25089-2

Putra, T. A., Rufaida, S. I., & Leu, J. S. (2020). Enhanced Skin Condition Prediction through Machine Learning Using Dynamic Training and Testing Augmentation. *IEEE Access*, *8*, 40536–40546. https://doi.org/10.1109/ACCESS.2020.2976045

Qader, S. M., Hassan, B. A., & Rashid, T. A. (2022). An improved deep convolutional neural network by using hybrid optimization algorithms to detect and classify brain tumor using augmented MRI images. *Multimedia Tools and Applications*, 1–35. https://doi.org/10.1007/s11042-022-13260-w

Qi, X., Zhang, L., Chen, Y., Pi, Y., Chen, Y., Lv, Q., & Yi, Z. (2019). Automated diagnosis of breast ultrasonography images using deep neural networks. *Medical Image Analysis*, *52*, 185–198. https://doi.org/10.1016/j.media.2018.12.006

Quintanilla-Domínguez, J., Ruiz-Pinales, J., Barrón-Adame, J. M., & Guzmán-Cabrera, R. (2018). Microcalcifications detection using image processing. *Computacion y Sistemas*, *22*(1), 291–300. https://doi.org/10.13053/CyS-22-1-2560

Raza, S. K., & Syed, S. M. (2021a). *Classi cation and Segmentation of Breast Tumor Using Mask R- CNN on Mammograms Classification and Segmentation of Breast Tumor using Mask*.

Raza, S. K., & Syed, S. M. (2021b). *Classi cation and Segmentation of Breast Tumor Using Mask R- CNN on Mammograms Classification and Segmentation of Breast Tumor using Mask*. *9*(1000180). https://doi.org/10.35248/2684-1258.22.9.180

Reiazi, R., Paydar, R., Ardakani, A. A., & Etedadialiabadi, M. (2018). *Mammography Lesion Detection Using Faster R-CNN Detector*. 111–115. https://doi.org/10.5121/csit.2018.80212

Reig, B., Heacock, L., J. Geras, K., & Moy, L. (2020). Machine Learning in Breast MRI. *Physiology & Behavior*, *176*(1), 139–148. https://doi.org/10.1002/jmri.26852.Machine

Ren, T., Lin, S., Huang, P., & Duong, T. Q. (2022). Convolutional Neural Network of Multiparametric MRI Accurately Detects Axillary Lymph Node Metastasis in Breast Cancer Patients With Pre Neoadjuvant Chemotherapy. *Clinical Breast Cancer*, *22*(2), 170–177. https://doi.org/10.1016/j.clbc.2021.07.002

Rojas, R. F., Huang, X., Romero, J., & Ou, K. L. (2017). fNIRS Approach to Pain Assessment for Non-verbal Patients. *Lecture Notes in Computer Science (Including Subseries Lecture Notes in Artificial Intelligence and Lecture Notes in Bioinformatics)*, *10637 LNCS*(May 2018), 778–787. https://doi.org/10.1007/978-3-319-70093-9_83

Roslidar, R., Saddami, K., Arnia, F., Syukri, M., & Munadi, K. (2019). A study of fine-tuning CNN models based on thermal imaging for breast cancer classification. *Proceedings: CYBERNETICSCOM 2019 - 2019 IEEE International Conference on Cybernetics and Computational Intelligence: Towards a Smart and Human-Centered Cyber World*, 77–81. https://doi.org/10.1109/CYBERNETICSCOM.2019.8875661

Runowicz, C. D., Leach, C. R., Henry, N. L., Henry, K. S., Mackey, H. T., Cowens-Alvarado, R. L., Cannady, R. S., Pratt-Chapman, M. L., Edge, S. B., Jacobs, L. A., Hurria, A., Marks, L. B., LaMonte, S. J., Warner, E., Lyman, G. H., & Ganz, P. A. (2016). American Cancer Society/American Society of Clinical Oncology Breast Cancer Survivorship Care Guideline. *CA: A Cancer Journal for Clinicians*, *66*(1), 43–73. https://doi.org/10.3322/caac.21319

Saffari, N., Rashwan, H. A., Abdel-Nasser, M., Singh, V. K., Arenas, M., Mangina, E., Herrera, B., & Puig, D. (2020). Fully automated breast density segmentation and classification using deep learning. *Diagnostics*, *10*(11), 1–

20. https://doi.org/10.3390/diagnostics10110988

Sannasi Chakravarthy, S. R., & Rajaguru, H. (2022). Automatic Detection and Classification of Mammograms Using Improved Extreme Learning Machine with Deep Learning. *Irbm*, *43*(1), 49–61. https://doi.org/10.1016/j.irbm.2020.12.004

Sarker, M. M. K., Makhlouf, Y., Craig, S. G., Humphries, M. P., Loughrey, M., James, J. A., Salto-tellez, M., O'Reilly, P., & Maxwell, P. (2021). A means of assessing deep learning-based detection of ICOS protein expression in colon cancer. *Cancers*, *13*(15), 1–21. https://doi.org/10.3390/cancers13153825

Sasikala, N., Swathipriya, V., Ashwini, M., Preethi, V., Pranavi, A., & Ranjith, M. (2020). Feature Extraction of Real-Time Image Using SIFT Algorithm. *European Journal of Electrical Engineering and Computer Science*, *4*(3), 1–7. https://doi.org/10.24018/ejece.2020.4.3.206

Senkamalavalli, R. (2017). Improved Classification of Breast Cancer Data Using Hybrid Techniques. *International Journal of Advanced Research in Computer Science*, *8*(8), 454–457. https://doi.org/10.26483/ijarcs.v8i8.4805

Sethy, P. K., Shanthi, S., Anitha, K., Devi, A. G., & Biswas, P. (2022). *Breast cancer detection using bimodal image fusion : Thermography and mammography images*. *16*(May), 1–5.

Sharma, S., Aggarwal, A., & Choudhury, T. (2018). Breast Cancer Detection Using Machine Learning Algorithms. *Proceedings of the International Conference on Computational Techniques, Electronics and Mechanical Systems, CTEMS 2018*, *Ml*, 114–118. https://doi.org/10.1109/CTEMS.2018.8769187

Shiji, T. P., Remya, S., & Thomas, V. (2017). ScienceDirect ScienceDirect Computer Aided Segmentation of Breast Ultrasound Images Using Scale Invariant Feature Transform (SIFT) and Bag Of Features. *Procedia*

Computer Science, *115*, 518–525. https://doi.org/10.1016/j.procs.2017.09.108

Silva, J., Borré, J. R., Piñeres Castillo, A. P., Castro, L., & Varela, N. (2019). Integration of data mining classification techniques and ensemble learning for predicting the export potential of a company. *Procedia Computer Science*, *151*(2018), 1194–1200. https://doi.org/10.1016/j.procs.2019.04.171

Sivasangari, A., Ajitha, P., Bevishjenila, Vimali, J. S., Jose, J., & Gowri, S. (2022). Breast Cancer Detection Using Machine Learning. *Lecture Notes on Data Engineering and Communications Technologies*, *68*(07), 693–702. https://doi.org/10.1007/978-981-16-1866-6_50

Smith, R. A., Andrews, K. S., Brooks, D., Fedewa, S. A., Manassaram-Baptiste, D., Saslow, D., Brawley, O. W., & Wender, R. C. (2018). Cancer screening in the United States, 2018: A review of current American Cancer Society guidelines and current issues in cancer screening. *CA: A Cancer Journal for Clinicians*, *68*(4), 297–316. https://doi.org/10.3322/caac.21446

Soltani, H., Amroune, M., Bendib, I., & Haouam, M. Y. (2021). Breast Cancer Lesion Detection and Segmentation Based On Mask R-CNn. *Proceedings - 2021 IEEE International Conference on Recent Advances in Mathematics and Informatics, ICRAMI 2021, November*. https://doi.org/10.1109/ICRAMI52622.2021.9585913

Sutton, E. J., Onishi, N., Fehr, D. A., Dashevsky, B. Z., Sadinski, M., Pinker, K., Martinez, D. F., Brogi, E., Braunstein, L., Razavi, P., El-Tamer, M., Sacchini, V., Deasy, J. O., Morris, E. A., & Veeraraghavan, H. (2020). A machine learning model that classifies breast cancer pathologic complete response on MRI post-neoadjuvant chemotherapy. *Breast Cancer Research*, *22*(1), 1–11. https://doi.org/10.1186/s13058-020-01291-w

Tahmooresi, M., Afshar, A., Bashari Rad, B., Nowshath, K. B., & Bamiah, M. A.

(2018). Early detection of breast cancer using machine learning techniques. *Journal of Telecommunication, Electronic and Computer Engineering*, *10*(3–2), 21–27.

Tamimi, R. M., Spiegelman, D., Smith-Warner, S. A., Wang, M., Pazaris, M., Willett, W. C., Eliassen, A. H., & Hunter, D. J. (2016). Population attributable risk of modifiable and nonmodifiable breast cancer risk factors in postmenopausal breast cancer. *American Journal of Epidemiology*, *184*(12), 884–893. https://doi.org/10.1093/aje/kww145

Tan, M., Chen, B., Pang, R., Vasudevan, V., Sandler, M., Howard, A., & Le, Q. V. (2019). Mnasnet: Platform-aware neural architecture search for mobile. *Proceedings of the IEEE Computer Society Conference on Computer Vision and Pattern Recognition*, *2019-June*, 2815–2823. https://doi.org/10.1109/CVPR.2019.00293

Tan, M., & Le, Q. V. (2021). *EfficientNetV2: Smaller Models and Faster Training*. http://arxiv.org/abs/2104.00298

Tang, L., Ma, S., Ma, X., & You, H. (2022). Research on Image Matching of Improved SIFT Algorithm Based on Stability Factor and Feature Descriptor Simplification. *Applied Sciences (Switzerland)*, *12*(17). https://doi.org/10.3390/app12178448

Timotius, I. K., & Setyawan, I. (2014). Evaluation of Edge Orientation Histograms in smile detection. *Proceedings - 2014 6th International Conference on Information Technology and Electrical Engineering: Leveraging Research and Technology Through University-Industry Collaboration, ICITEE 2014*, 2–6. https://doi.org/10.1109/ICITEED.2014.7007905

Ting, F. F., Tan, Y. J., & Sim, K. S. (2019). Convolutional neural network improvement for breast cancer classification. *Expert Systems with Applications*, *120*, 103–115. https://doi.org/10.1016/j.eswa.2018.11.008

Wang, L. (2017). Early diagnosis of breast cancer. *Sensors (Switzerland)*, *17*(7). https://doi.org/10.3390/s17071572

Wang, M., & Chen, H. (2020). Chaotic multi-swarm whale optimizer boosted support vector machine for medical diagnosis. *Applied Soft Computing Journal*, *88*, 105946. https://doi.org/10.1016/j.asoc.2019.105946

Webber, C., Whitehead, M., Eisen, A., Holloway, C. M. B., & Groome, P. A. (2020). Breast cancer diagnosis and treatment wait times in specialized diagnostic units compared with usual care: A population-based study. *Current Oncology*, *27*(4), e377–e385. https://doi.org/10.3747/co.27.6115

Xi, P., Shu, C., & Goubran, R. (2018). Abnormality Detection in Mammography using Deep Convolutional Neural Networks. *MeMeA 2018 - 2018 IEEE International Symposium on Medical Measurements and Applications, Proceedings*, *3528725544*, 1–6. https://doi.org/10.1109/MeMeA.2018.8438639

Y. Wu, A. K., Massa, F., Lo, W.-Y., & Girshick, R. (2019). *Digging into Detectron 2 — part 1 | by Hiroto Honda | Medium*. https://medium.com/@hirotoschwert/digging-into-detectron-2-47b2e794fabd

Yari, Y., Nguyen, T. V., & Nguyen, H. T. (2020). Deep learning applied for histological diagnosis of breast cancer. *IEEE Access*, *8*, 162432–162448. https://doi.org/10.1109/ACCESS.2020.3021557

Yassin, N. I. R., Omran, S., El Houby, E. M. F., & Allam, H. (2018). Machine learning techniques for breast cancer computer aided diagnosis using different image modalities: A systematic review. *Computer Methods and Programs in Biomedicine*, *156*, 25–45. https://doi.org/10.1016/j.cmpb.2017.12.012

Ye, G., He, S., Pan, R., Zhu, L., Zhou, D., & Lu, R. L. (2022). Research on DCE-MRI Images Based on Deep Transfer Learning in Breast Cancer Adjuvant

Curative Effect Prediction. *Journal of Healthcare Engineering*, *2022*. https://doi.org/10.1155/2022/4477099

Zhang, Y., Chan, S., Park, V. Y., Chang, K. T., Mehta, S., Kim, M. J., Combs, F. J., Chang, P., Chow, D., Parajuli, R., Mehta, R. S., Lin, C. Y., Chien, S. H., Chen, J. H., & Su, M. Y. (2022). Automatic Detection and Segmentation of Breast Cancer on MRI Using Mask R-CNN Trained on Non–Fat-Sat Images and Tested on Fat-Sat Images. *Academic Radiology*, *29*, S135–S144. https://doi.org/10.1016/j.acra.2020.12.001

Zhang, Y., Chu, J., Leng, L., & Miao, J. (2020). Mask-Refined R-CNN: A Network for Refining Object Details in Instance Segmentation. *Sensors*, *20*(4).

Zhao, Y., Zhang, J., Hu, D., Qu, H., Tian, Y., & Cui, X. (2022). Application of Deep Learning in Histopathology Images of Breast Cancer: A Review. *Micromachines*, *13*(12), 1–30. https://doi.org/10.3390/mi13122197

Zheng, J., Lin, D., Gao, Z., Wang, S., He, M., & Fan, J. (2020). Deep Learning Assisted Efficient AdaBoost Algorithm for Breast Cancer Detection and Early Diagnosis. *IEEE Access*, *8*, 96946–96954. https://doi.org/10.1109/ACCESS.2020.2993536

Zhou, J., Zhang, Y., Chang, K. T., Lee, K. E., Wang, O., Li, J., Lin, Y., Pan, Z., Chang, P., Chow, D., Wang, M., & Su, M. Y. (2020). Diagnosis of Benign and Malignant Breast Lesions on DCE-MRI by Using Radiomics and Deep Learning With Consideration of Peritumor Tissue. *Journal of Magnetic Resonance Imaging*, *51*(3), 798–809. https://doi.org/10.1002/jmri.26981

Zhou, K., Li, W., & Zhao, D. (2022). Deep learning-based breast region extraction of mammographic images combining pre-processing methods and semantic segmentation supported by Deeplab v3. *Technology and Health Care*, *30*(S1), S173–S190. https://doi.org/10.3233/THC-228017

Zhu, Z. (2020). *Detecting Coronavirus Disease 2019 Pneumonia*. *2507*(February), 1–9.

Zhu, Z., Wang, S. H., & Zhang, Y. D. (2023). A Survey of Convolutional Neural Network in Breast Cancer. *CMES - Computer Modeling in Engineering and Sciences*, *136*(3), 2127–2172. https://doi.org/10.32604/cmes.2023.025484

Zuluaga-Gomez, J., Al Masry, Z., Benaggoune, K., Meraghni, S., & Zerhouni, N. (2021). A CNN-based methodology for breast cancer diagnosis using thermal images. *Computer Methods in Biomechanics and Biomedical Engineering: Imaging and Visualization*, *9*(2), 131–145. https://doi.org/10.1080/21681163.2020.1824685

APPENDICES

Appendices A

In this appendix, the first comparative is illustrated by using machine learning algorithms (Breast cancer recognition based on performance evaluation of machine learning algorithms) The results are displayed in the following tables and figures.

Table A. 1 Classification results for feature set diagnosis

No. of datasets	No. of Method	KNN	ANN	SVM	DT	RF	Ada Boost
Dataset (920)	HOG	94.13%	94.13%	88.7%	87.93%	91.9%	88.8%
	EOH	85.2%	89.2%	88.4%	86.52%	88.3%	86.96%
	SIFT	88.9%	85.87%	88.4%	87.83%	88.04%	88.04%
	LBP	88.18%	88%	88%	87.18%	88.59%	88%
	Bo W	89.1%	90%	89.9%	92%	89.1%	92.3%
Dataset (400)	HOG	92.3%	89%	87.3%	86.75%	88.75%	87.5%
	EOH	85.5%	87%	87.5%	87%	87.25%	87.5%
	SIFT	89.25%	82.75%	87.25%	87%	86.75%	87.25%
	LBP	85.25%	85.75%	87.5%	87%	88.25	86%
	Bo W	95%	96%	95%	97%	95%	99%
Dataset (1280)	HOG	97.89%	98.20%	93.67%	93.59%	95.3%	93.67%
	EOH	9.78%	93.36%	93.75%	93.75%	93.59%	93.75%

	SIFT	89.38%	93.67%	93.75%	93.59%	93.75%	93.75%
	LBP	91.32%	93.81%	93.75%	93.28%	93.82%	93.75%
	Bo W	96%	97%	96%	98%	96%	99%

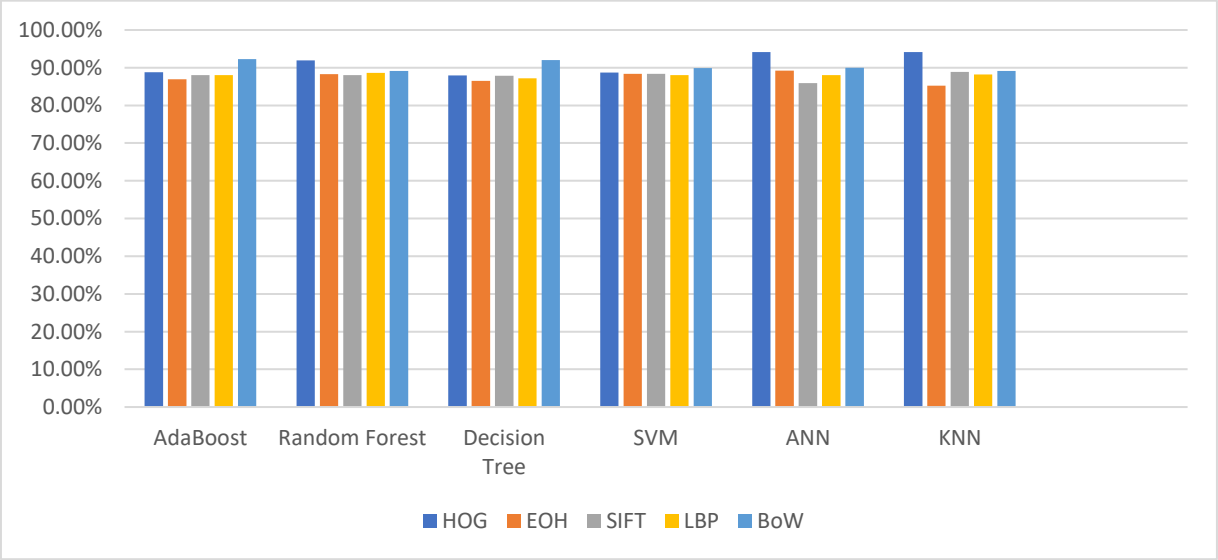

Figure A. 1 Dataset: Erbil and Sulaymaniyah breast MRI

Figure A. 2 Dataset: Breast Cancer MRI

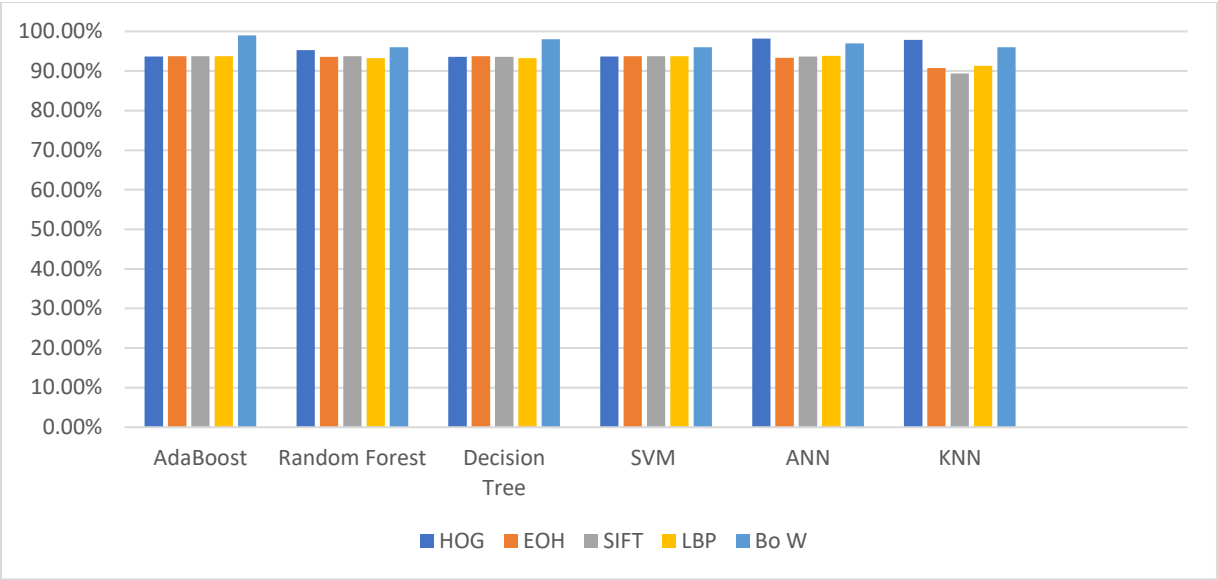

Figure A. 3 Dataset: ACRIN-Contralateral-Breast-MRI

Table A. 2 MRI image diagnostic accuracy test breast cancer private dataset

Method	Algorithms	Test Accuracy	Train Accuracy	Test Result		
				Sensitivity	f- measure	Precision
HOG (920) images	KNN	92.8%	95.6%	95.6%	95.8%	96.0%
	ANN	95.4%	95.8%	95.9%	95.9%	96.0%
	Decision Tree	88.0%	91.0%	91.1%	90.%3	90.1%
	Random Forest	90.8%	93.6%	93.7%	92.%6	93.7%
	AdaBoost	87.6%	91.9%	92.0%	91.%1	91.2%
	SVM	88.0%	91.3%	91.3%	89.0%	92.1%
EOH (920)	KNN	86.0%	86.5%	86.5%	86.5%	86.5%
	ANN	87.6%	88.2%	88.2%	85.4%	85.2%
	Decision Tree	87.3%	87.6%	87.2%	83.3%	82.4%
	Random Forest	87.3%	88.0%	88.0%	83.5%	82.4%

images	AdaBoost	88.0%	88.6%	80.7%	84.0%	90.0%
	SVM	88.0%	88.0%	88.0%	93.6%	88.0%
Sift (920) images	KNN	88.6%	90.8%	90.9%	90.5%	90.2%
	ANN	83.2%	87.8%	87.8%	88.2%	86.8%
	Decision Tree	87.82%	87.8%	87.8%	82.3%	81.6%
	Random Forest	88.0%	88.0%	88.7%	81.8%	88.0%
	AdaBoost	86.9%	88.0%	88.0%	81.9%	88.0%
	SVM	87.0%	88.6%	88.0%	82.5%	83.6%
LBP (920) images	KNN	86.3%	93.4%	96.0%	96.3%	95.6%
	ANN	84.7%	92.6%	96.5%	95.3%	95.1%
	Decision Tree	87.3%	90.2%	95.8%	94.9%	93.3%
	Random Forest	88.5%	93%	98.5%	96.1%	93.9%
	AdaBoost	87.3%	88.9%	98.8%	94.0%	89.7%
	SVM	87.6%	88.2%	100%	93.8%	88.3%
Bo W (920) images	KNN	87%	100%	98.5%	100%	99.5%
	ANN	88.5%	90%	100%	94.1%	88.9%
	Decision Tree	92.5%	100%	99.5%	100%	94.9%
	Random Forest	86.6%	100%	99.8%	100%	99.6%
	AdaBoost	91.0%	100%	99.8%	100%	99.9%
	SVM	88.5%	90%	100%	94.1%	88.1%

Table A. 3 Breast cancer diagnostic public dataset image accuracy test percentage

Method	Algorithms	Test Accuracy	Train Accuracy	Test Result		
				Sensitivity	f- measure	Precision
HOG (400) images	KNN	93.0%	94.0%	94.0%	94.2%	94.5%
	ANN	89.0%	90.0%	90.0%	90.3%	90.7%
	Decision Tree	87.5%	88.0%	88.0%	83.2%	89.5%
	Random Forest	89.0%	93.0%	93.0%	92.3%	92.7%
	AdaBoost	87.5%	88.5%	88.5%	87.7%	87.3%
	SVM	87.5%	89.5%	89.5%	86.2%	90.6%
EOH (400) images	KNN	89.94%	92.0%	92.0%	92.2%	0.923
	ANN	88.44%	91.0%	91.0%	89.0%	90.9%
	Decision Tree	86.56%	90.4%	90.5%	90.4%	90.3%
	Random Forest	90.04%	91.9%	92.0%	91.3%	91.3%
	AdaBoost	87.06%	87.9%	87.9%	87.5%	87.1%
	SVM	87.43%	87.5%	89.6%	93.4%	87.8%
Sift (400) images	KNN	91.5%	96.5%	96.5%	98.0%	96.5%
	ANN	83.5%	85.5%	85.5%	85.4%	85.3%
	Decision Tree	87.5%	87.5%	87.5%	83.3%	83.5%
	Random Forest	87.0%	88.5%	88.5%	84.0%	89.8%
	AdaBoost	85.5%	86.0%	86.0%	82.3%	81.6%
	SVM	86.0%	88.5%	88.5%	86.8%	86.6%
LBP (400) images	KNN	82.0%	91.0%	94.3%	94.9%	95.4%
	ANN	85.0%	91.0%	98.3%	95.1%	92.0%
	Decision Tree	84.5%	87.5%	100%	93.3%	87.4%
	Random Forest	86.0%	92.0%	98.9%	95.6%	92.6%

	AdaBoost	87.0%	90.0%	97.7%	94.5%	91.5%
	SVM	87.0%	88.0%	100%	93.6%	88.0%
Bo W (400) images	KNN	82.0%	91.0%	94.3%	94.9%	95.4%
	ANN	8.5%	91.0%	98.3%	95.1%	92.0%
	Decision Tree	84.5%	87.5%	100%	93.3%	87.4%
	Random Forest	86.0%	92.0%	98.9%	95.6%	92.6%
	AdaBoost	87.0%	90.0%	97.7%	94.5%	91.5%
	SVM	87.0%	88.0%	100%	93.6%	88.0%

Table A. 4 Diagnostic test accuracy for breast cancer images on the public dataset

Method	**Algorithms**	**Test Accuracy**	**Train Accuracy**	**Test Result**		
				Sensitivity	**f- measure**	**Precision**
HOG (1280) images	KNN	98.1%	98.9%	99.8%	98.9%	99.0%
	ANN	97.5%	97.8%	97.8%	97.%4	97.4%
	Decision Tree	93.3%	95.4%	95.0%	92.1%	94.9%
	Random Forest	94.0%	97.0%	97.0%	96.6%	97.1%
	AdaBoost	93.5%	94.5%	94.5%	92.7%	94.1%
	SVM	93.3%	95.5%	95.3%	94.1%	95.1%
EOH (1280) images	KNN	89.0%	94.0%	94.1%	94.0%	93.9%
	ANN	92.1%	95.8%	92.8%	90.2%	87.8%
	Decision Tree	93.2%	93.4%	93.8%	90.6%	87.9%
	Random Forest	93.7%	94.3%	93.7%	93.4%	93.8%
	AdaBoost	93.5%	93.7%	100%	90.6%	93.8%
	SVM	93.7%	93.7%	93.7%	96.8%	93.8%
Sift (1280) images	KNN	88.9%	90.8%	90.8%	90.9%	92.5%
	ANN	92.8%	94.6%	94.8%	94.7%	94.6%
	Decision Tree	93.5%	93.5%	93.6%	91.2%	87.9%

	Random Forest	93.7%	94.0%	94.1%	91.5%	94.4%
	AdaBoost	93.7%	93.9%	93.9%	91.4%	92.3%
	SVM	93.7%	95.5%	95.8%	95.1%	95.4%
LBP (1280) images	KNN	93.0%	94.2%	96.5%	96.9%	97.3%
	ANN	92.3%	95.4%	99.9%	97.6%	96.1%
	Decision Tree	93.9%	94.5%	99.2%	97.1%	95.2%
	Random Forest	93.7%	95.4%	100%	97.6%	95.4%
	AdaBoost	93.4%	93.4%	99.7%	96.6%	93.9%
	SVM	93.7%	93.7%	100%	96.8%	93.8%
BoW (1280) images	KNN	99.0%	100%	100%	100%	100%
	ANN	99.0%	100%	100%	100%	100%
	Decision Tree	99.0%	100%	100%	100%	100%
	Random Forest	99.0%	100%	100%	100%	100%
	AdaBoost	99.0%	100%	100%	100%	100%
	SVM	99.0%	100%	100%	100%	100%

پوختە

شێرپەنجەی مەمک، کە تووشی ژنان دەبێت لە سەرانسەری جیهاندا نەخۆشییەکی باو و مەترسیدارە بۆ سەر ژیان. دۆزینەوەی پێشوەختەی ورد ڕۆڵێکی گرنگ دەگێڕێت لە باشترکردنی دەرئەنجامەکانی نەخۆش و ڕێژەی مانەوە.

مۆدێلی فێربوونی قوواڵ وەک ئامرازێکی بەهێز بۆ شیکاری وێنەی پزیشکی دەرکەوتووە، کە توانای یارمەتیدان لە دەستنیشانکردنی ئۆتۆماتیکی شێرپەنجەی مەمک پێشکەش دەکات. لەم بوارەدا چەندین لێکۆڵینەوە ئەنجام دراون، هەروەها لەو ڕاپرسیانەی کە ئەنجام دراوە، بۆشایی زۆر هەیە کە پێویستە لەبەرچاو بگیرێت.

بەو پێیەی هیچکۆمەڵە داتایەکی پەیوەست بە نەخۆشخانەکانی هەرێمی کوردستانی عێراق (KRI) نییە، کە وێنەکان بۆ پۆلێنکردنی حاڵەتەکانی شێرپەنجەی مەمک پشتی پێ ببەستن. بەشێکی زۆری نووسینەکان لەسەر ئەم بابەتە لەسەر وردی پۆلێنکردن بووە بەبێ ئەوەی تا ئێستا باس لە متمانەپێکردن بکرێت. ئەم دیزێرتەیشنە بە مەبەستی پەرەپێدانی مۆدێلێکی ئۆتۆماتیکی لەسەر بنەمای فێربوونی ئامێرە، کە دەتواندرێت بۆ دیاریکردنی شێرپەنجەی مەمک بەکاربهێندرێت.

بۆ ئەوەی بتواندرێت بە خێرایی و بەشێوەیەکی کاریگەر حاڵەتەکانی شێرپەنجەی مەمک دەستنیشان بکرێت. لەم لێکۆڵینەوەیەدا، ڕێگەی زۆربەهێز بۆ دیاریکردنی شێرپەنجەی مەمک دیاریکرا، بەتایبەتی مەمک بڕین و دەرهێنانی گرێیەکە، واتە (WLE) پەرەی پێدرا. کۆمەڵە داتاکانی شێرپەنجەی مەمک کە دروستکراون بریتین لە؛ وێنەگرتنی دەنگدانەوەی موگناتیسی (MRI)، وێنەگرتنی دەنگدانەوەی موگناتیسی بەبەکارهێنانی کۆنتراستی داینامیکی (DCE-MRI) و مامۆگرافی. ئەم دیزێرتەیشنە بە مەبەستی پەرەپێدانی مۆدێلێکی ئۆتۆماتیکی لەسەر بنەمای

فێربوونی قوواڵ که دەتواندرێت بەکاربهێندرێت بۆ دیاریکردنی شێرپەنجەی مەمک سێ ڕێگای سەرەکی دەخاتەڕوو، کە دەتواندرێت بەم شێوەیە پۆلێنبکرێن:

شێوازی یەکەم؛ شێوازێکی نوێیە بۆ پۆلێنکردنی وێنەکانی (MRI) شێرپەنجەی مەمک. پرۆسەی شێوازی پێشنیارکراو لە سێ ئاست پێکدێت: دەستنیشانکردنی شێرپەنجەی مەمک لەسەر بنەمای هەڵسەنگاندنێک بە بەکارهێنانی سێ کۆمەڵە داتا، کە بە سێ قۆناغدا تێدەپەڕێت. لە قۆناغی یەکەمدا دوای هاوردەکردنی وێنەکان پرۆسەی بەشکردن دەستدەکات بە بەراوردکردنی یاخود جیاکردنەوەی ڕەنگی ڕەش و سپی لە وێنەکان، پاشان دەرهێنانی تایبەتمەندی بە بەکارهێنانی پێنج شێواز دەست پێدەکات، لە کۆتاییدا پرۆسەی پۆلێنکردن بە بەکارهێنانی حەوت ئەلگۆریثم بۆ هەڵسەنگاندنی ئەدای کارکردن دەست پێدەکات.

وردی پۆلێنکردنی وێنە پێشنیارکراوەکانی (MRI) شێرپەنجەی مەمک لە نەخۆشخانەکانی هەولێر و سلێمانی 91.9% بوو، ئەنجامی جۆری داتای ACRIN نزیکەی 97% بوو، هەروەها ئەنجامی WDBC 92.3% بوو.

مۆدێلی دووەم؛ بریتین لە CNN, ResNet152V2, Mask R-CNN بەکارهاتوون بۆ پەرەپێدانی مۆدێلی پۆلێنکردنی وێنەی مامۆگرافی شێرپەنجە و ناسینەوەی لە وێنە ڕەسەنەکانەوە بەکاتێکی کەمتری ڕاهێنان و تێچووی هەژمارکردن، بەڵام وردبینی و بیرهێنانەوەی بەرز، کە دەبێتە ئامانجی تاقیکردنەوەکان ئێمە گەیشتوینەتە ئەو ئەنجامەی، کە ResNet152V2 بەڕێژەی ١٠٠٪ لە ناسینەوەی جۆری چڕی مەمک و وێنەی ئاسایی یان نائاسایی وردبینییەکی بەرزتری بەدەستهێناوە. CNN دەستکاریکراو بەکارهێنراوە بۆ دیاریکردنی ئەوەی، کە ئایا وێنەی مەمۆگرامەکە چەپ یان ڕاستە. ئەم مۆدێلە Mask RCNN ی بەکارهێنا بۆ جیاکردنەوەی نێوان وەرەمی شێرپەنجەیی سووک و دۆزینەوەی قەبارەی وەرەمەکە.

مۆدێلی سێیەم؛ ژمارەی تایبەتمەندییە قوولەکان لە وێنەکانی MRIی شێرپەنجە وDCE-MRI زیاد دەکات بە بەکارهێنانی ڕێبازە جیاوازەکانی فێربوونی قوول. ئەم مۆدێلە خاوەنی EfficientNetV2L و Mask RCNN و Detestron2 و Detestron2ە، لەگەڵ Faster RCNN. لەم مۆدێلەدا لەبری Mask RCNN هەڵساین بە بەکارهێنا YoloV7. ئێمە گەیشتووین بەو ئەنجامەی، کە ماسک RCNN بەڕێژەی زیاتر لە ١٠٪ لە چاو YoloV7 وردبینییەکی بەرزتری لە ناسینەوەدا بەدەستهێناوە. ئەم کارە گرنگی پێدراوە بۆ دۆزینەوەی ئۆتۆماتیکی شێرپەنجەی مەمک بۆ مەمکبڕین یان WLE، واتە تەنها دەرهێنانی گرێیەکە بە بەکارهێنانی مۆدێلی جیاوازی فێربوونی قوول.

لە کۆتاییدا، جێگیرکردنی مۆدێلی فێربوونی قوول لە دەستنیشانکردنی شێرپەنجەی مەمکدا دەرئەنجامی ئومێدبەخش لە ڕووی وردبینی و کاراییەوە بەدەست دەهێنێت. ئەم مۆدێلانە توانای ئەوەیان هەیە، کە بۆ پزیشکانی تیشک و نەخۆشی لە دۆزینەوە و پۆلێنکردنی شێرپەنجەی مەمک ببنە ئامرازێکی بەسوود.

دەستنیشانکردنی شێرپەنجەی مەمک بە بەکارهێنانی مۆدێلی فێربوونی قوول

دیزێرتەیشن

پێشکەشی ئەنجومەنی کۆلێژی تەکنیکی ئەندازیاری کراوە لە زانکۆی پۆلیتەکنیکی هەولێر وەکو بەشێك لە پێداویستیەکانی بەدەست هێنانی دکتۆرای فەلسەفە

لە بەشی ئەندازیاری سیستەمی زانیاری

لەلایەن

چیمن حیدر سالح

بەکالۆریۆس لە زانستی کۆمپیوتەر

ماستەر لە ئەندازیاری ئەلیکترۆنی کارەبایی

بەسەرپەرشتیاری

پ.ی.د. عباس محمد علی

2023